Nonlinear Vibrations of Doubly Curved Cross-Ply Shallow Shells

Khaled A. Alhazza

Dissertation submitted to the Faculty of the

Virginia Polytechnic Institute and State University

in partial fulfillment of the requirements for the degree of

Doctor of Philosophy

in

Mechanical Engineering

Ali H. Nayfeh, Co-Chairman

Mehdi Ahmadian, Co-Chairman

Daniel J. Inman

Donald J. Leo

Ziyad N. Masoud

December 5, 2002

Blacksburg, Virginia

Keywords: Shallow Shells, Nonlinear Vibrations, Galerkin Discretization, Modal Interactions, Resonance.

Nonlinear Vibrations of Doubly Curved Cross-Ply Shallow Shells

Khaled Alhazza

(ABSTRACT)

The objective of this work is to study the local and global nonlinear vibrations of isotropic single-layered and multi-layered cross-ply doubly curved shallow shells with simply supported boundary conditions. The study is based-on the full nonlinear partial-differential equations of motion for shells. These equations of motion are based-on the von Kármán-type geometric nonlinear theory and the first-order shear-deformation theory, they are developed by using a variational approach. Many approximate shell theories are presented.

We used two approaches to study the responses of shells to a primary resonance: a *direct* approach and a *discretization* approach. In the discretization approach, the nonlinear partial-differential equations are discretized using the Galerkin procedure to reduce them to an infinite system of nonlinearly coupled second-order ordinary-differential equations. An approximate solution of this set is then obtained by using the method of multiple scales for the case of primary resonance. The resulting equations describing the modulations of the amplitude and phase of the excited mode are used to generate frequency- and force-response curves. The effect of the number of modes retained in the approximation on the predicted responses is discussed and the shortcomings of using low-order discretization models are demonstrated. In the direct approach, the method of multiple scales is applied directly to the nonlinear partial-differential equations of motion and associated boundary conditions for the same cases treated using the discretization approach. The results obtained from these two approaches are compared.

For the global analysis, a finite number of equations are integrated numerically to calculate the limit cycles and their stability, and hence their bifurcations, using Floquet theory. The use of this theory requires integrating $2n + (2n)^2$ nonlinear first-order ordinary-differential equations simultaneously, where n is the number of modes retained in the discretization. A

convergence study is conducted to determine the number of modes needed to obtain robust results.

The discretized system of equation are used to study the nonlinear vibrations of shells to subharmonic resonances of order one-half. The effect of the number of modes retained in the approximation is presented. Also, the effect of the number of layers on the shell parameters is shown.

Modal interaction between the first and second modes in the case of a two-to-one internal resonance is investigated. We use the method of multiple scales to determine the modulation equations that govern the slow dynamics of the response. A pseudo-arclength scheme is used to determine the fixed points of the modulation equations and the stability of these fixed points is investigated. In some cases, the fixed points undergo Hopf bifurcations, which result in dynamic solutions. A combination of a long-time integration and Floquet theory is used to determine the detailed solution branches and chaotic solutions and their stability. The limit cycles may undergo symmetry-breaking, saddle node, and period-doubling bifurcations.

بِسْمِ اللَّهِ الرَّحْمَنِ الرَّحِيمِ

In the Name of God (Allah), the Most Benevolent, the Most Merciful.

Dedication

To my Mother and Father, with love, admiration, and gratitude.

Acknowledgments

I feel very fortunate to have Dr. Ali H. Nayfeh as a supervisor. I would like to thank him for his invaluable guidance, priceless encouragement, and thoughtfulness. His help from the beginning of my Ph.D. and resourcefulness are greatly admired. It has been my pleasure to have him as a teacher, exemplar, friend, and mentor. I will not forget his help for the rest of my life.

I would like to thank Dr. Mehdi Ahmadian for his support, invaluable comments, and willingness to help. His patience and understanding are greatly admired. I would also like to thank my committee members: Dr. Daniel J. Inman, Dr. Donald J. Leo, Dr. Dean T. Mook, and Dr. Ziyad N. Masoud for their indispensable help and thoughtfulness.

The accomplishment of this work would not have been possible without the assistance of Dr. Haider Arafat for his guidance, comments, and understanding, and Dr. Eihab Abdulrahman, Dr. Osama Ashour, Samir Emam, Waleed Faris, Mohammed Younis, and Pramod Malatkar for their friendship, willingness to help, and suggestions.

A special thanks to my closest friends, Dr. Ziyad Masoud, Mohammed Daqaq, and Nasser Al-Fraih, for their understanding and patience. I would like to thank them for helping me go through my toughest times. I really believe that the accomplishment of this work would not have been possible without their friendship.

Most importantly, I would like to thank my family. I would have never succeeded with out their support and inspiration. I would like to thank my father, Ahmed Alhazza, and my

mother for their boundless energy, invaluable guidance, love, endless kindness, and never-ending devotion.

Contents

List of Figures

xv

Chapter 1

Introduction

1.1 Linear Shell Theory

Shells are used in many structural parts of various modern vehicles and civil engineering structures. A significant number of historical and modern buildings contains shell-type structures. These structures were designed long before the advent of modern engineering analysis. Examples include the Dome of the Rock Mosque, Fig. 1.1, which stood for almost one thousand years, the Pantheon of Ancient Rome, Fig. 1.2, which stood for about two thousand years, and the United States Capital Dome, Fig. 1.3. The static and dynamic studies of these and many other structures give us a better understanding of their behaviors.

A *shell* can be defined as a curved, thin-walled surface. It can be made from a single layer or multilayers of isotropic or anisotropic materials. Shells can be classified according to their curvatures: plates (where both curvatures are zero), cylindrical (where one curvature is zero), spherical (where both curvatures are equal), conical (where one of the curvatures is zero and the other changes linearly with the axial length), and doubly curved (where the two curvatures are different).

Linear isotropic shell theory was first developed by Germaine (1821). She neglected the

in-plane deflection of a cylindrical shell, but her equations contained some errors. Aron (1874) derived five equations expressed in curvilinear coordinates to describe shell behaviors. He showed that these equations reduce to the plate equations when the curvatures are set equal to zero. Love (1888) introduced a simplification for both of the in-plane and transverse motions. The equations of Love started the basic development of the theory of vibration of continuous structures with small thickness, such as those of Galerkin (1934,1942) and Timoshenko and Woinowsky-Krieger (1959). In particular, Galerkin (1934) developed a method to obtain all of the shell equations from the general theory of elasticity. His work was widely used by Lur'ye (1940), Vlasov (1949), Novozhilov (1953), Vorovich (1956), Mushtari and Galimov (1957), Mushtari and Teregulov (1959), Gol'denveiser (1961, 1979), and Gol'denveiser et al. (1993). Their work laid the fundamental principles for the linear and nonlinear theories of isotropic and anisotropic shells.

Anisotropic shells were studied in the 1920's by Shtaerman (1924), Flügge (1934, 1962), Mushtari and Galimov (1957), and Mushtari and Teregulov (1959). However, the complete theory of anistropic shells was presented by Ambartsumian (1974). He also developed the theory of multi-layered orthotropic shells with an arbitrary layer lay-up through the thickness. Grigolyuk (1953) and Grigolyuk and Chulkov (1964) developed the theory of sandwich shells as well as general multi-layered shells, including viscoelastic multi-layered shells.

1.2   Nonlinear Shell Theory

A shell is said to behave nonlinearly if the deflection at any point is not proportional to the magnitude of the applied load. There are two types of nonlinearities: geometric and material. The geometric nonlinearity is the result of nonlinear strain-displacement relations, and the material nonlinearity is the result of nonlinear stress-strain relations. Most of the work done on nonlinear shells takes into account the geometric nonlinearity because traditional engineering materials, such as steel and aluminum, behave linearly when the principal strains

Figure 1.1: The Dome of the Rock Mosque.

remain small. An attempt was made by Zerna (1960) to formulate nonlinear material shell theories.

Mushtari and Galimov (1957), Mushtari and Teregulov (1959), and Galimove (1977) made outstanding contributions to the nonlinear geometric shell theory based on the general nonlinear theory of elasticity and Kirchhoff-Love's hypotheses. Novozhilov (1953, 1964) developed a general approach to the problem of nonlinear deformation of flexible bodies and the nonlinear equations of thin shells in orthogonal coordinates. Some important results on the nonlinear equations were made by Donnell (1933), Chien (1943, 1944a, 1944b), Grigolyuk (1953), Sokolnikoff (1956), Sanders (1959, 1963), Zerna (1960), Naghdi and Berry (1964), Grigolyuk and Chulkov (1964), Koiter (1966), and Grigolyuk and Mamai (1974).

Relatively, a small number of papers addressed the nonlinear theory of laminated shells. Prusakov (1971) developed a nonlinear theory of shallow laminated shells and Gershtein (1971) and Kulikov (1979) developed nonlinear equations for multi-layered shells in tensor

Figure 1.2: The Pantheon of Ancient Rome.

form. Many contributions and reviews were made by Libai and Simmonds (1988), Vorovich
(1990), Bogdanovich (1991), Mirza (1991), Qatu (1992), Leissa (1993), Pshenichnov (1993),
Soedel (1993), Liew et al. (1997), and Gould (1998).

1.3   Methods of Solution

There are three methods for solving the nonlinear equations of motion: numerical methods
such as Galerkin, Rayleigh-Ritz, finite elements, and finite differences (Meirovitch, 1997); an-
alytical methods such as perturbation techniques (Nayfeh, 1981, 1993); and a combination
of both. In the Rayleigh-Ritz method, the vibration modes are expressed as a linear combi-
nation of a set of assumed shape functions, which satisfy the geometric boundary conditions.
In the combined approach, the partial-differential equations of motion and the associated
boundary conditions are first discretized into a set of nonlinear ordinary-differential equa-
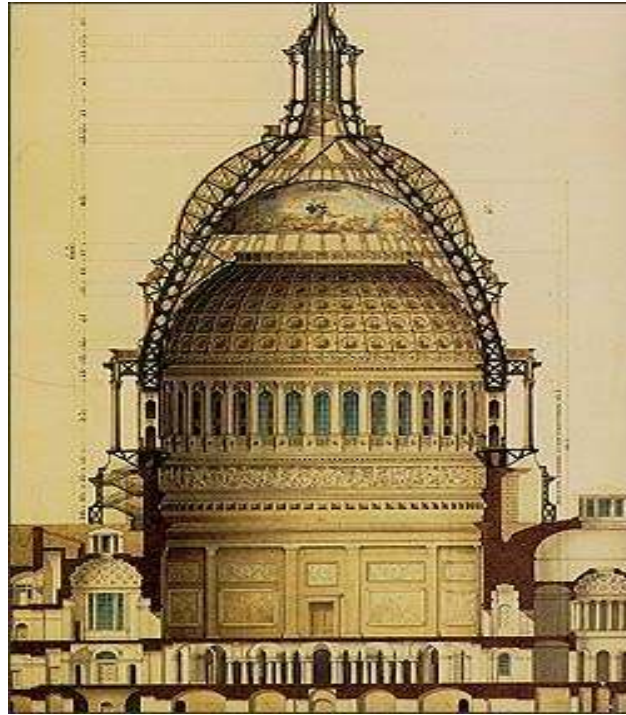
Figure 1.3: The United States Capital dome.

tions. One of the most commonly used methods for discretization is the Galerkin approach in which the weighting functions are the linear spatial mode shapes. These equations are truncated into a finite number of equations and then solved analytically in time domain. Most researchers retain one or two modes in the approximation. As a result, the obtained responses may be quantitatively and/or qualitatively erroneous (Raouf, 1989; Nayfeh and coworkers, 1988, 1992, 1996, 1997; Troger and Steindl, 1991).

1.4   Equations of Motion

To study the elastic deformation of plates and shells, one needs a complete and consistent theory. During the last three decades, composite materials have received considerable attention. Most of the work was done on plates and cylindrical shells. Nash and Modeer (1959) derived approximate equations governing the nonlinear behavior of plates with finite

amplitudes. Delpak et al. (1986) developed a simplified energy method for studying the geometric nonlinear behavior of elastic structures. Gol'denveizer et al. (1993) discussed linear Timoshenko-Reissner theories for isotropic plates and shells. These theories take into account the shear deformation and the rotational inertia.

The ring problem attracted some attention. Simmonds (1979, 1985) derived a set of geometric nonlinear equations for the in-plane motion of an elastic homogeneous circular ring and developed the equations of motion for shells of revolution. Maganty and Bickford (1987) derived an accurate set of geometric nonlinear equations of motion for circular rings. Efstathiadis (1971) derived the equations of motion governing the free undamped vibrations of nonuniform circular plates.

Large deflections of initially flat isotropic plates have been proposed by Berger (1955). He neglected the second invariant of the middle surface strains in the potential energy. This approximation is also used by Nowinski (1958a, 1958b, 1959). A great summary on the mechanics of laminated plates is presented in the book by Reddy (1997).

The nonlinear behavior of isotropic shells was studied by Sathyamoorthy (1994, 1997). He presented a geometric nonlinear theory of moderately thick isotropic spherical shells. Connor (1962) derived the equations of motion for axisymmetric nonlinear isotropic shallow spherical shells.

A small number of works is dedicated to the derivation of the nonlinear equations of motion of multi-layered and anistropic shells. Reddy and Liu (1985) developed a higher-order shear-deformation theory for elastic shells with laminated orthotropic layers. Librescu (1987) used a Lagrangian formulation to refine the geometric nonlinear theory of anisotropic laminated shells of arbitrary shape. Leissa and Qatu (1991) derived equations of motion for laminated composite shallow shells in terms of arbitrary-oriented shell coordinates. Pai and Nayfeh (1992) developed a general nonlinear theory for the dynamics of elastic anistropic circular cylindrical shells.

1.5 Plates

A large number of publications has been devoted to the linear vibrations of plates. The Galerkin procedure, the Raylegh-Ritz method, and the finite element method have been widely used in the analysis.

Free vibrations were studied by Alfonso and Hinton (1995), Barik and Mukhopadhyay (1998), Farag and Pan (1998), and Ghazi (1998). Ding (1996) used a static beam function as a shape function to study the vibration characteristics of thin, isotropic rectangular plates using the Rayleigh-Ritz method. Cheung and Zhou (1999) studied the free vibrations of a wide range of nonuniform rectangular plates.

Large-amplitude vibrations of rectangular plates were studied by Cummings (1964), Chia (1980), and Prathap and Varadan (1997). Hui (1983a, 1985) investigated the effects of geometric imperfections on the large-amplitude vibrations of circular plates. He found out that geometric imperfections may significantly raise the linear vibration frequencies and may cause a qualitative change in the behavior of plates.

Free vibrations of composite plates have been studied by Anderson and Nayfeh (1996), Chai (1996), Cunha (1997), and De Almeida and Hansen (1997). Fan and Ye (1990) introduced an exact solution for laminated plates. Qatu and Leissa (1991) used the Ritz method to determine the vibration frequencies of completely free laminated plates and shallow shells. Anderson and Nayfeh (1996) built and tested composite plates in cantilever, free-free, and clamped configurations. The experimental results were in agreement with their finite element results. They showed that, for the same accuracy, the Ritz method requires fewer degrees of freedom when compared with the finite element method. Rajalingham et al. (1996) studied the vibration of rectangular plates using the plate characteristic functions as the deflection shapes in the Rayleigh-Ritz method. Lee et al. (1997) analyzed the free vibrations of symmetrically laminated composite rectangular plates using the Rayleigh-Ritz and Kantorovich methods. Chandrashekhara and Kolli (1997) used the finite element method to study the

free vibration characteristics of laminated plates.

The nonlinear dynamic behavior of plates was studied by Tenneti and Chandrashekhara (1994), Young and Chen (1995), and Harichandran and Naja (1997). Sridhar et al. (1975, 1978) studied the nonlinear behavior of uniform circular plates to harmonic excitations. Ramesh and Krishnamoorthy (1995) investigated the application of the dynamic relaxation method to analyze the geometric nonlinear behavior of plates and shells. Abe et al. (1998a) used a single-mode Galerkin procedure to reduce the equations of motion of a laminated plate to a Duffing-type equation in terms of the transverse displacement. They analyzed solutions of the resulting equation using the method of multiple scales. They investigated the influence of the lamination sequence, the thickness ratio, the number of layers, and the in-plane boundary conditions on the subharmonic resonance response.

Multi-mode responses of plates were studied by Sridhar et al. (1975), Zhu et al. (1995) and Oh and Nayfeh (1998). Maganty and Bickford (1987) derived an accurate set of geometrically nonlinear equations of motion of circular rings. They concluded that, for nonresonant motions, the initial out-of-plane amplitude has a marginal effect on the initial in-plane oscillations, whereas the effect of the initial in-plane amplitude on the out-of-plane oscillations is significant. For resonance motions, they indicated that there is an exchange of energy between the in-plane and out-of-plane motions. Hadian and Nayfeh (1990) used the method of multiple scales to study the responses of circular plates to a harmonic external excitation. They found out that the multi-mode response loses stability through a Hopf bifurcation, resulting in harmonically and chaotically modulated motions of the plate. Leung and Mao (1995) used Galerkin method to study the dynamics of beams and plates. They compared their results with those obtained by using Runge-Kutta integration for an undamped system. Abe et al. (1998b, 1998c) investigated two-mode and three-mode responses of simply supported laminated plates to harmonic excitations by using a combination of the Galerkin procedure and the method of multiple scales. They compared their analytical results with numerical integration results and found good agreement.

1.6 Cylindrical Shells

Cylindrical shells received considerable attention due to their importance. A rich bibliography on the dynamics of cylindrical shells has been presented by Grigolyuk and Kabanov (1967, 1978) and Bert (1969). Linear vibrations were studied by Nowacki (1963). He presented analytical solutions for the vibrations of simply supported cylindrical shallow shells with a rectangular planform. Khdeir (1993) constructed a closed-form solution for the dynamic response of cross-ply laminated circular cylindrical shells using state variables. Suzuki et al. (1994) presented an exact solution for the free vibration of laminated noncircular cylindrical shells using a power-series expansion. Timarci and Soldates (1995) investigated the linear free vibrations of cross-ply laminated cylindrical shells subjected to different boundary conditions. Ip et al. (1996) developed an analytical model to predict the modal characteristics of thin-walled circular cylindrical laminated shells with free ends by Rayleigh-Ritz method. Zenkour (1998) studied the free vibrations of axisymmetric shear-deformable laminated cylindrical shells. He developed a third-order shear deformation theory of elastic shells with orthotropic layers.

Fluid loaded cylindrical shells were studied by Ahmed and Lee (1975). They developed a mathematical theory to study the nonlinear flexural response of an elastic, infinitely long, thin cylindrical shell submerged in an acoustic medium. Amabili et al. (1998) studied the nonlinear free and forced vibrations of a simply supported circular cylindrical Donnell shallow shell in contact with a fluid. They presented the results numerically and by using the normal forms (Nayfeh 1993). In another paper (1999), they investigated the nonlinear dynamics and stability of simply supported circular cylindrical shells containing a fluid.

Nonlinear free vibrations of cylindrical shells have been studied by a number of researchers. Moussaoui et al. (2000) studied the nonlinear free vibrations of an infinitely long circular cylindrical shell. They showed that the nonlinearity can significantly affect the stress in the shell. Killian et al. (1983) used the method of composite expansions to obtain approximations to the natural frequencies of prestressed, clamped cylindrical shells.

Investigations have been conducted into the forced nonlinear vibrations of cylindrical shells. Mente (1973) numerically studied the nonlinear elastic response of thin cylindrical shells to a time-dependent asymmetric pressure loading. Andianov and Kholod (1993) used an asymptotic method to study the nonlinear vibrations of shallow cylindrical shells. Andrianov and Kholod (1996) used an asymptotic procedure to study the dynamics of geometrically nonlinear thin circular cylindrical shells. Foale et al. (1998) numerically studied the nonlinear vibrations of a shallow cylindrical shell to a periodic axial forcing using the inertial manifold approximation. The influence of geometric imperfections on the dynamics of cylindrical shells was studied by Watawala and Nash (1983) and Hui (1984).

Nowinski (1963) studied the transverse vibrations of elastic orthotropic cylindrical shells using a single-mode Galerkin approximation. Bieniek et al. (1966) studied the dynamic stability of a cylindrical shell subjected to a uniform radial pressure. They used a combination of the Galerkin procedure and perturbation methods to analyze the dynamics. Chen and Babcock (1975) analyzed the large-amplitude vibrations of thin-walled cylindrical shells. They used a single-mode approximation and a perturbation method to solve for the steady-state forced vibrations. They indicated that the response contains a frequency that is twice that of the fundamental mode.

Recently, modal interactions in cylindrical shells have attracted some attention. McIvor (1966) and McIvor and Lovell (1968) analyzed the stability of the breathing mode of finite-length isotropic cylindrical shells under a uniform radial impulse. Atluri (1972) studied the nonlinear free vibrations of circular cylindrical shells using the Galerkin method. Fu and Chia (1993) studied the nonlinear free vibrations of generally laminated circular and cylindrical shells, including shear deformations, rotatory inertia, and geometrical initial imperfections using a multi-mode Galerkin approximation and the method of harmonic balance. They found out that the rotatory inertia has a very small effect on the frequency-response curve (Nayfeh and Mook, 1979) whereas, the transverse shear has a significant effect. Raouf and Palazotto (1994) studied the nonlinear free vibrations of a curved simply supported orthotropic panel using a combination of the Galerkin method and the Lindstédt-Poincaré

perturbation technique. They concluded that modes with even indeces do not affect the nonlinear vibration of the shell. Popov et al. (1998) studied the nonlinear vibrations of parametrically excited cylindrical shells. They used a continuation technique to study the interaction between modes.

1.7   Spherical and Conical Shells

A relatively small number of publications has studied the vibrations of spherical and conical shells. Sinharay and Banerjee (1985) studied large deflections of elastic spherical and cylindrical shells. Mukherjee and Chakraborty (1985) developed an exact solution for large-amplitude free and forced oscillations of spherical shells using finite-deformation theory. Alwar and Narasimhan (1991) studied the static deflections of laminated orthotropic spherical shells subjected to nonaxisymmetric loadings. They used a combination of a Fourier series and the Chebyshev-Galerkin spectral method.

Connor (1962) studied the nonlinear axisymmetric vibrations of shallow spherical shells. Evenson and Fulton (1965) studied the nonlinear dynamic responses of spherical shells. Grossman et al. (1969) studied axisymmetric vibrations of isotropic spherical caps with various boundary conditions. Leissa and Kadi (1971) studied the large-amplitude vibrations of spherical shells. They showed that the nonlinearity of spherical shells is of the softening type. Hui (1983) studied the effect of geometric imperfections on the large-amplitude vibrations of shallow spherical shells. He found out that the presence of geometric imperfections of the order of a fraction of the shell thickness may significantly raise the vibration frequencies and may produce a qualitative difference in the frequency-response curves. Hui and Leissa (1983) investigated the effect of initial geometric uni-directional imperfections on the nonlinear vibrations of a pressurized spherical shell. They showed that the imperfections significantly reduce the natural frequencies of the shell. Yasuda and Kushida (1984) studied axisymmetric forced oscillations of a shallow spherical shell subjected to harmonic

excitations. They concluded that the character of the oscillations is greatly influenced by internal resonances. Cheung and Fu (1995) studied the nonlinear vibrations of symmetric cross-ply spherical shallow shells with a circular hole, including shear deformation, by using the orthogonal collection method. They concluded that shear deformation does not alter the nature of the nonlinear static and dynamic behaviors of the shell, but it decreases the buckling load and increases the amplitude of vibration.

Very little work exists on the vibration of conical shells. Stricklin et al. (1971) studied the nonlinear dynamic behavior of shells of revolution under symmetric and asymmetric loads using the matrix displacement method. Chandrashekhara and Karekar (1992) studied the vibrations of conical shell subjected to asymmetric loads. Ye (1997) studied numerically the nonlinear vibrations and dynamic instability of thin shallow spherical and conical shells subjected to periodic transverse and in-plane loads by using a single-mode Galerkin approximation. He determined the nonlinear vibration frequencies and instability regions. Liew and Feng (2000) studies the three-dimentional linear vibration characteristics of on conical shell panels.

1.8   Doubly Curved Shells

Doubly curved shells are considered to be one of the most difficult type of shells to analyze due to the presence of both curvatures in the nonlinear equations of motion. The work done on this type of shells is small compared to the work done on cylindrical shells. Free vibrations have constituted most of this work. Singh and Kumar (1996) investigated numerically the linear free vibrational characteristics of doubly curved laminated shells. They compared the Ritz method with the finite-element method and found out that the Ritz method produces more accurate results. Liew and Lim (1996) studied the natural frequencies and linear vibratory characteristics of doubly curved shallow shells using the Ritz minimization method and taking into account high-order shear deformation. Stavridis (1998) studied the linear

dynamic responses of thin shallow shells with a rectangular layout. He used beam eigen-functions and assumed the shell to be a system of two independent plates in the context of a Galerkin solution procedure. He showed that the series solution obtained in this way converges rapidly and provides acceptable results.

El-Zaouk and Dym (1973) used a single-mode Galerkin approximation to evaluate the effect of the curvatures, the material orthotropicity, and an internal pressure on the non-linear vibrations of shallow shells. Chia (1988) used the method of harmonic balance and a generalized double Fourier series with time-dependent coefficients to study the nonlinear free vibrations of doubly curved symmetrically laminated shallow shells with rectangular planform. They used a single-mode approximation. Their numerical results show that the harmonic amplitudes of modes higher than the fourth are negligibly small. Abe et al. (2000) studied the nonlinear free-vibration characteristics of the first and second vibration modes of laminated shallow shells with rigidly clamped edges. They used the Ritz method to obtain the first and second vibration modes. Then, the Galerkin procedure was used to derive two nonlinearly coupled ordinary-differential equations. They showed that the motion of the first mode affects the vibrations of the second mode.

Leissa and Narita (1984) studied the free vibrations of shallow shells using the Ritz method. Li et al. (1990) analyzed the free vibrations of doubly curved shells using the spline finite-strip method. Fan and Luah (1995) developed a spline finite-element technique to study the free vibrations of arbitrary thin shell structures. Kobayashi and Leissa (1995) studied the effect of the thickness and the curvature on the large-amplitude free-vibrations of shallow shells using the Galerkin procedure.

A small number of publications has dealt with the forced vibrations of doubly curved shells. Leissa et al. (1983) studied the vibrations of cantilevered doubly curved shallow shells using the Ritz method. Jiashen and Lei (1991) studied the behavior of a shell under an earthquake loading using a Fourier series. Qatu and Leissa (1991) used the Ritz method to study the effect of shell parameters on its natural frequencies. In another paper, Qatu and Leissa (1993)

investigated the vibrations of shallow shells with two adjacent edges clamped and the others free by using the Ritz method. Fan and Zhang (1992) established an analytical solution for the static and dynamic behavior of doubly curved shells with orthotropic layers using the Cayley-Hamilton theorem. Wu and Liu (1994) used a Fourier series expansion to study the displacement and stresses in thick doubly curved laminated shells. Masunaga (1999) studied the effects of high-order shear deformations on the natural frequencies and buckling loads of thick shallow shells with rectangular planform and subjected to uniaxial and biaxial in-plane stresses. He concluded that a nine-mode approximation was accurate enough for extremely thick shallow shells. Wu and Chi (1999) developed an analytical solution for doubly curved laminated shells with various boundary conditions by using an asymptotic method.

Maewal (1978) solved the equations of motion by using an asymptotic analysis without going through the Galerkin method and indicated a correction to the frequency-response curves reported in the literature. Zhang et al. (2001) used a single-mode Galerkin approximation to study the nonlinear dynamics and stability of doubly curved orthotropic shallow shells with simply supported boundary conditions under impact.

1.9   Reduced-Order Models

Recently, multi-mode approximation has attracted a great attention due to their effect on the accuracy of the predicted response. Many papers and a book (Nayfeh, 2000) were published by Nayfeh and his co-workers on the effects of multi-mode approximation on the stability of continuous systems. They showed the shortcomings of using a single-mode discretization in the analysis of different continuous systems with quadratic and cubic nonlinearities.

Nayfeh and Raouf (1987) used the Galerkin procedure to study the nonlinear forced responses of infinitely long cylindrical shells in the case of one-to-one internal resonance. In another paper, they (1990) studied the nonlinear responses of infinitely long cylinders to a primary resonance excitation. Pakdemirli et al. (1995) showed that treatment of a low-order

discretized system may lead to different responses compared to those obtained by the direct approach for the nonlinear vibrations of cables.

Chin and Nayfeh (1996) studied the nonlinear vibrations of infinitely long cylindrical shells. They compared the results obtained using a two-mode discretization with those obtained by directly attacking the governing partial-differential equations of motion. They showed that a two-mode discretization approach may produce erroneous results. In another paper, Chin and Nayfeh (2001) investigated the nonlinear response and stability of an infinitely long circular cylindrical shell to a primary resonance excitation involving one-to-one and two-to-one internal resonances.

Nayfeh and Lacarbonara (1997) compared the results obtained by low-order Galerkin approximations with those obtained by directly attacking the partial-differential equations governing the dynamics of an Euler-Bernoulli beam resting on a nonlinear foundation. They showed that a single-mode approximation leads to erroneous qualitative and quantitative predictions. Lacarbonara et al. (1998) demonstrated experimentally that a single-mode Galerkin approximation of the dynamics of a buckled beam may produce quantitative and qualitative errors in the frequency-response curves. Nayfeh (1998) developed a procedure to produce reduced-order models that overcome the shortcomings of the Galerkin method. The results obtained by analyzing these reduced-order systems are in agreement with those obtained experimentally and by directly attacking the partial-differential equations and associated boundary conditions. Lacarbonara (1999) studied the nonlinear vibrations of nonlinear spatially continuous systems with general quadratic and cubic nonlinearities using the direct approach and low-order Galerkin discretization. He showed that a low-order Galerkin discretization may produce inadequate qualitative and quantitative responses. Abe et al. (1998) studied two-mode responses of thin rectangular laminated plates to harmonic excitations using the Galerkin procedure and the method of multiple scales. They concluded that the two-mode approximation may predict a behavior different from that predicted by a single-mode approximation. Kobayashi et al. (1999) used single-mode and two-mode approximations to analyze the nonlinear responses of doubly-curved shells to primary-resonance

excitations. Rega et al. (1999) studied the nonlinear three-dimensional responses of an elastic suspended shallow cable to a harmonic excitation. They showed that a low-order Galerkin approximation produces qualitative and quantitative differences in the frequency-response curves compared with those produced by the direct approach. Abe et. al. (2001) studied the responses of cross-ply laminated shallow shells. They used an improved displacement function to overcome the shortcomings of the Galerkin approximation.

Emam and Nayfeh (2002) investigated the nonlinear vibrations of a clamped-clamped buckled beam subjected to a harmonic excitation. They showed that a single-mode approximation may lead to quantitative and qualitative errors in the static and dynamic behaviors of the beam. Nayfeh and Arafat (2002) investigated the nonlinear forced vibrations of shallow suspended cables. They compared between the results obtained by using the direct and discretization approaches. They found out that using a low-order discretization may lead to significant quantitative and qualitative errors in the effective nonlinearity.

Chapter 2

Equations of Motion

There are many theories of shells which can be classified depending on the assumptions made in each of them. Next, we present an introduction of them. For more comprehensive details, we refer the reader to Leissa (1993), Soedel (1993), Bogdanovich (1990), Novozhilov (1953), Pshenichnov (1993), and Reddy (1997).

2.1   Infinitesimal Distance in Shell Layers

The derivation of the equations of motion is based on two assumptions. The first assumption is that the shell has small deflections. The second assumption is that the shell thickness is small compared to its radii of curvature. The theoretical approach presented here is based on the works of Love (1888, 1944) and Reissner (1941).

With these assumptions, any location on the neutral surface can be defined by two-dimensional curvilinear surface coordinates α_1 and α_2 instead of three-dimensional Cartesian coordinates. We choose α_1 and α_2 along the principal curvatures, Fig. 4. The location of point P on the neutral surface can be expressed as

$$x_1 = f_1(\alpha_1, \alpha_2), \;\; x_2 = f_2(\alpha_1, \alpha_2), \;\; x_3 = f_3(\alpha_1, \alpha_2) \tag{2.1}$$

or in vector form as

$$\bar{r}(\alpha_1, \alpha_2) = f_1(\alpha_1, \alpha_2)\bar{e}_1 + f_2(\alpha_1, \alpha_2)\bar{e}_2 + f_3(\alpha_1, \alpha_2)\bar{e}_3 \tag{2.2}$$

Next, we consider a point P' close to P on the neutral surface. Then, the location of P' can be expressed in terms of that of P as

$$\bar{r} + d\bar{r} \tag{2.3}$$

where the differential change in the vector $\bar{r}$ can be written as

$$d\bar{r} = \frac{\partial \bar{r}}{\partial \alpha_1} d\alpha_1 + \frac{\partial \bar{r}}{\partial \alpha_2} d\alpha_2 \tag{2.4}$$

Hence, the magnitude ds of $d\bar{r}$ is obtained from

$$(ds)^2 = d\bar{r} \cdot d\bar{r} \tag{2.5}$$

Expanding this equation in orthogonal curvilinear coordinates leads to

$$(ds)^2 = \frac{\partial \bar{r}}{\partial \alpha_1} \cdot \frac{\partial \bar{r}}{\partial \alpha_1}(d\alpha_1)^2 + \frac{\partial \bar{r}}{\partial \alpha_2} \cdot \frac{\partial \bar{r}}{\partial \alpha_2}(d\alpha_2)^2 \tag{2.6}$$

or

$$(ds)^2 = A_1^2(d\alpha_1)^2 + A_2^2(d\alpha_2)^2 \tag{2.7}$$

where A_1 and A_2 are called *Lame parameters* and defined as

$$A_1^2 = \frac{\partial \bar{r}}{\partial \alpha_1} \cdot \frac{\partial \bar{r}}{\partial \alpha_1} \tag{2.8}$$

$$A_2^2 = \frac{\partial \bar{r}}{\partial \alpha_2} \cdot \frac{\partial \bar{r}}{\partial \alpha_2} \tag{2.9}$$

To define the distance between two points on the shell, we take a point P_1 along the normal to the neutral surface through point P and at a distance α_3 from P, and we take another
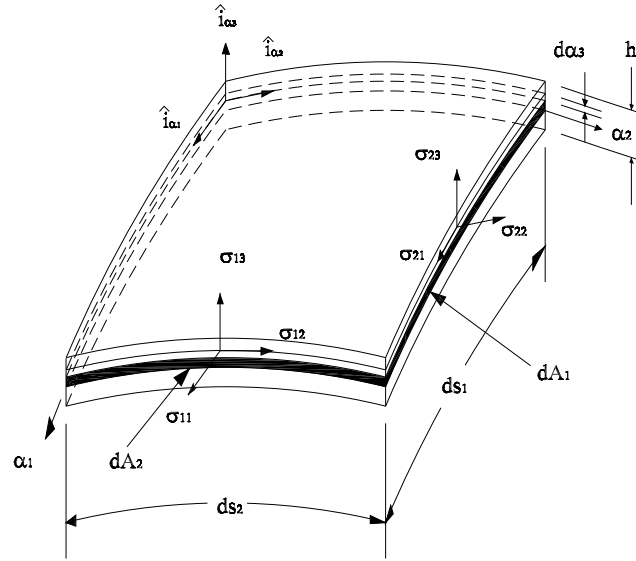
Figure 2.1: Stresses in a shell element.

point P_1' along the normal to the neutral surface through P' and at a distance $\alpha_3 + d\alpha_3$ from P'. Therefore, the location of P_1 can be expressed as

$$\bar{R}(\alpha_1, \alpha_2, \alpha_3) = \bar{r}(\alpha_1, \alpha_2) + \alpha_3 \bar{n}(\alpha_1, \alpha_2) \tag{2.10}$$

where $\bar{n}$ is a unit vector normal to the neutral surface through P. Then, $d\bar{R}$ can be expressed as

$$d\bar{R} = d\bar{r} + \alpha_3 d\bar{n} + \bar{n} d\alpha_3 \tag{2.11}$$

where

$$d\bar{n} = \frac{\partial \bar{n}}{\partial \alpha_1} d\alpha_1 + \frac{\partial \bar{n}}{\partial \alpha_2} d\alpha_2 \tag{2.12}$$

Next, we calculate the magnitude dS of $d\bar{R}$ by taking the dot product of the vector $d\bar{R}$ with itself. The result is

$$(dS)^2 = d\bar{R} \cdot d\bar{R} = d\bar{r} \cdot d\bar{r} + \alpha_3^2 d\bar{n} \cdot d\bar{n} + (d\alpha_3)^2 + 2\alpha_3 d\bar{r} \cdot d\bar{n}$$
$$+ 2d\alpha_3(d\bar{r} \cdot \bar{n}) \tag{2.13}$$

where (Soedel, 1993)

$$d\bar{r} \cdot d\bar{r} = A_1^2(d\alpha_1)^2 + A_2^2(d\alpha_2)^2 \tag{2.14}$$

$$d\bar{n} \cdot d\bar{n} = \frac{A_1^2}{R_1^2}(d\alpha_1)^2 + \frac{A_2^2}{R_2^2}(d\alpha_2)^2 \tag{2.15}$$

$$d\bar{r} \cdot d\bar{n} = \frac{A_1^2}{R_1}(d\alpha_1)^2 + \frac{A_2^2}{R_2}(d\alpha_2)^2 \tag{2.16}$$

and R_1 and R_2 are the radii of curvature along the α_1 and α_2 axes, respectively.

Substituting Eqs. (2.14)-(2.16) into Eq. (2.13) gives

$$(dS)^2 = A_1^2\left(1 + \frac{\alpha_3}{R_1}\right)^2(d\alpha_1)^2 + A_2^2\left(1 + \frac{\alpha_3}{R_2}\right)^2(d\alpha_2)^2 + (d\alpha_3)^2 \tag{2.17}$$

2.2 Stress-Strain Relationships

Most engineering materials have linear stress-strain relationships. These relationships can be expressed as

$$\sigma_{ii} = E\varepsilon_{ii} \tag{2.18}$$

$$\sigma_{ij} = G\varepsilon_{ij} \tag{2.19}$$

These relationships are known as *Hooke's Law*, after the English mathematician Robert Hooke (1635-1703), where E is the *modulus of elasticity*, the ε_{ii} are the normal strains, the σ_{ii} are the normal stresses, G is the *modulus of rigidity*, the σ_{ij} are the shearing stresses, and the ε_{ij} are the shearing strains. In order to express the strain components ε_{ij} in terms of the stress components σ_{ij}, we use the principle of superposition, which states that the effect of a given combined loading on a structure can be obtained by determining separately the effects of the various loads and combining the results. Assuming that each effect is linearly

related to the load which produces it and that the deformation resulting from any given load is small, the relations provided by these assumptions are referred to as *the generalized Hooke Law*, which can be expressed mathematically as

$$\varepsilon_{11} = \frac{1}{E}[\sigma_{11} - \nu(\sigma_{22} + \sigma_{33})] \tag{2.20}$$

$$\varepsilon_{22} = \frac{1}{E}[\sigma_{22} - \nu(\sigma_{11} + \sigma_{33})] \tag{2.21}$$

$$\varepsilon_{33} = \frac{1}{E}[\sigma_{33} - \nu(\sigma_{11} + \sigma_{22})] \tag{2.22}$$

$$\varepsilon_{12} = \frac{1}{G}\sigma_{12} \tag{2.23}$$

$$\varepsilon_{13} = \frac{1}{G}\sigma_{13} \tag{2.24}$$

$$\varepsilon_{23} = \frac{1}{G}\sigma_{23} \tag{2.25}$$

where ν is Poisson's ratio.

2.3   Strain-Displacement Relationships

The strain-displacement relationships in orthogonal curvilinear coordinates based on the three-dimensional theory of elasticity can be written as (Sokolnikoff, 1956)

$$\varepsilon_{ii} = \frac{\partial}{\partial \alpha_i}\left(\frac{U_i}{\sqrt{g_i}}\right) + \frac{1}{2g_i}\sum_{k=1}^{3}\frac{\partial g_i}{\partial \alpha_k}\frac{U_k}{\sqrt{g_k}} \qquad i = 1, 2, 3 \tag{2.26}$$

$$\varepsilon_{ij} = \frac{1}{\sqrt{g_i g_j}}\left[g_i\frac{\partial}{\partial \alpha_j}\left(\frac{U_i}{\sqrt{g_i}}\right) + g_j\frac{\partial}{\partial \alpha_i}\left(\frac{U_j}{\sqrt{g_j}}\right)\right] \qquad i, j = 1, 2, 3 \quad i \neq j \tag{2.27}$$

where g_1, g_2, and g_3 are defined as

$$g_1 = \left[A_1 \left(1 + \frac{\alpha_3}{R_1} \right) \right]^2 \tag{2.28}$$

$$g_2 = \left[A_2 \left(1 + \frac{\alpha_3}{R_2} \right) \right]^2 \tag{2.29}$$

$$g_3 = 1 \tag{2.30}$$

and the U_i are the deflections along the α_i directions. Substituting Eqs. (2.28)-(2.30) into Eqs. (2.26) and (2.27) leads

$$\varepsilon_{11} = \frac{1}{1 + \frac{\alpha_3}{R_1}} \left(\frac{1}{A_1} \frac{\partial U_1}{\partial \alpha_1} + \frac{U_2}{A_1 A_2} \frac{\partial A_1}{\partial \alpha_2} + \frac{U_3}{R_1} \right) \tag{2.31}$$

$$\varepsilon_{22} = \frac{1}{1 + \frac{\alpha_3}{R_2}} \left(\frac{1}{A_2} \frac{\partial U_2}{\partial \alpha_2} + \frac{U_1}{A_1 A_2} \frac{\partial A_2}{\partial \alpha_1} + \frac{U_3}{R_2} \right) \tag{2.32}$$

$$\varepsilon_{33} = \frac{\partial U_3}{\partial \alpha_3} \tag{2.33}$$

$$\varepsilon_{12} = \frac{A_1 \left(1 + \frac{\alpha_3}{R_1} \right)}{A_2 \left(1 + \frac{\alpha_3}{R_2} \right)} \frac{\partial}{\partial \alpha_2} \left[\frac{U_1}{A_1 \left(1 + \frac{\alpha_3}{R_1} \right)} \right] + \frac{A_2 \left(1 + \frac{\alpha_3}{R_2} \right)}{A_1 \left(1 + \frac{\alpha_3}{R_1} \right)} \frac{\partial}{\partial \alpha_1} \left[\frac{U_2}{A_2 \left(1 + \frac{\alpha_3}{R_2} \right)} \right] \tag{2.34}$$

$$\varepsilon_{13} = \frac{1}{A_1 \left(1 + \frac{\alpha_3}{R_1} \right)} \frac{\partial U_3}{\partial \alpha_1} + A_1 \left(1 + \frac{\alpha_3}{R_1} \right) \frac{\partial}{\partial \alpha_3} \left[\frac{U_1}{A_1 \left(1 + \frac{\alpha_3}{R_1} \right)} \right] \tag{2.35}$$

$$\varepsilon_{23} = \frac{1}{A_2 \left(1 + \frac{\alpha_3}{R_2} \right)} \frac{\partial U_3}{\partial \alpha_2} + A_2 \left(1 + \frac{\alpha_3}{R_2} \right) \frac{\partial}{\partial \alpha_3} \left[\frac{U_2}{A_2 \left(1 + \frac{\alpha_3}{R_2} \right)} \right] \tag{2.36}$$

Next, we classify different theories used to derive the equations of motion.

2.4   Classical Theories and Assumptions

2.4.1   Love's Approximations

Love (1888) made four approximations in the classical theory of small displacements of thin shells, referred to as the *first approximation*. These approximations have been accepted by almost all of the following researchers. These approximations can be summarized as:

1. The shell thickness h is small compared with the radii of curvature; that is,

$$\frac{h}{R_1} \quad \text{and} \quad \frac{h}{R_2} << 1 \tag{2.37}$$

2. The transverse normal stress can be neglected compared to the other stresses; that is,

$$\sigma_{33} = 0 \tag{2.38}$$

3. The displacements and strains are very small so that the second-order terms in the strain-displacement relations can be neglected.

4. The normals to the undeformed middle-surface of the shell remain straight through out the deformation and suffer no extension. This assumption is known as Kirchhoff's hypothesis. This set of approximations leads to the rules

$$\varepsilon_{13} = \varepsilon_{23} = \varepsilon_{33} = 0$$

$$\sigma_{13} = \sigma_{23} = 0 \tag{2.39}$$

In order to satisfy Kirchhoff's hypothesis, we assume that the displacements along the α_1 and α_2 directions change linearly through the shell thickness, whereas the displacements in the α_3 direction are independent of the shell thickness. These assumptions can be expressed as

$$U_1(\alpha_1, \alpha_2, \alpha_3) = u_1(\alpha_1, \alpha_2) + \alpha_3 \beta_1(\alpha_1, \alpha_2) \tag{2.40}$$

$$U_2(\alpha_1, \alpha_2, \alpha_3) = u_2(\alpha_1, \alpha_2) + \alpha_3\beta_2(\alpha_1, \alpha_2) \tag{2.41}$$

$$U_3(\alpha_1, \alpha_2, \alpha_3) = u_3(\alpha_1, \alpha_2) \tag{2.42}$$

where β_1 and β_2 are the rotations of the normals to the middle surface during deformation about α_1 and α_2, respectively. Substituting Eqs. (2.40)-(2.42) into Eqs. (2.35) and (2.36) leads to the following relations:

$$\beta_1 = \frac{u_1}{R_1} - \frac{\partial u_3}{A_1 \partial \alpha_1} \tag{2.43}$$

$$\beta_2 = \frac{u_2}{R_2} - \frac{\partial u_3}{A_2 \partial \alpha_2} \tag{2.44}$$

2.4.2 Flügge, Gol'denveizer, Novozhilov, Byrne, and Lur'ye Equations

The strain-displacement equations used by Flügge, Gol'denveizer, Novozhilov, Byrne, and Lur'ye can be derived by substituting Eqs. (2.40)-(2.42) into Eqs. (2.31)-(2.34) and obtaining

$$\varepsilon_{11} = \frac{1}{1 + \frac{\alpha_3}{R_1}}(\epsilon_{11} + \alpha_3 \kappa_{11}) \tag{2.45}$$

$$\varepsilon_{22} = \frac{1}{1 + \frac{\alpha_3}{R_2}}(\epsilon_{22} + \alpha_3 \kappa_{22}) \tag{2.46}$$

$$\varepsilon_{12} = \frac{1}{(1 + \frac{\alpha_3}{R_2})(1 + \frac{\alpha_3}{R_1})}\left[\left(1 - \frac{\alpha_3^2}{R_1 R_2}\right)\epsilon_{12} + \alpha_3\tau\left(1 + \frac{\alpha_3}{2R_1} + \frac{\alpha_3}{2R_2}\right)\right] \tag{2.47}$$

where the ϵ_{ii} are the normal strain in the middle surface in the α_i directions, ϵ_{12} is the shear strain in the middle surface, τ is the middle surface twist, and κ_{11} and κ_{22} are the changes in the curvature in the middle surface. These quantities can written as

$$\epsilon_{11} = \frac{1}{A_1}\frac{\partial u_1}{\partial \alpha_1} + \frac{u_2}{A_1 A_2}\frac{\partial A_1}{\partial \alpha_2} + \frac{u_3}{R_1} \tag{2.48}$$

$$\epsilon_{22} = \frac{1}{A_2}\frac{\partial u_2}{\partial \alpha_2} + \frac{u_1}{A_1 A_2}\frac{\partial A_2}{\partial \alpha_1} + \frac{u_3}{R_2} \tag{2.49}$$

$$\epsilon_{12} = \frac{A_1}{A_2}\frac{\partial}{\partial \alpha_2}\left(\frac{u_1}{A_1}\right) + \frac{A_2}{A_1}\frac{\partial}{\partial \alpha_1}\left(\frac{u_2}{A_2}\right) \tag{2.50}$$

$$\kappa_{11} = \frac{1}{A_1}\frac{\partial \beta_1}{\partial \alpha_1} + \frac{\beta_2}{A_1 A_2}\frac{\partial A_1}{\partial \alpha_2} \tag{2.51}$$

$$\kappa_{22} = \frac{1}{A_2}\frac{\partial \beta_2}{\partial \alpha_2} + \frac{\beta_1}{A_1 A_2}\frac{\partial A_2}{\partial \alpha_1} \tag{2.52}$$

$$\tau = \frac{A_1}{A_2}\frac{\partial}{\partial \alpha_2}\left(\frac{\beta_1}{A_1}\right) + \frac{A_2}{A_1}\frac{\partial}{\partial \alpha_1}\left(\frac{\beta_2}{A_2}\right) + \frac{1}{R_1}\left(\frac{1}{A_2}\frac{\partial u_1}{\partial \alpha_2} - \frac{u_2}{A_1 A_2}\frac{\partial A_2}{\partial \alpha_1}\right)$$
$$+ \frac{1}{R_2}\left(\frac{1}{A_1}\frac{\partial u_2}{\partial \alpha_1} - \frac{u_1}{A_1 A_2}\frac{\partial A_1}{\partial \alpha_2}\right) \tag{2.53}$$

2.4.3   Love and Timoshenko Equations

Love and Timoshenko assumed that the terms $\frac{\alpha_3}{R_1}$ and $\frac{\alpha_3}{R_2}$ are small in Eqs. (2.45)-(2.47). Hence,

$$\varepsilon_{11} = \epsilon_{11} + \alpha_3 \kappa_{11} \tag{2.54}$$

$$\varepsilon_{22} = \epsilon_{22} + \alpha_3 \kappa_{22} \tag{2.55}$$

$$\varepsilon_{12} = \epsilon_{12} + \alpha_3 \tau \tag{2.56}$$

2.4.4   Reissner, Naghdi, and Berry Equations

Reissner, Naghdi, and Berry used the same simplification as Love and Timoshenko, α_3/R_1 and $\alpha_3/R_2 << 1$, but they used it earlier in the derivation, Eqs. (2.31), (2.32), and (2.34), which gives the following set of equations:

$$\varepsilon_{11} = \frac{1}{A_1}\frac{\partial U_1}{\partial \alpha_1} + \frac{U_2}{A_1 A_2}\frac{\partial A_1}{\partial \alpha_2} + \frac{U_3}{R_1} \tag{2.57}$$

$$\varepsilon_{22} = \frac{1}{A_2}\frac{\partial U_2}{\partial \alpha_2} + \frac{U_1}{A_1 A_2}\frac{\partial A_2}{\partial \alpha_1} + \frac{U_3}{R_2} \tag{2.58}$$

$$\varepsilon_{12} = \frac{A_1}{A_2}\frac{\partial}{\partial \alpha_2}\left(\frac{U_1}{A_1}\right) + \frac{A_2}{A_1}\frac{\partial}{\partial \alpha_1}\left(\frac{U_2}{A_2}\right) \tag{2.59}$$

Consequently, the midsurface twist τ can be expressed as

$$\tau = \frac{A_1}{A_2}\frac{\partial}{\partial \alpha_2}\left(\frac{\beta_1}{A_1}\right) + \frac{A_2}{A_1}\frac{\partial}{\partial \alpha_1}\left(\frac{\beta_2}{A_2}\right) \tag{2.60}$$

2.4.5 Vlasov Equations

Assuming that the terms α_3/R_1 and $\alpha_3/R_2 << 1$, Vlasov expanded the term $(1 + \alpha_3/R_i)^{-1}$ in a geometric series as

$$\frac{1}{1 + \alpha_3/R_i} = \sum_{n=1}^{\infty}\left(-\frac{\alpha_3}{R_i}\right)^n \tag{2.61}$$

Substituting Eqs. (2.40)-(2.61) into Eqs. (2.31), (2.32), and (2.34) gives

$$\varepsilon_{11} = (\epsilon_{11} + \alpha_3 \kappa_{11})\sum_{n=1}^{\infty}\left(-\frac{\alpha_3}{R_1}\right)^n \tag{2.62}$$

$$\varepsilon_{22} = (\epsilon_{22} + \alpha_3 \kappa_{22})\sum_{n=1}^{\infty}\left(-\frac{\alpha_3}{R_2}\right)^n \tag{2.63}$$

$$\begin{aligned}
\varepsilon_{12} = &\frac{A_1}{A_2}\left(1 + \frac{\alpha_3}{R_1}\right)\sum_{n=1}^{\infty}\left(-\frac{\alpha_3}{R_2}\right)^n\left\{\frac{\partial}{\partial \alpha_2}\left[\frac{u_1 + \alpha_3 \beta_1}{A_1}\sum_{m=1}^{\infty}\left(-\frac{\alpha_3}{R_1}\right)^m\right]\right\} \\
&+ \frac{A_2}{A_1}\left(1 + \frac{\alpha_3}{R_2}\right)\sum_{n=1}^{\infty}\left(-\frac{\alpha_3}{R_1}\right)^n\left\{\frac{\partial}{\partial \alpha_1}\left[\frac{u_2 + \alpha_3 \beta_2}{A_2}\sum_{m=1}^{\infty}\left(-\frac{\alpha_3}{R_2}\right)^m\right]\right\}
\end{aligned} \tag{2.64}$$

Considering only $n = 1$ and $m = 1$, a linear relationships in α_3, one can write Eqs. (2.62)-(2.64) as

$$\varepsilon_{11} = \epsilon_{11} + \alpha_3 \kappa_{11} - \alpha_3\frac{\epsilon_{11}}{R_1} \tag{2.65}$$

$$\varepsilon_{22} = \epsilon_{22} + \alpha_3 \kappa_{22} - \alpha_3 \frac{\epsilon_{22}}{R_2} \tag{2.66}$$

$$\varepsilon_{12} = \epsilon_{12} + \tau \alpha_3 \tag{2.67}$$

where

$$\tau = \left(\frac{1}{R_1} - \frac{1}{R_2} \right) \left[\frac{A_1}{A_2} \frac{\partial}{\partial \alpha_2} \left(\frac{u_1}{A_1} \right) - \frac{A_2}{A_1} \frac{\partial}{\partial \alpha_1} \left(\frac{u_2}{A_2} \right) \right]$$
$$- \frac{2}{A_1 A_2} \left(\frac{\partial^2 u_3}{\partial \alpha_1 \partial \alpha_2} - \frac{1}{A_2} \frac{\partial A_2}{\partial \alpha_1} \frac{\partial u_3}{\partial \alpha_2} - \frac{1}{A_1} \frac{\partial A_1}{\partial \alpha_2} \frac{\partial u_3}{\partial \alpha_1} \right) \tag{2.68}$$

2.4.6 Donnell and Mushtari Equations

Donnell and Mushtari neglected the effect of the tangential displacement in their derivation. They obtained the strains equations

$$\varepsilon_{11} = \epsilon_{11} + \alpha_3 \kappa_{11} \tag{2.69}$$

$$\varepsilon_{22} = \epsilon_{22} + \alpha_3 \kappa_{22} \tag{2.70}$$

$$\varepsilon_{12} = \epsilon_{12} + \alpha_3 \tau \tag{2.71}$$

where ϵ_{11}, ϵ_{22}, and ϵ_{12} are given by Eqs. (2.48)-(2.50). The middle surface change in the curvatures and twist, κ_{11}, κ_{22}, and τ, are

$$\kappa_{11} = -\frac{1}{A_1} \frac{\partial}{\partial \alpha_1} \left(\frac{1}{A_1} \frac{\partial u_3}{\partial \alpha_1} \right) - \frac{1}{A_1 A_2^2} \frac{\partial A_1}{\partial \alpha_2} \frac{\partial u_3}{\partial \alpha_2} \tag{2.72}$$

$$\kappa_{22} = -\frac{1}{A_2} \frac{\partial}{\partial \alpha_2} \left(\frac{1}{A_2} \frac{\partial u_3}{\partial \alpha_2} \right) - \frac{1}{A_1^2 A_2} \frac{\partial A_2}{\partial \alpha_1} \frac{\partial u_3}{\partial \alpha_1} \tag{2.73}$$

$$\tau = -\frac{A_2}{A_1} \frac{\partial}{\partial \alpha_1} \left(\frac{1}{A_2^2} \frac{\partial u_3}{\partial \alpha_2} \right) - \frac{A_1}{A_2} \frac{\partial}{\partial \alpha_2} \left(\frac{1}{A_1^2} \frac{\partial u_3}{\partial \alpha_1} \right) \tag{2.74}$$
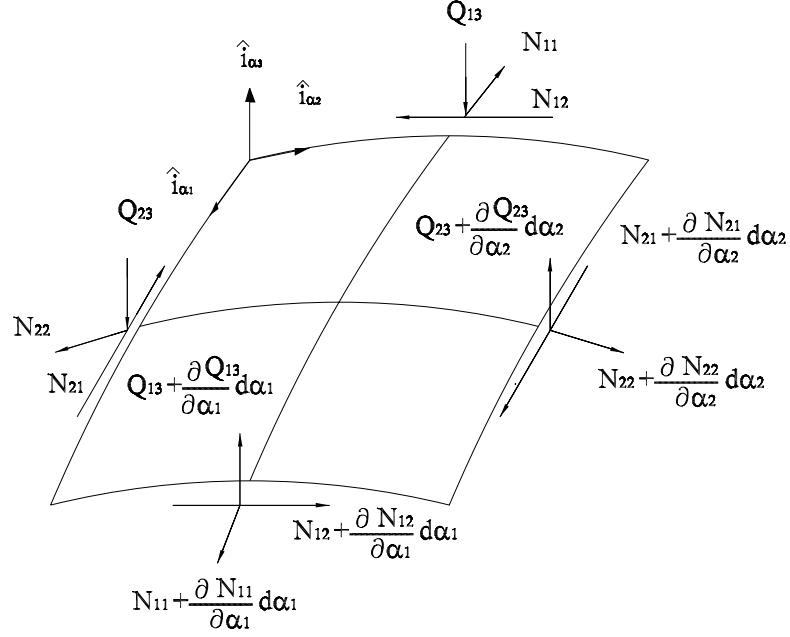
Figure 2.2: Forces resultants in shell coordinates.

2.5 Energy Expressions

The equations of motion can be derived by calculating the strain and kinetic energies stored in an infinitesimal element. The strain energy produced by the stresses σ_{ij} can be expressed as

$$dU = \frac{1}{2}\left(\sigma_{11}\varepsilon_{11} + \sigma_{22}\varepsilon_{22} + \sigma_{11}\varepsilon_{11} + \sigma_{13}\varepsilon_{13} + \sigma_{23}\varepsilon_{23} + \sigma_{33}\varepsilon_{33}\right)dV \tag{2.75}$$

Using Love assumptions, we can neglect the effect of the last term in Eq. (2.75). Integrating Eq. (2.75) over the volume

$$dV = A_1 A_2 \left(1 + \frac{\alpha_3}{R_1}\right)\left(1 + \frac{\alpha_3}{R_2}\right) d\alpha_1 d\alpha_2 d\alpha_3 \tag{2.76}$$

gives

$$U = \int_{\alpha_1}\int_{\alpha_2}\int_{\alpha_3} \frac{1}{2}\left(\sigma_{11}\varepsilon_{11} + \sigma_{22}\varepsilon_{22} + \sigma_{11}\varepsilon_{11} + \sigma_{13}\varepsilon_{13} + \sigma_{23}\varepsilon_{23}\right)dV \tag{2.77}$$

For an infinitesimal element, the kinetic energy K is given by

$$dK = \frac{1}{2}\rho \left(\dot{U}_1^2 + \dot{U}_2^2 + \dot{U}_3^2 \right) dV \tag{2.78}$$

where ρ is the density and the overdot indicates the time derivative. Substituting Eqs. (2.40)-(2.42) and (2.76) into Eq. (2.78) gives

$$K = \frac{1}{2}\rho \int_{\alpha_1} \int_{\alpha_2} \int_{\alpha_3} [\dot{u}_1^2 + \dot{u}_2^2 + \dot{u}_3^2 + \alpha_3(\alpha_3\dot{\beta}_1^2 + \alpha_3\dot{\beta}_2^2 + 2\dot{\beta}_1\dot{u}_1 + 2\dot{\beta}_2\dot{u}_2)]$$
$$\times A_1 A_2 \left(1 + \frac{\alpha_3}{R_1} \right) \left(1 + \frac{\alpha_3}{R_2} \right) d\alpha_1 d\alpha_2 d\alpha_3 \tag{2.79}$$

For small deflections, we can neglect the terms $\frac{\alpha_3}{R_2}$ and $\frac{\alpha_3}{R_2}$. Integrating Eq. (2.79) over the thickness α_3 from $\frac{1}{2}h$ to $-\frac{1}{2}h$ yields,

$$K = \frac{1}{2}\rho h \int_{\alpha_1} \int_{\alpha_2} [\dot{u}_1^2 + \dot{u}_2^2 + \dot{u}_3^2 + \frac{1}{12}h^2(\dot{\beta}_1^2 + \dot{\beta}_2^2)]A_1 A_2 d\alpha_1 d\alpha_2 \tag{2.80}$$

Now, we calculate the variation of the energy due to the forces q_1, q_2, and q_3 acting on the neutral surface of the shell as

$$\delta E_L = \int_{\alpha_1} \int_{\alpha_2} (q_1\delta u_1 + q_2\delta u_2 + q_3\delta u_3)A_1 A_2 d\alpha_1 d\alpha_2 \tag{2.81}$$

Variation of the energy due to the boundary forces along α_1 and α_2, Fig. 2.2, can be expressed as

$$\delta E_B = \int_{\alpha_1} (\delta u_2 N_{22}^* + \delta u_1 N_{21}^* + \delta u_3 Q_{23}^* + \delta\beta_2 M_{22}^* + \delta\beta_1 M_{21}^*)A_1 d\alpha_1$$
$$+ \int_{\alpha_2} (\delta u_1 N_{11}^* + \delta u_2 N_{12}^* + \delta u_3 Q_{13}^* + \delta\beta_1 M_{11}^* + \delta\beta_1 M_{12}^*)A_2 d\alpha_2 \tag{2.82}$$

where the N_{ii}^* are the boundary forces acting normal to the surface, the N_{ij}^* are the shear forces acting in the tangent plane, the M_{ii}^* are the moments in the α_i^* directions, the M_{ij}^* are the twisting moments in the α_j^* directions, and the Q_{ij}^* are the shear forces.

2.6   Hamilton's Principle

There are several ways in which we can derive Lagrange's equations, such as the generalized principle of d'Alembert and using Hamilton's principle. Hamilton's principle is a minimiza-
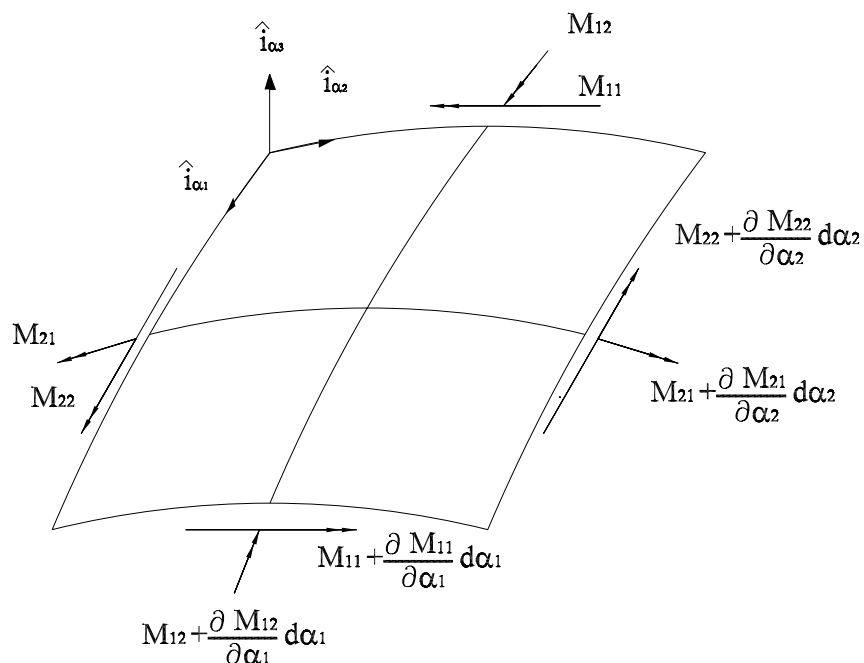
Figure 2.3: Moment resultants in shell coordinates.

tion principle, which seems to apply to all problems of mechanics and most classical physics. It states that, while there are more than one path along which a dynamic system may move from one point to another in space and time, the system actually follows the path that minimizes the time integral of the difference between the kinetic and potential energies. In the derivation of the equations of motion using Hamilton's principle, there are two steps that must be done. First, one uses integration by parts to eliminate the generalized virtual velocities. Second, one sets the coefficients of the generalized virtual displacements equal to zero. The mathematical version of this principle, developed by Euler and Bernoulli in the eighteenth century, can be written as

$$\delta \int_{t_0}^{t_1} (U - K - E_L - E_B)dt = 0 \qquad \delta \bar{r}_i = 0 \qquad (2.83)$$

where the $\delta \bar{r}_i$ are variations of the displacement and δ is the variational symbol, which is treated mathematically like a differential symbol. Taking the variational operator inside the

integral in Eq. (2.83) leads to

$$\int_{t_0}^{t_1} (\delta U - \delta K - \delta E_L - \delta E_B) dt = 0 \tag{2.84}$$

We start with δK from Eq. (2.80); that is,

$$\int_{t_0}^{t_1} \delta K \, dt = \rho h \int_{t_0}^{t_1} \int_{\alpha_1} \int_{\alpha_2} \left[\dot{u}_1 \delta \dot{u}_1 + \dot{u}_2 \delta \dot{u}_2 + \dot{u}_3 \delta \dot{u}_3 + \frac{h^2}{12} (\dot{\beta}_1 \delta \dot{\beta}_1 + \dot{\beta}_2 \delta \dot{\beta}_2) \right] A_1 A_2 d\alpha_1 d\alpha_2 dt \tag{2.85}$$

We integrate each term in Eq. (2.85) by parts. As an example,

$$\int_{t_0}^{t_1} \dot{u}_1 \delta \dot{u}_1 dt = [\dot{u}_1 \delta u_1]_{t_0}^{t_1} - \int_{t_0}^{t_1} \ddot{u}_1 \delta u_1 dt \tag{2.86}$$

Knowing that the virtual displacements are zero at t_0 and t_1, we rewrite Eq. (2.85) as

$$\int_{t_0}^{t_1} \delta K \, dt = -\rho h \int_{t_0}^{t_1} \int_{\alpha_1} \int_{\alpha_2} \left[\ddot{u}_1 \delta u_1 + \ddot{u}_2 \delta u_2 + \ddot{u}_3 \delta u_3 + \frac{h^2}{12} (\ddot{\beta}_1 \delta \beta_1 + \ddot{\beta}_2 \delta \beta_2) \right] A_1 A_2 d\alpha_1 d\alpha_2 dt \tag{2.87}$$

Neglecting the influence of the rotatory inertia $\ddot{\beta}_1$ and $\ddot{\beta}_2$ and following the classical Bernoulli-Euler beam theory, we reduce Eq. (2.87) to

$$\int_{t_0}^{t_1} \delta K \, dt = -\rho h \int_{t_0}^{t_1} \int_{\alpha_1} \int_{\alpha_2} [\ddot{u}_1 \delta u_1 + \ddot{u}_2 \delta u_2 + \ddot{u}_3 \delta u_3] A_1 A_2 d\alpha_1 d\alpha_2 dt \tag{2.88}$$

Evaluating the variation of the energy due to the external load δE_L from Eq. (2.81), we have

$$\int_{t_0}^{t_1} \delta E_L dt = \int_{t_0}^{t_1} \int_{\alpha_1} \int_{\alpha_2} (q_1 \delta u_1 + q_2 \delta u_2 + q_3 \delta u_3) A_1 A_2 d\alpha_1 d\alpha_2 dt \tag{2.89}$$

Next, we evaluate variation of the energy due to the boundary energy δE_B from Eq. (2.82) and obtain

$$\int_{t_0}^{t_1} \delta E_B = \int_{t_0}^{t_1} \int_{\alpha_1} (\delta u_2 N_{22}^* + \delta u_1 N_{21}^* + \delta u_3 Q_{23}^* + \delta \beta_2 M_{22}^* + \delta \beta_1 M_{21}^*) A_1 d\alpha_1 dt$$
$$+ \int_{t_0}^{t_1} \int_{\alpha_2} (\delta u_1 N_{11}^* + \delta u_2 N_{12}^* + \delta u_3 Q_{13}^* + \delta \beta_1 M_{11}^* + \delta \beta_1 M_{12}^*) A_2 d\alpha_2 dt \tag{2.90}$$

Finally, we evaluate the integral of the variation of the strain energy δU from Eq. (2.77) and obtain

$$\int_{t_0}^{t_1} \delta U\, dt = \int_{t_0}^{t_1} \int_{\alpha_1} \int_{\alpha_2} \int_{\alpha_3} \delta F\, dV\, dt \tag{2.91}$$

where

$$F = \frac{1}{2}\left(\sigma_{11}\varepsilon_{11} + \sigma_{22}\varepsilon_{22} + \sigma_{12}\varepsilon_{12} + \sigma_{13}\varepsilon_{13} + \sigma_{23}\varepsilon_{23}\right) \tag{2.92}$$

Applying the differential operator and using the chain rule on F leads to

$$\delta F = \frac{\partial F}{\partial \varepsilon_{11}}\delta\varepsilon_{11} + \frac{\partial F}{\partial \varepsilon_{22}}\delta\varepsilon_{22} + \frac{\partial F}{\partial \varepsilon_{12}}\delta\varepsilon_{12} + \frac{\partial F}{\partial \varepsilon_{13}}\delta\varepsilon_{13} + \frac{\partial F}{\partial \varepsilon_{23}}\delta\varepsilon_{23} \tag{2.93}$$

Expanding the first term in Eq. (2.93) yields,

$$\frac{\partial F}{\partial \varepsilon_{11}}\delta\varepsilon_{11} = \frac{1}{2}\left(\frac{\partial \sigma_{11}}{\partial \varepsilon_{11}}\varepsilon_{11} + \sigma_{11} + \frac{\partial \sigma_{22}}{\partial \varepsilon_{11}}\varepsilon_{22}\right)\delta\varepsilon_{11} \tag{2.94}$$

Considering the Love simplification $\sigma_{33}=0$ and solving for the stresses in the generalized Hooke law gives

$$\sigma_{11} = \frac{E}{1-\nu^2}(\varepsilon_{11} + \nu\varepsilon_{22}) \tag{2.95}$$

$$\sigma_{22} = \frac{E}{1-\nu^2}(\varepsilon_{22} + \nu\varepsilon_{11}) \tag{2.96}$$

$$\sigma_{12} = G\varepsilon_{12} \tag{2.97}$$

Substituting Eqs. (2.95)-(2.97) into Eq. (2.94) gives

$$\frac{\partial F}{\partial \varepsilon_{11}}\delta\varepsilon_{11} = \sigma_{11}\delta\varepsilon_{11} \tag{2.98}$$

Thus, Eq. (2.91) can be written as

$$\int_{t_0}^{t_1} \delta U\, dt = \int_{t_0}^{t_1} \int_{\alpha_1} \int_{\alpha_2} \int_{\alpha_3} \left(\sigma_{11}\delta\varepsilon_{11} + \sigma_{22}\delta\varepsilon_{22} + \sigma_{12}\delta\varepsilon_{12} + \sigma_{13}\delta\varepsilon_{13} + \sigma_{23}\delta\varepsilon_{23}\right)$$
$$\times A_1 A_2 \left(1 + \frac{\alpha_3}{R_1}\right)\left(1 + \frac{\alpha_3}{R_2}\right) d\alpha_1 d\alpha_2 d\alpha_3\, dt \tag{2.99}$$

Now, we substitute the Love and Timoshenko strain-displacement equations, Eqs. (2.54)-(2.56), into Eqs. (2.95)-(2.97) and obtain

$$\sigma_{11} = \frac{E}{1 - \nu^2}\left[\epsilon_{11} + \nu\epsilon_{22} + \alpha_3(\kappa_{11} + \nu\kappa_{22})\right] \tag{2.100}$$

$$\sigma_{22} = \frac{E}{1 - \nu^2}\left[\epsilon_{22} + \nu\epsilon_{11} + \alpha_3(\kappa_{22} + \nu\kappa_{11})\right] \tag{2.101}$$

$$\sigma_{12} = G(\epsilon_{12} + \alpha_3\tau) \tag{2.102}$$

The total force acting on an element $d\alpha_2$ in the α_1 direction can be expressed as

$$\int_{\alpha_3=-h/2}^{\alpha_3=h/2} \sigma_{11}A_2\left(1 + \frac{\alpha_3}{R_2}\right)d\alpha_2 d\alpha_3 \tag{2.103}$$

Hence, the force per unit length N_{11} acting on the A_2 surface can be expressed as

$$N_{11} = \int_{-h/2}^{h/2} \sigma_{11}A_2\left(1 + \frac{\alpha_3}{R_2}\right)d\alpha_3 \tag{2.104}$$

Neglecting the term $\frac{\alpha_3}{R_2}$ in Eq. (2.104) yields

$$N_{11} = \int_{-h/2}^{h/2} \sigma_{11}A_2 d\alpha_3 \tag{2.105}$$

Substituting Eq. (2.100) into Eq. (2.105) gives

$$N_{11} = \bar{K}(\epsilon_{11} + \nu\epsilon_{22}) \tag{2.106}$$

where the membrane stiffness $\bar{K}$ can be written as

$$\bar{K} = \frac{Eh}{1 - \nu^2} \tag{2.107}$$

Similarly, one can write N_{22} and N_{12} as

$$N_{22} = \bar{K}(\epsilon_{22} + \nu\epsilon_{11}) \tag{2.108}$$

$$N_{12} = N_{21} = \frac{1}{2}\bar{K}(1 - \nu)\epsilon_{12} \tag{2.109}$$

The total bending moments acting on an element $d\alpha_2$ in the α_1 direction is

$$\int_{\alpha_3=-h/2}^{\alpha_3=h/2} \sigma_{11}\alpha_3 A_2 \left(1 + \frac{\alpha_3}{R_2}\right) d\alpha_2 d\alpha_3 \tag{2.110}$$

Hence, the total bending moment per unit length M_{11} acting on the A_2 surface is

$$M_{11} = \int_{-h/2}^{h/2} \sigma_{11}\alpha_3 A_2 \left(1 + \frac{\alpha_3}{R_2}\right) d\alpha_3 \tag{2.111}$$

Neglecting the terms containing $\frac{\alpha_3}{R_2}$ in Eq. (2.111) gives

$$M_{11} = \int_{-h/2}^{h/2} \sigma_{11}\alpha_3 A_2 d\alpha_3 \tag{2.112}$$

Substituting Eq. (2.100) into Eq. (2.112) yields,

$$M_{11} = D(\kappa_{11} + \nu\kappa_{22}) \tag{2.113}$$

where D is the bending rigidity, which can be expressed as

$$D = \frac{Eh^3}{12(1 - \nu^2)} \tag{2.114}$$

Similarly, one can write M_{22} and M_{12} as

$$M_{22} = D(\kappa_{22} + \nu\kappa_{11}) \tag{2.115}$$

$$M_{12} = M_{21} = \frac{1}{2}D(1 - \nu)\kappa_{12} \tag{2.116}$$

The transverse shear forces are

$$Q_{13} = \int_{-h/2}^{h/2} \sigma_{13} d\alpha_3 \tag{2.117}$$

$$Q_{23} = \int_{-h/2}^{h/2} \sigma_{23} d\alpha_3 \tag{2.118}$$

Using Eqs. (2.106), (2.108), (2.109), (2.113), (2.115), and (2.116) to solve for the strains and substituting the results into Eqs. (2.100)-(2.102) gives

$$\sigma_{11} = \frac{N_{11}}{h} + \frac{12M_{11}}{h^3}\alpha_3 \tag{2.119}$$

$$\sigma_{22} = \frac{N_{22}}{h} + \frac{12M_{22}}{h^3}\alpha_3 \tag{2.120}$$

$$\sigma_{12} = \frac{N_{12}}{h} + \frac{12M_{12}}{h^3}\alpha_3 \tag{2.121}$$

Next, we neglect the terms α_3/R_1 and α_3/R_2, substitute the Love and Timoshenko strain-displacement relations into Eq. (2.99), and integrate the result with respect to α_3. The first term in the resulting equation is

$$\int_{t_0}^{t_1} \int_{\alpha_1} \int_{\alpha_2} \int_{\alpha_3} \sigma_{11}\delta\varepsilon_{11}A_1A_2 \, d\alpha_1 \, d\alpha_2 \, d\alpha_3 \, dt =$$
$$\int_{t_0}^{t_1} \int_{\alpha_1} \int_{\alpha_2} \int_{\alpha_3} \left[\sigma_{11}\left(A_2\frac{\partial(\delta u_1)}{\partial\alpha_1} + \delta u_2\frac{\partial A_1}{\partial\alpha_2} + \frac{A_1A_2}{R_1}\delta u_3 \right) + \alpha_3\sigma_{11}\left(A_2\frac{\partial(\delta\beta_2)}{\partial\alpha_1} + \delta\beta_2\frac{\partial A_1}{\partial\alpha_2} \right) \right]$$
$$\cdot \, d\alpha_1 \, d\alpha_2 \, d\alpha_3 \, dt \tag{2.122}$$

Substituting Eqs. (2.106) and (2.113) into Eq. (2.122) gives

$$\int_{t_0}^{t_1} \int_{\alpha_1} \int_{\alpha_2} \int_{\alpha_3} \sigma_{11}\delta\varepsilon_{11}A_1A_2 \, d\alpha_1 \, d\alpha_2 \, d\alpha_1 \, dt =$$
$$\int_{t_0}^{t_1} \int_{\alpha_1} \int_{\alpha_2} \left[N_{11}\left(A_2\frac{\partial(\delta u_1)}{\partial\alpha_1} + \delta u_2\frac{\partial A_1}{\partial\alpha_2} + \frac{A_1A_2}{R_1}\delta u_3 \right) + M_{11}\left(A_2\frac{\partial(\delta\beta_1)}{\partial\alpha_1} + \delta\beta_2\frac{\partial A_1}{\partial\alpha_2} \right) \right]$$
$$\cdot \, d\alpha_1 \, d\alpha_2 \, dt \tag{2.123}$$

Integrating the first term by parts leads to

$$\int_{\alpha_1} \int_{\alpha_2} N_{11}A_2\alpha_1\frac{\partial(\delta u_1)}{\partial\alpha_1}d\alpha_1 \, d\alpha_2 = \int_{\alpha_2} N_{11}A_2\delta u_1 d\alpha_2 - \int_{\alpha_1} \int_{\alpha_2} \frac{\partial(N_{11}A_2)}{\partial\alpha_1}\delta u_1 \, d\alpha_1 \, d\alpha_2 \tag{2.124}$$

Integrating by parts all of the terms in Eq. (2.99) gives

$$
\begin{aligned}
\int_{t_0}^{t_1} \delta U \, dt = \int_{t_0}^{t_1} \int_{\alpha_1} \int_{\alpha_2} & \left[\left(-\frac{\partial(N_{11}A_2)}{\partial\alpha_1} - \frac{\partial(N_{21}A_1)}{\partial\alpha_2} - N_{12}\frac{\partial A_1}{\partial\alpha_2} + N_{22}\frac{\partial A_2}{\partial\alpha_1} - Q_{13}\frac{A_1 A_2}{R_1} \right) \delta u_1 \right. \\
& + \left(-\frac{\partial(N_{12}A_2)}{\partial\alpha_1} - \frac{\partial(N_{22}A_1)}{\partial\alpha_2} + N_{11}\frac{\partial A_1}{\partial\alpha_2} - N_{21}\frac{\partial A_2}{\partial\alpha_1} - Q_{23}\frac{A_1 A_2}{R_2} \right) \delta u_2 \\
& + \left(N_{11}\frac{A_1 A_2}{R_1} + N_{22}\frac{A_1 A_2}{R_2} - \frac{\partial(Q_{13}A_2)}{\partial\alpha_1} - \frac{\partial(Q_{23}A_1)}{\partial\alpha_2} \right) \delta u_3 \\
& + \left(-\frac{\partial(M_{21}A_1)}{\partial\alpha_2} - M_{12}\frac{\partial A_1}{\partial\alpha_2} + M_{22}\frac{\partial A_2}{\partial\alpha_1} - \frac{\partial(M_{11}A_2)}{\partial\alpha_1} + Q_{13}A_1 A_2 \right) \delta\beta_1 \\
& + \left. \left(-\frac{\partial(M_{12}A_2)}{\partial\alpha_1} - M_{21}\frac{\partial A_2}{\partial\alpha_1} + M_{11}\frac{\partial A_1}{\partial\alpha_2} - \frac{\partial(M_{22}A_1)}{\partial\alpha_2} + Q_{23}A_1 A_2 \right) \delta\beta_2 \right] d\alpha_1 d\alpha_2 dt \\
& + \int_{t_0}^{t_1} \int_{\alpha_2} \left(N_{11}\delta u_1 + M_{11}\delta\beta_1 + N_{12}\delta u_2 + M_{12}\delta\beta_2 + Q_{13}\delta u_3 \right) A_2 \, d\alpha_2 dt \\
& + \int_{t_0}^{t_1} \int_{\alpha_1} \left(N_{22}\delta u_2 + M_{22}\delta\beta_2 + N_{21}\delta u_1 + M_{21}\delta\beta_1 + Q_{23}\delta u_2 \right) A_1 \, d\alpha_1 dt
\end{aligned}
$$

$$(2.125)$$

Substituting Eqs. (2.79) and (2.88)-(2.90) into Eq. (2.125) gives

$$
\begin{aligned}
\int_{t_0}^{t_1} \int_{\alpha_1} \int_{\alpha_2} &\left[\left(\frac{\partial(N_{11}A_2)}{\partial\alpha_1} + \frac{\partial(N_{21}A_1)}{\partial\alpha_2} + N_{12}\frac{\partial A_1}{\partial\alpha_2} - N_{22}\frac{\partial A_2}{\partial\alpha_1} + Q_{13}\frac{A_1A_2}{R_1} \right.\right. \\
&+ (q_1 - \rho h\ddot{u}_1)A_1A_2 \bigg)\delta u_1 + \left(\frac{\partial(N_{12}A_2)}{\partial\alpha_1} + \frac{\partial(N_{22}A_1)}{\partial\alpha_2} - N_{11}\frac{\partial A_1}{\partial\alpha_2} + N_{21}\frac{\partial A_2}{\partial\alpha_1} \right. \\
&+ Q_{23}\frac{A_1A_2}{R_2} + (q_2 - \rho h\ddot{u}_2)A_1A_2 \bigg)\delta u_2 \\
&+ \left(-N_{11}\frac{A_1A_2}{R_1} - N_{22}\frac{A_1A_2}{R_2} + \frac{\partial(Q_{13}A_2)}{\partial\alpha_1} + \frac{\partial(Q_{23}A_1)}{\partial\alpha_2} + (q_3 - \rho h\ddot{u}_3)A_1A_2 \right)\delta u_3 \\
&+ \left(\frac{\partial(M_{21}A_1)}{\partial\alpha_2} + M_{12}\frac{\partial A_1}{\partial\alpha_2} - M_{22}\frac{\partial A_2}{\partial\alpha_1} + \frac{\partial(M_{11}A_2)}{\partial\alpha_1} - Q_{13}A_1A_2 \right)\delta\beta_1 \\
&+ \left(\frac{\partial(M_{12}A_2)}{\partial\alpha_1} + M_{21}\frac{\partial A_2}{\partial\alpha_1} - M_{11}\frac{\partial A_1}{\partial\alpha_2} + \frac{\partial(M_{22}A_1)}{\partial\alpha_2} - Q_{23}A_1A_2 \right)\delta\beta_2 \bigg] d\alpha_1 d\alpha_2 dt \\
&+ \int_{t_0}^{t_1} \int_{\alpha_2} \left[(N_{11}^* - N_{11})\delta u_1 + (M_{11}^* - M_{11})\delta\beta_1 + (N_{12}^* - N_{12})\delta u_2 + (M_{12}^* - M_{12})\delta\beta_2 \right. \\
&+ (Q_{13}^* - Q_{13})\delta u_3 \bigg] A_2 d\alpha_2 dt + \int_{t_0}^{t_1} \int_{\alpha_1} \left[(N_{22}^* - N_{22})\delta u_2 + (M_{22}^* - M_{22})\delta\beta_2 + (N_{21}^* - N_{21})\delta u_1 \right. \\
&+ (M_{21}^* - M_{21})\delta\beta_1 + (Q_{23}^* - Q_{23})\delta u_2 \bigg] A_1 d\alpha_1 dt
\end{aligned}
$$

$$(2.126)$$

To satisfy Eq. (2.126) requires that each double and triple integral must equal to zero individually. Also, each integral equation can not be satisfied unless the coefficients of the variational displacement are zero. Setting the triple integrals equal to zero gives

$$\frac{\partial(N_{11}A_2)}{\partial\alpha_1} + \frac{\partial(N_{21}A_1)}{\partial\alpha_2} + N_{12}\frac{\partial A_1}{\partial\alpha_2} - N_{22}\frac{\partial A_2}{\partial\alpha_1} + Q_{13}\frac{A_1A_2}{R_1} + (q_1 - \rho h\ddot{u}_1)A_1A_2 = 0 \quad (2.127)$$

$$\frac{\partial(N_{12}A_2)}{\partial\alpha_1} + \frac{\partial(N_{22}A_1)}{\partial\alpha_2} - N_{11}\frac{\partial A_1}{\partial\alpha_2} + N_{21}\frac{\partial A_2}{\partial\alpha_1} + Q_{23}\frac{A_1A_2}{R_2} + (q_2 - \rho h\ddot{u}_2)A_1A_2 = 0 \quad (2.128)$$

$$-N_{11}\frac{A_1A_2}{R_1} - N_{22}\frac{A_1A_2}{R_2} + \frac{\partial(Q_{13}A_2)}{\partial\alpha_1} + \frac{\partial(Q_{23}A_1)}{\partial\alpha_2} + (q_3 - \rho h\ddot{u}_3)A_1A_2 = 0 \qquad (2.129)$$

$$\frac{\partial(M_{21}A_1)}{\partial\alpha_2} + M_{12}\frac{\partial A_1}{\partial\alpha_2} - M_{22}\frac{\partial A_2}{\partial\alpha_1} + \frac{\partial(M_{11}A_2)}{\partial\alpha_1} - Q_{13}A_1A_2 = 0 \qquad (2.130)$$

$$\frac{\partial(M_{12}A_2)}{\partial\alpha_1} + M_{21}\frac{\partial A_2}{\partial\alpha_1} - M_{11}\frac{\partial A_1}{\partial\alpha_2} + \frac{\partial(M_{22}A_1)}{\partial\alpha_2} - Q_{23}A_1A_2 = 0 \qquad (2.131)$$

Equations (2.127)-(2.131) are known as Love's equations; they define the motion of a shell due to any type of load. These equations of motion can be also obtained by taking a differential element of the shell having a thickness h and set the summation of the forces, Fig. 2.2, and summation of the moments, Fig. 2.3, equal to zero. Summation of the forces gives the first three equations of motion, Eqs. (2.127)-(2.129), while summation of the moments in the α_1 and α_2 directions leads to the remaining two equations, Eqs. (2.130) and (2.131).

2.7   Shallow Shell Theory

A shallow shell can be defined as a slightly curved plate or a shell whose smallest radius of curvature at every point is large compared with the greatest length measured along the middle surface of the shell. In shallow shell theory, the terms Q_{13} and Q_{23} are neglected, the tangential loads q_1 and q_2 are zero, only the transverse load $q_3 \neq 0$, and the tangentional accelerations $\ddot{u}_1$ and $\ddot{u}_2$ are neglected.

2.8   Classical Laminate Theory

The classical laminate theory is based on the following assumptions:

1. The layers are perfectly bonded together.

2. The material of each layer is linearly elastic.

3. The material has two planes of material symmetry (orthotropic).

4. The strains and displacements are small.

5. The transverse shear stresses on the top and bottom surfaces are zero.

Chapter 3

Response of a Shallow Shell to a Primary Resonance

We consider nonlinear forced vibrations of a doubly curved cross-ply laminated shallow shell with simply supported boundary conditions. We investigate its response to a primary resonance of its fundamental mode (i.e., $\Omega \approx \omega_{11}$). The nonlinear partial-differential equations governing the motion of the shell are based on the von Kármán-type geometric nonlinear theory and the first-order shear-deformation theory.

Due to the complexity of the nonlinear partial-differential equations, relatively a limited number of papers has been presented on the nonlinear vibrations of doubly curved shells. A common approach for analyzing the problem is to use the Galerkin method. Accordingly, the weighted functions are chosen as the eigenfunctions of the linearized problem. In particular, if the shell is excited near the natural frequency of a specific linear mode, only that mode is used in the analysis. Such an approach is referred to as a single-mode discretization. Using such an approach may lead to quantitative and in some cases qualitative errors in the predicted response.

An approximation based on the Galerkin method is used to reduce the partial-differential
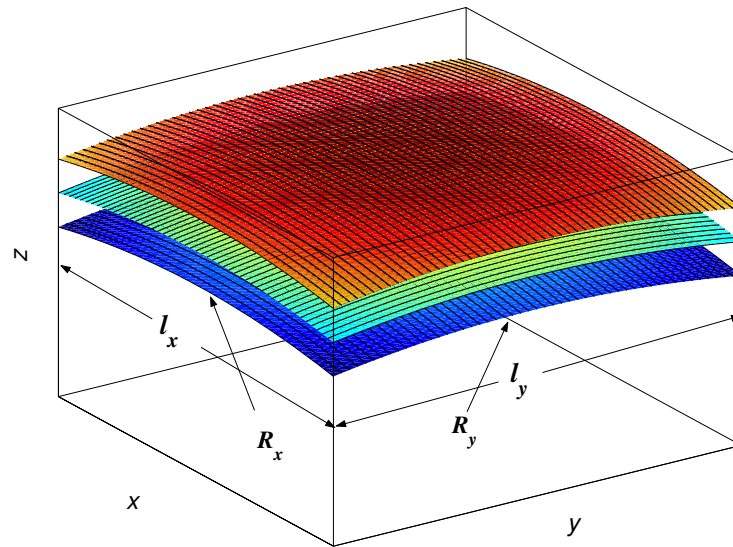
Figure 3.1: A doubly curved shell with three layers ($k = 3$).

equations of motion and associated boundary conditions to an infinite system of nonlinearly coupled second-order ordinary-differential equations. These equations are solved by using the method of multiple scales. Numerical results for isotropic and single-layered shells are obtained. The influence of the number of modes retained in the discretization on the predicted shell response is investigated. We found that symmetric modes do not have any effect on the predicted response for the case of primary resonance of the fundamental mode of vibration. It is shown that using a single-mode approximation can lead to quantitatively and in some cases to qualitatively erroneous results. A multi-mode approximation that includes as many modes as needed for convergence is used to study the shell responses. Furthermore, we identify the regions in the parameter space in which the nonlinearity of the shell is of the hardening or softening type as well as the regions in which two-to-one internal resonances may be activated.

3.1 Formulation

The equations of motion for the doubly curved cross-ply shallow shell, shown in Fig. 3.1, in Cartesian coordinates are obtained from Eqs. (2.127)-(2.131) by changing the transverse displacement u_3 to w, changing the shell coordinates α_1 and α_2 to x and y, setting the shell curvatures as $k_x = 1/R_x$ and $k_y = 1/R_y$, changing the forces N_{11}, N_{12}, and N_{22} to N_x, N_{xy}, and N_y, changing the moments M_{11}, M_{12}, and M_{22} to M_x, M_{xy}, and M_y, and setting $A_1 = A_2 = 1$. Furthermore, for a shallow shell, $N_{12} = N_{21}$ and $M_{12} = M_{21}$. Also, the terms Q_{13} and Q_{23} are neglected and the tangential accelerations $\ddot{u}_1$ and $\ddot{u}_2$ are set equal to zero. Substituting these quantities into the equations of motion leads to

$$\frac{\partial N_x}{\partial x} + \frac{\partial N_{xy}}{\partial y} = 0 \tag{3.1}$$

$$\frac{\partial N_{xy}}{\partial x} + \frac{\partial N_y}{\partial y} = 0 \tag{3.2}$$

$$\frac{\partial}{\partial x}\left(N_x \frac{\partial w}{\partial x} + N_{xy}\frac{\partial w}{\partial y}\right) + \frac{\partial}{\partial y}\left(N_{xy}\frac{\partial w}{\partial x} + N_y \frac{\partial w}{\partial y}\right) + \frac{\partial^2 M_x}{\partial x^2} + \frac{\partial^2 M_y}{\partial y^2} + 2\frac{\partial^2 M_y}{\partial y \partial x}$$
$$- k_x N_x - k_y N_y = \rho h \frac{\partial^2 w}{\partial t^2} + C\frac{\partial w}{\partial t} + F\cos(\Omega t) \tag{3.3}$$

where ρ is the mass density and C is the linear viscous damping coefficient. The moment resultants are related to the transverse displacement $w(x,y,t)$ for cross-ply composites by (Reddy, 1997)

$$\begin{bmatrix} M_x \\ \\ M_y \\ \\ M_{xy} \end{bmatrix} = - \begin{bmatrix} D_{11} & D_{12} & D_{16} \\ \\ D_{12} & D_{22} & D_{26} \\ \\ D_{16} & D_{26} & D_{66} \end{bmatrix} \begin{bmatrix} \frac{\partial^2 w}{\partial x^2} \\ \\ \frac{\partial^2 w}{\partial y^2} \\ \\ 2\frac{\partial^2 w}{\partial y \partial x} \end{bmatrix} \tag{3.4}$$

For a cross-ply laminate composed of k layers which are symmetrically distributed about the midplane,

$$D_{ij} = \frac{1}{3}\sum_{k=1}^{N} Q_{ij}^k (z_{k+1}^3 - z_k^3) \tag{3.5}$$

where

$$Q_{11}^k = \frac{E_1^k}{1 - \nu_{12}^k \nu_{21}^k}, \quad Q_{12}^k = \frac{\nu_{21}^k E_1^k}{1 - \nu_{12}^k \nu_{21}^k},$$

$$Q_{22}^k = \frac{E_2^k}{1 - \nu_{12}^k \nu_{21}^k}, \quad Q_{16}^k = Q_{26}^k = 0,$$

$$Q_{66}^k = G_{12}^k, \quad Q_{44}^k = G_{23}^k, \quad Q_{55}^k = G_{13}^k \tag{3.6}$$

We introduce the stress function $\Phi(x, y, t)$ such that

$$N_x = \Phi_{yy}, \quad N_y = \Phi_{xx}, \quad N_{xy} = -\Phi_{xy} \tag{3.7}$$

As a result, Eqs. (3.1) and (3.2) are satisfied exactly and Eq. (3.3) becomes

$$D_{11} \frac{\partial^4 w}{\partial x^4} + 2(D_{12} + 2D_{66}) \frac{\partial^4 w}{\partial y^2 \partial x^2} + D_{22} \frac{\partial^4 w}{\partial y^4} + k_x \frac{\partial^2 \Phi}{\partial y^2} + k_y \frac{\partial^2 \Phi}{\partial x^2} + C \frac{\partial w}{\partial t} + \rho h \frac{\partial^2 w}{\partial t^2}$$

$$= \frac{\partial^2 \Phi}{\partial y^2} \frac{\partial^2 w}{\partial x^2} + \frac{\partial^2 \Phi}{\partial x^2} \frac{\partial^2 w}{\partial y^2} - 2 \frac{\partial^2 \Phi}{\partial y \partial x} \frac{\partial^2 w}{\partial y \partial x} + F \cos(\Omega t) \tag{3.8}$$

A second equation is obtained from the compatibility conditions for cross-ply shells as (Bogdanovich, 1990)

$$-K_{11} \frac{\partial^4 \Phi}{\partial x^4} - (2K_{12} + K_{66}) \frac{\partial^4 \Phi}{\partial y^2 \partial x^2} - K_{22} \frac{\partial^4 \Phi}{\partial y^4} + k_x \frac{\partial^2 w}{\partial y^2} + k_y \frac{\partial^2 w}{\partial x^2}$$

$$= -\left(\frac{\partial^2 w}{\partial y \partial x} \right)^2 + \frac{\partial^2 w}{\partial x^2} \frac{\partial^2 w}{\partial y^2} \tag{3.9}$$

where

$$[K]_{ij} = [A]_{ij}^{-1} \quad \text{and} \quad A_{ij} = \sum_{k=1}^{N} Q_{ij}^k (z_{k+1} - z_k) \tag{3.10}$$

We nondimensionalize the governing equations using the following:

$$\hat{w} = \frac{w}{h} \ , \ \hat{x} = \frac{x}{l_x} \ , \ \hat{y} = \frac{y}{l_y} \ , \ \hat{\Omega} = l_x^2 \sqrt{\frac{\rho h}{D^*}} \Omega,$$

$$D^* = \frac{E_2 h^3}{12(1 - \nu_{12}\nu_{21})} \ , \ \hat{t} = \frac{1}{l_x^2} \sqrt{\frac{D^*}{\rho h}} t,$$

$$\hat{\Phi} = \Phi D^*, \quad \hat{F} = -\frac{l_x^4}{D^* h} F \ , \ \hat{C} = \frac{l_x^4}{D^* h} C \tag{3.11}$$

where l_x and l_y are the shell lengths in the x and y directions, respectively. In what follows, we drop the hat for convenience.

Using the Galerkin procedure, we express the transverse displacement and the stress function in the form

$$w = \sum_{m=1}^{\infty} \sum_{n=1}^{\infty} \sin(n\pi x) \sin(m\pi y) \, W_{nm}(t) \tag{3.12}$$

$$\Phi = \sum_{m=1}^{\infty} \sum_{n=1}^{\infty} \sin(n\pi x) \sin(m\pi y) \, \Phi_{nm}(t) \tag{3.13}$$

which satisfies the boundary conditions. The first four antisymmetric modes are shown in Fig 3.2. Substituting Eqs. (3.12) and (3.13) into Eqs. (3.8) and (3.9), multiplying the resulting equations by $\sin(\eta\pi x)\sin(\nu\pi y)$, and integrating over the domain, we obtain the following system of nonlinear ordinary-differential equations:

$$\Phi_{\eta\nu}(t) = \frac{A2_{\eta\nu}}{A1_{\eta\nu}} W_{\eta\nu}(t) + \frac{A3}{A1_{\eta\nu}} \sum_{n,m}^{\infty} \sum_{l,j}^{\infty} \left(nlmj\bar{G}_{\eta\nu nmlj} - n^2 j^2 G_{\eta\nu nmlj} \right) \cdot W_{nm}(t) W_{lj}(t) \tag{3.14}$$

$$C1_{\eta\nu} W_{\eta\nu}(t) + C2_{\eta\nu} \Phi_{\eta\nu}(t) + C3_{\eta\nu} \dot{W}_{\eta\nu}(t) + C4 \ddot{W}_{\eta\nu}(t) + C5$$
$$\cdot \sum_{n,m}^{\infty} \sum_{l,j}^{\infty} \left[\left(n^2 j^2 + m^2 l^2 \right) G\eta\nu nmlj - 2mnlj\bar{G}_{\eta\nu nmlj} \right] W_{nm}(t) \Phi_{lj}(t) = F_{\eta\nu} \cos(\Omega t) \tag{3.15}$$

where the $A's$ and the $C's$ are defined in Appendix A. Using Eq. (3.14) to eliminate the $\Phi_{\eta\nu}(t)$ from Eq. (3.15), we obtain

$$\ddot{W}_{\eta\nu} + 2\mu_{\eta\nu} \dot{W}_{\eta\nu} + \omega_{\eta\nu}^2 W_{\eta\nu} + \sum_{n,m=1}^{\infty} \sum_{l,j=1}^{\infty} P_{\eta\nu nmlj} W_{nm} W_{lj}$$
$$+ \sum_{n,m=1}^{\infty} \sum_{l,j=1}^{\infty} \sum_{p,q=1}^{\infty} \sum_{r,s=1}^{\infty} S_{\eta\nu nmljpqrs} W_{nm} W_{rs} W_{pq} = F_{\eta\nu} \cos(\Omega t) \tag{3.16}$$

where the $P_{\eta\nu nmlj}$ and $S_{\eta\nu nmljpqrs}$ are given in Appendix A.
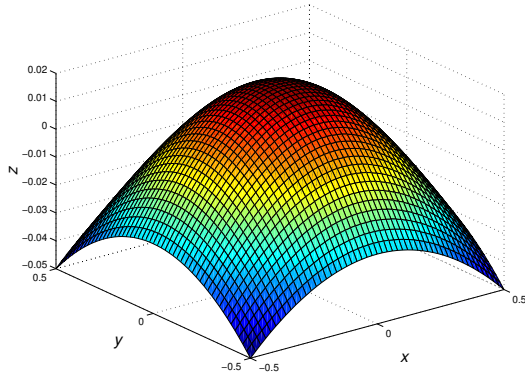
(a) First mode $n = 1$ and $m = 1$
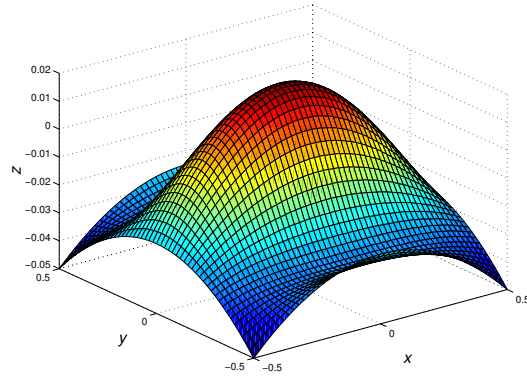
(b) Second mode $n = 3$ and $m = 1$
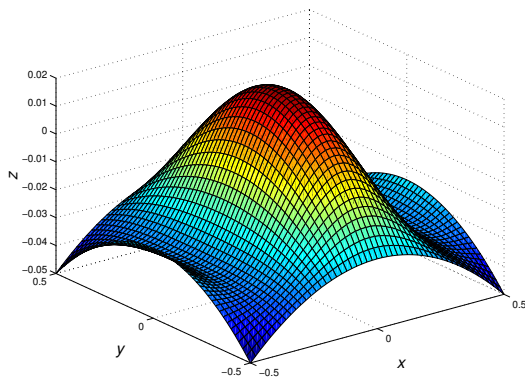
(c) Third mode $n = 1$ and $m = 3$
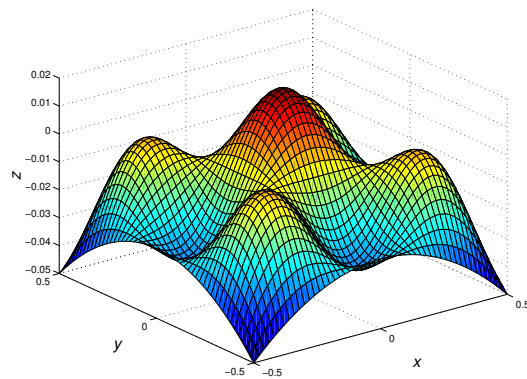
(d) Fourth mode $n = 3$ and $m = 3$

Figure 3.2: The first four antisymmetric mode shapes for a doubly curved shallow shell with $k_x = 0.1$, $k_y = 0.1$, $l_x = 1$, and $l_y = 1$.

3.2   Perturbation Solution

An approximate solution for the system of weakly nonlinear equations, Eqs. (3.16), can be obtained by a number of perturbation techniques. Here, we use the method of multiple scales (Nayfeh, 1973, 1981). Accordingly, we express the solution in terms of different time scales as

$$W_{11}(t; \epsilon) = \epsilon W_{11}^{(1)}(T_0, T_2) + \epsilon^2 W_{11}^{(2)}(T_0, T_2) + \epsilon^3 W_{11}^{(3)}(T_0, T_2) + \cdots \tag{3.17}$$

$$W_{nm}(t; \epsilon) = \epsilon^2 W_{nm}^{(2)}(T_0, T_2) + \cdots, \quad n, m \neq 1 \tag{3.18}$$

where $T_0 = t$ and $T_2 = \epsilon^2 t$. Because in the presence of damping the homogeneous solution of every mode that is not directly or indirectly excited by an internal resonance decays with time, the long-time response of the shell does not contain these homogeneous solutions. Therefore, we scale W_{11} at $O(\epsilon)$ and W_{nm} for $n \neq 1$ and $m \neq 1$ at $O(\epsilon^2)$. In the present analysis, we consider the case in which the fundamental mode is not involved in an internal resonance with any other mode.

To express the nearness of the excitation frequency Ω to the fundamental natural frequency ω_{11}, we introduce the detuning parameter σ defined as

$$\Omega = \omega_{11} + \epsilon^2 \sigma \tag{3.19}$$

Furthermore, we scale the damping and the excitation amplitude as

$$\mu_{\eta\nu} \to \epsilon^2 \mu_{\eta\nu} \quad \text{and} \quad F_{\eta\nu} \to \epsilon^3 f_{\eta\nu} \tag{3.20}$$

Substituting Eqs. (3.17)-(3.20) into Eq. (3.16) and equating coefficients of like powers of ϵ, we obtain

Order ϵ^1

$$D_0^2 W_{11}^{(1)} + \omega_{11}^2 W_{11}^{(1)} = 0 \tag{3.21}$$

Order ϵ^2

$$D_0^2 W_{nm}^{(2)} + \omega_{nm}^2 W_{nm}^{(2)} = -P_{nm1111}\left(W_{11}^{(1)}\right)^2 \tag{3.22}$$

Order ϵ^3

$$D_0^2 W_{11}^{(3)} + \omega_{11}^2 W_{11}^{(3)} = -2D_0 D_2 W_{11}^{(1)} - \sum_{n,m=1}^{N,M} P_{11nm11} W_{11}^{(1)} W_{nm}^{(2)} - \sum_{l,k=1}^{N,M} P_{1111lk} W_{lk}^{(2)} W_{11}^{(1)}$$

$$- \sum_{i,j=1}^{N,M} S_{1111ij1111}\left(W_{11}^{(1)}\right)^3 - 2\mu_{11} D_0 W_{11}^{(1)} + f_{11}\cos(\omega_{11}T_0 + \sigma T_2) \tag{3.23}$$

where $D_n = \frac{\partial}{\partial T_n}$. One can show that $P_{\eta\nu nmlk} = 0$ if any of the indices η, ν, n, m, l, k is an even number. Thus, the even modes do not influence the response of the fundamental mode to a primary-resonance excitation.

The solution of Eq. (3.21) can be expressed as

$$W_{11}^{(1)} = a(T_2)\cos\left[\omega_{11}T_0 + \beta(T_2)\right] \tag{3.24}$$

where $a(T_2)$ and $\beta(T_2)$ are determined by eliminating the secular terms from the higher-order approximations. Substituting Eq. (3.24) into Eq. (3.22) and solving for $W_{nm}^{(2)}$ gives

$$W_{nm}^{(2)} = -P_{nm1111}a^2 \left\{ \frac{1}{2(\omega_{nm}^2 - 4\omega_{11}^2)}\cos\left[2\omega_{11}T_0 + 2\beta(T_2)\right] + \frac{1}{2\omega_{nm}^2} \right\} \tag{3.25}$$

Then, substituting Eqs. (3.24) and (3.25) into Eq. (3.23) leads to

$$D_0^2 W_{11}^{(3)} + \omega_{11}^2 W_{11}^{(3)} = 2\omega_{11}a'\sin(\omega_{11}T_0 + \beta) + 2\omega_{11}a\beta'\cos(\omega_{11}T_0 + \beta)$$

$$\left\{ \sum_{i,j}^{N,M}(P_{11ij11} + P_{1111ij})\left[\frac{P_{ij1111}}{8\omega_{11}(\omega_{ij}^2 - 4\omega_{11}^2)} + \frac{P_{ij1111}}{4\omega_{11}\omega_{ij}^2}\right] - \sum_{i,j}^{N,M}\frac{3S_{1111ij11}}{8\omega_{11}} \right\}$$

$$\times \cos(\omega_{11}T_0 + \beta) + 2\mu_{11}\omega_{11}\sin(\omega_{11}T_0 + \beta)$$

$$+ f_{11}\left[\cos\left(\omega_{11}T_0 + \beta\right)\cos\left(\sigma T_2 - \beta\right) - \sin\left(\omega_{11}T_0 + \beta\right)\sin\left(\sigma T_2 - \beta\right)\right] + NST \tag{3.26}$$

where NST stand for nonsecular terms. Eliminating the terms that produce secular terms from Eq. (3.26) yields

$$a' = -\frac{1}{2}\mu_{11}a + \frac{f_{11}}{2\omega_{11}}\sin(\gamma) \tag{3.27}$$

$$2\omega_{11}a\beta' + f\cos(\gamma) + 2\omega_{11}\alpha_e a^3 = 0 \tag{3.28}$$

where α_e is the effective nonlinearity given by

$$\alpha_e = \sum_{i,j}^{N,M} (P_{11ij11} + P_{1111ij}) \left[\frac{P_{ij1111}}{8\omega_{11}(\omega_{ij}^2 - 4\omega_{11}^2)} + \frac{P_{ij1111}}{4\omega_{11}\omega_{ij}^2} \right] - \sum_{i,j}^{N,M} \frac{3S_{1111ij11}}{8\omega_{11}} \tag{3.29}$$

and

$$\gamma = \sigma T_2 - \beta \tag{3.30}$$

Using Eq. (3.30) to eliminate $\beta(T_2)$ from Eq. (3.28) gives

$$a\gamma' = \sigma a + \alpha_e a^3 + \frac{f_{11}}{2\omega_{11}}\cos\gamma \tag{3.31}$$

It follows from Eq. (3.29) that $\alpha_e \to \infty$ if any $\omega_{ij} \to 2\omega_{11}$, which corresponds to a two-to-one internal resonance.

3.3   Numerical Results

Next, we use Eqs. (3.27) and (3.31) to investigate the influence of the number of terms retained in the Galerkin approximation on the accuracy of the calculated response and the effect of the curvatures, k_x and k_y, on the dynamics of simply supported isotropic, single-layered, and multi-layered shallow shells.

3.3.1   Isotropic Shells

We consider an isotropic shell with the following parameters:

$$\nu_{12} = 0.3, \quad l_x = 1, \quad l_y = 1, \quad f = 10,$$
$$E_1 = 21 \times 10^9, \quad \frac{G_{12}}{E_1} = 0.79 \tag{3.32}$$

We start with investigating the influence of the number of terms retained in the approximation on the accuracy of the predicted response. In Fig. 3.3, we show the frequency-response curves obtained for a spherical isotropic shell using 1, 2, 3, 4, and 16-mode approximations. All of the curves are bent to the left, indicating a softening-type nonlinearity. However, the extent of the bending depends on the number N of modes retained in the approximation. Increasing N from 1 to 2 increases the bending of the curve. Increasing N from 2 to 3 also increases the bending of the curve. However, increasing N beyond 4 has a small effect. In fact, the results obtained with $N = 4$ are very close to those obtained with $N = 16$. To get a better picture of the influence of the number of modes retained in the approximation on the effective nonlinearity, we use Eq. (3.29) to calculate the variation of α_e with N; the results are shown in Fig. 3.4. Increasing N from 1 to 2 leads to a change in α_e from -5.2 to -6.3. However, increasing N from 2 to 3 leads to a similar change in α_e from -6.3 to -7.44. Increasing N from 3 to 4 leads to a small change (from -7.44 to -7.56) in α_e, and increasing N to 6 leads to a slight decrease in α_e to -7.58. Increasing N beyond 6 has a negligible effect on α_e. It is clear from Figs. 3.3 and 3.4 that using a one-mode approximation, as usually done, would lead to a quantitative error in the predicted response. Hence, one needs to check the convergence of the predicted results as the number of modes retained in the approximation is increased.

Next, we consider two examples for which low-order Galerkin approximations predict not only quantitatively but also qualitatively erroneous results. In the first example, we consider a cylindrical isotropic shell with the curvatures $k_x = 0$ and $k_y = 0.05588$. It follows from Fig. 3.5 that retaining one mode in the approximations produces a frequency-response curve that is bent to the right, indicating a hardening-type nonlinearity. Retaining two modes in the approximation produces a linear-like frequency-response curve. However, retaining three modes in the approximation yields a frequency-response curve bent to the left, indicating a softening-type nonlinearity. Increasing the number of retained modes further leads only to quantitative rather than qualitative changes in the predicted response. In Fig. 3.6, we show variation of the effective nonlinearity α_e with the number N of retained modes in the
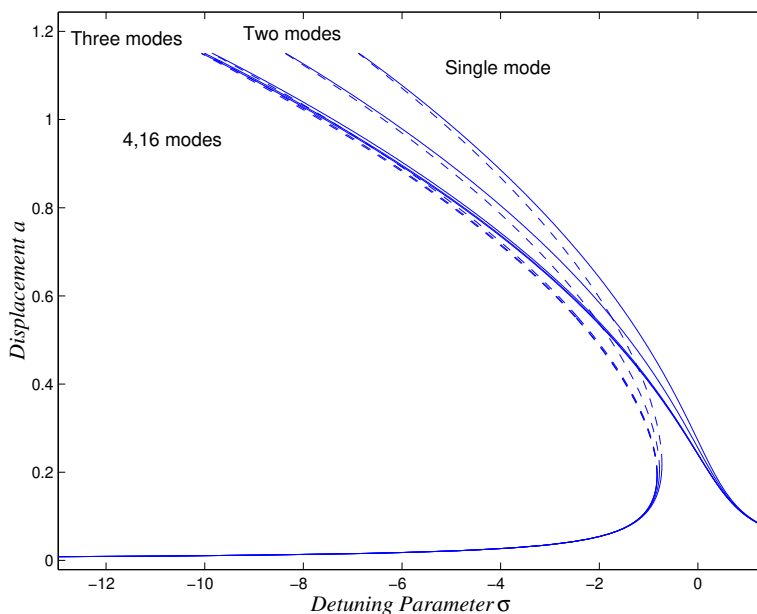
Figure 3.3: Frequency-response curves of an isotropic spherical shell when $k_x = 0.1$ and $k_y = 0.1$.

approximation. When $N = 1$, $\alpha_e > 0$, indicating a hardening-type behavior. When $N = 2$, $\alpha_e \approx 0$, indicating a linear-like behavior. When $N \geq 3$, $\alpha_e < 0$, indicating a softening-type behavior. In fact, $\alpha_e \approx 0$ when $N = 2$ whereas $\alpha_e \approx -0.092$ when $N = 3$ and $\alpha_e \approx -0.106$ when $N = 4$. The value of α_e converges to -0.113 as N approaches 11.

In the second example, we consider a doubly-curved isotropic shell with the curvatures $k_x = -0.2$ and $k_y = 0.2553$. Again, it follows from Fig. 3.7 that retaining one, two, or three modes in the approximation predicts frequency-response curves bent to the right, whereas retaining four or more modes in the approximation predicts frequency-response curves bent to the left. It follows from Fig. 3.8 that α_e changes from 0.006 when $N = 3$ to -0.0075 when $N = 4$. As N increases, the predicted α_e continues to decrease, indicating a softening-type behavior, and finally converges to -0.013 as N approaches 11.

In Figs. 3.9 and 3.10, we show three-dimensional plots of the variation of the effective non-linearity of a doubly curved shell with the curvatures k_x and k_y when using single-mode and
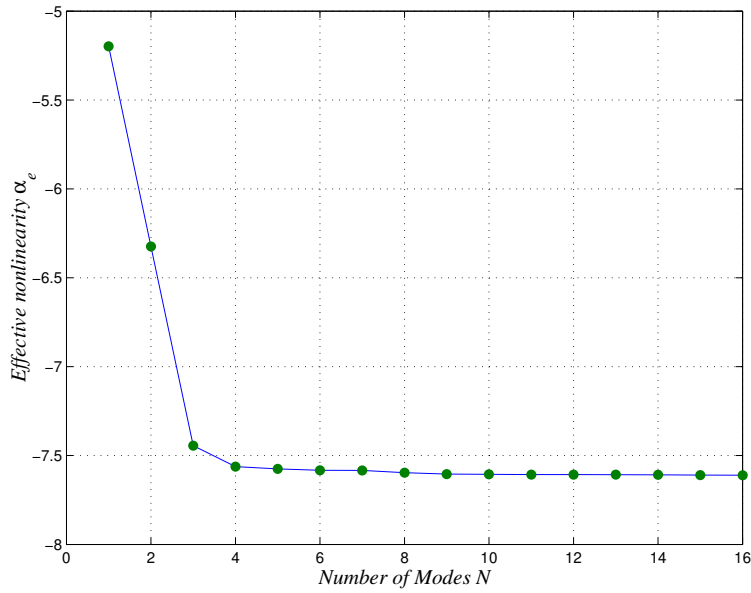
Figure 3.4: Effective nonlinearity for an isotropic spherical when $k_x = 0.1$ and $k_y = 0.1$.
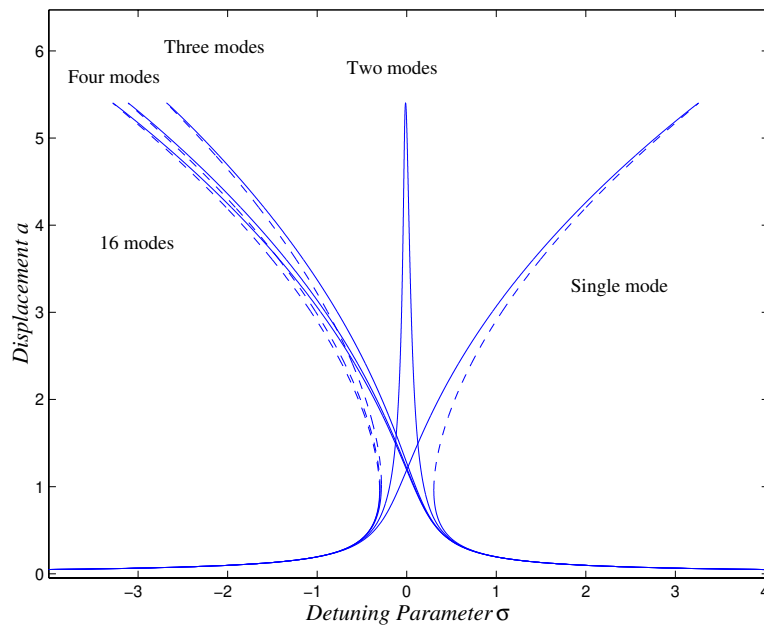
Figure 3.5: Frequency-response curves of an isotropic cylindrical shell when $k_x = 0.0$ and $k_y = 0.05588$.
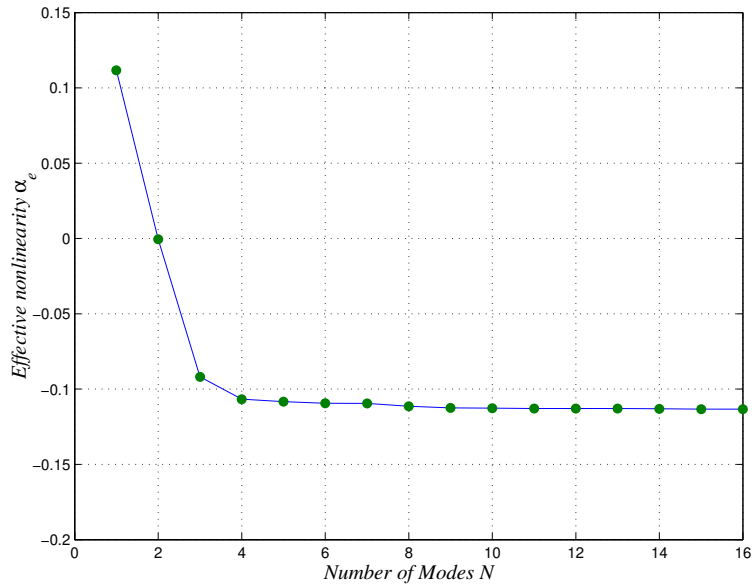
Figure 3.6: Effective nonlinearity for an isotropic cylindrical shell when $k_x = 0.0$ and $k_y = 0.05588$.
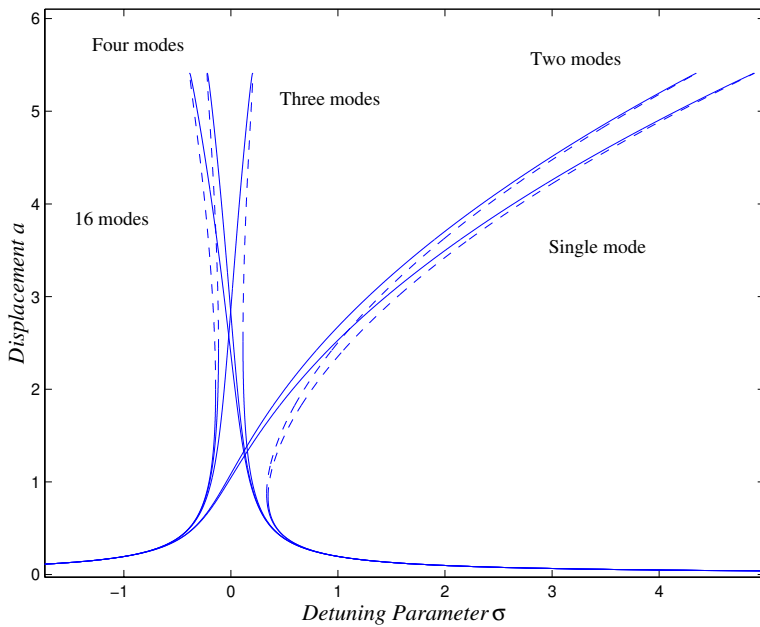
Figure 3.7: Frequency-response curves of an isotropic doubly-curved shell when $k_x = -0.2$ and $k_y = 0.2553$.
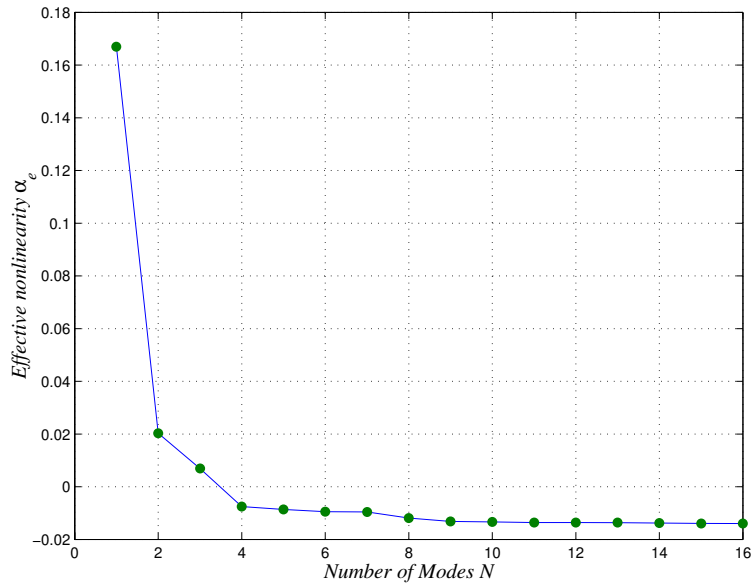
Figure 3.8: Effective nonlinearity for an isotropic doubly-curved shell when $k_x = -0.2$ and $k_y = 0.2553$.

nine-mode approximations, respectively. Clearly, the value and sign of the effective nonlinearity depend on the curvature values and the number of retained modes in the approximation. In Fig. 3.10, we can see that the shell has a harding-type nonliearity when $k_x/k_y = -1$. In Fig 3.11, we show the hardening and softening regions in the k_x and k_y plane. Between these regions, there are ranges of curvatures where the one-mode approximation predicts a positive α_e, indicating a hardening-type nonlinearity, whereas the nine-mode approximation predicts a negative α_e, indicating a softening-type nonlinearity. Moreover, the results in Fig. 3.10 show spikes, which correspond to the case of a two-to-one internal resonance involving the fundamental mode of the shell and a higher-order mode, as mentioned in Section 3.2. In Fig 3.12, we show the possible activation of two-to-one internal resonance involving the second, third, and fourth modes. The behavior of shells having two-to-one internal resonace is treated in Chapter 5.
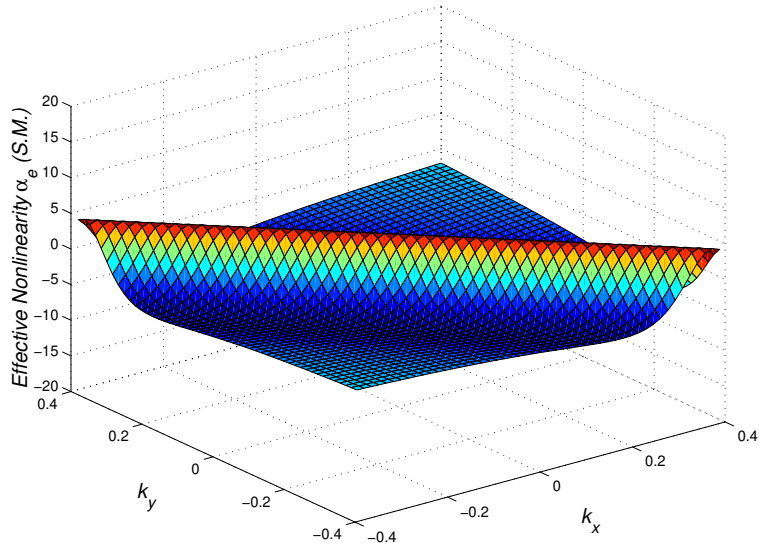
Figure 3.9: Effective nonlinearity for an isotropic shell using a single-mode approximation.
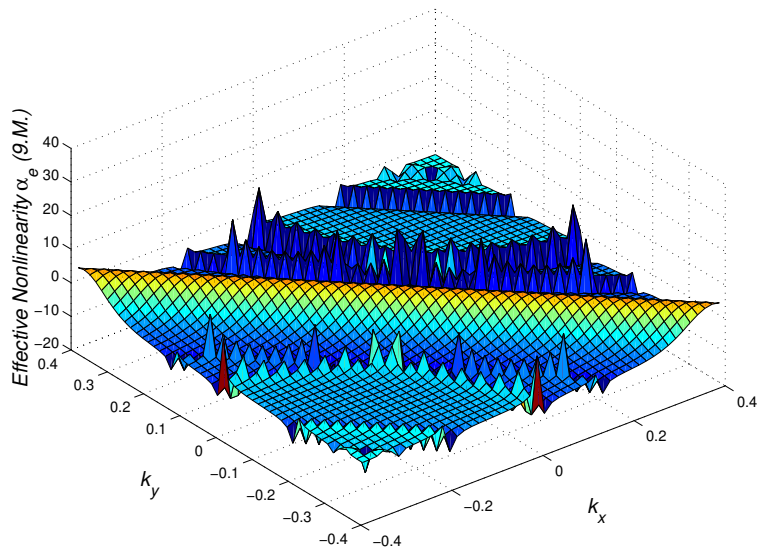
Figure 3.10: Effective nonlinearity for an isotropic shell using a nine-mode approximation.
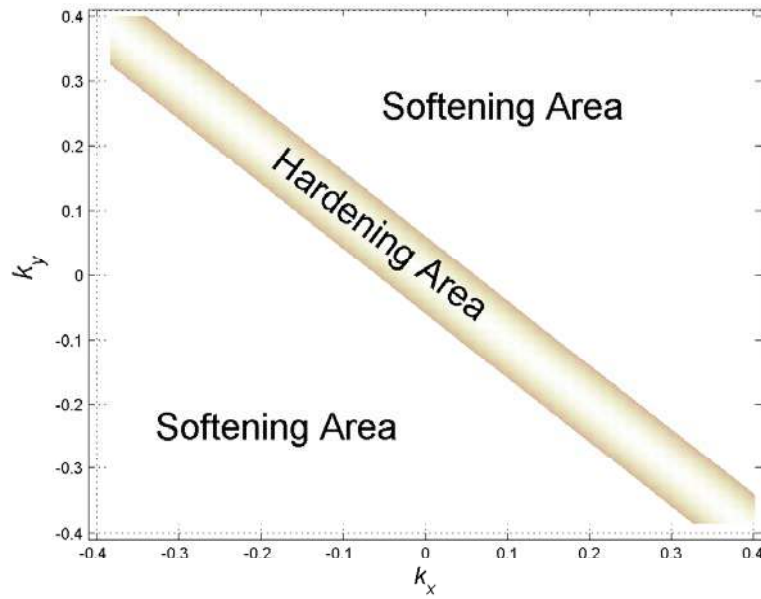
Figure 3.11: The softening and hardening regions in the isotropic shell using a nine-mode approximation.
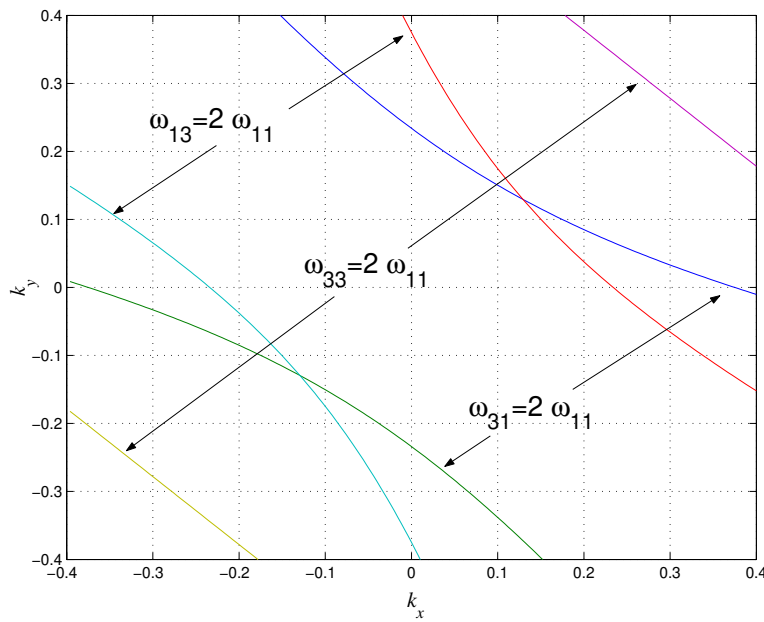
Figure 3.12: Conditions for the activation of a two-to-one internal resonance in the dynamics of an isotropic shell.

3.3.2   Single-Layered Shells

Next, we use Eqs. (3.27) and (3.31) to investigate the dynamic behavior of a single-layered shell and the influence of the number of terms retained in the Galerkin approximation on the accuracy of the calculated response. We consider a graphite/epoxy shell with the following parameters:

$$\nu_{12} = 0.3, \quad l_x = 1, \quad l_y = 1, \quad f_{11} = 30,$$
$$\frac{E_1}{E_2} = 15.4, \quad \frac{G_{12}}{E_2} = 0.79, \quad \frac{G_{23}}{E_2} = 0.5 \qquad (3.33)$$

In Fig. 3.13, we show the frequency-response curves obtained for a spherical single-layered shell with $k_x = k_y = 0.1$ using 1, 2, 3, 4, and 16-mode approximations. All of the curves are bent to the left, indicating a softening-type nonlinearity. However, the extent of the bending depends on the number N of modes retained in the approximation. Increasing N from 1 to 2 has a small effect on the bending of the curve. However, increasing N from 2 to 3 has a large effect. Increasing N beyond 3 has a small effect. In fact, the results obtained with $N = 4$ are very close to those obtained with $N = 16$. To get a better picture of the influence of the number of modes retained in the approximation on the effective nonlinearity, we use Eq. (3.29) to calculate the variation of α_e with N; the results are shown in Fig. 3.14. Increasing N from 1 to 2 leads to a small decrease in α_e. However, increasing N from 2 to 3 leads to a large decrease in α_e from -2.8 to -4.8. Increasing N from 3 to 4 leads to a small decrease (from -4.8 to -4.9) in α_e, and increasing N to 6 leads to a slight decrease in α_e to -4.92. Increasing N beyond 6 has a negligible effect on α_e. It is clear from Figs. 3.13 and 3.14 that using a one-mode approximation, as usually done, would lead to a quantitative error in the predicted response.

Next, we consider a cylindrical single-layered shell with the curvatures $k_x = 0$ and $k_y = 0.0935$. It follows from Fig. 3.15 that retaining one or two modes in the approximations produces frequency-response curves that are bent to the right, indicating a hardening-type nonlinearity. However, retaining three modes in the approximation yields a frequency-

response curve bent to the left, indicating a softening-type nonlinearity. Increasing the number of retained modes further leads only to quantitative rather than qualitative changes in the predicted response. In Fig. 3.16, we show variation of the effective nonlinearity α_e with the number N of the retained modes in the approximation. When $N = 1$ or 2, $\alpha_e > 0$, indicating a hardening-type behavior. When $N \geq 3$, $\alpha_e < 0$, indicating a softening-type behavior. In fact, $\alpha_e \approx 0.068$ when $N = 2$ whereas $\alpha_e \approx -0.55$ when $N = 3$ and $\alpha_e \approx -0.58$ when $N = 4$. The value of α_e converges to -0.62 as N approaches 11.

In another example, we consider a doubly-curved single-layered shell with the curvatures $k_x = -0.194$ and $k_y = 0.1$. Again, it follows from Fig. 3.17 that retaining one or two modes in the approximations predicts frequency-response curves bent to the right, whereas retaining three or more modes in the approximation predicts frequency-response curves bent to the left. It follows from Fig. 3.18 that α_e changes from 0.11 when $N = 2$ to -0.26 when $N = 3$. As N increases, the predicted α_e continues to decrease, indicating a softening-type behavior, and finally converges to -0.29 as N approaches 11.

To have a better understanding of the behavior of a single-layered shell, we show three-dimensional plots, Figs. 3.19 and 3.20, of the variation of the effective nonlinearity of a doubly curved shell with the curvatures k_x and k_y by using single-mode and nine-mode approximations, respectively. As in the case of isotropic shells, the value and sign of the effective nonlinearity depend on the curvature values and the number of retained modes in the approximation. In Fig 3.21, we show the softening and hardening regions in the k_x and k_y plane for a single-layered shell. The harding region is larger than that for an isotropic shell, Fig 3.11, which indicates that the nonlinear behavior of the shell also depends on its lay-up. Again, there are ranges of curvatures between the two regions where the one-mode approximation predicts a positive α_e, indicating a hardening-type nonlinearity, whereas the nine-mode approximation predicts a negative α_e, indicating a softening-type nonlinearity. As in the case of isotropic shells, the results in Fig. 3.20 show spikes, corresponding to the case of a two-to-one internal resonance involving the fundamental mode. A projection of the internal-resonance curves is shown in Fig 3.22.
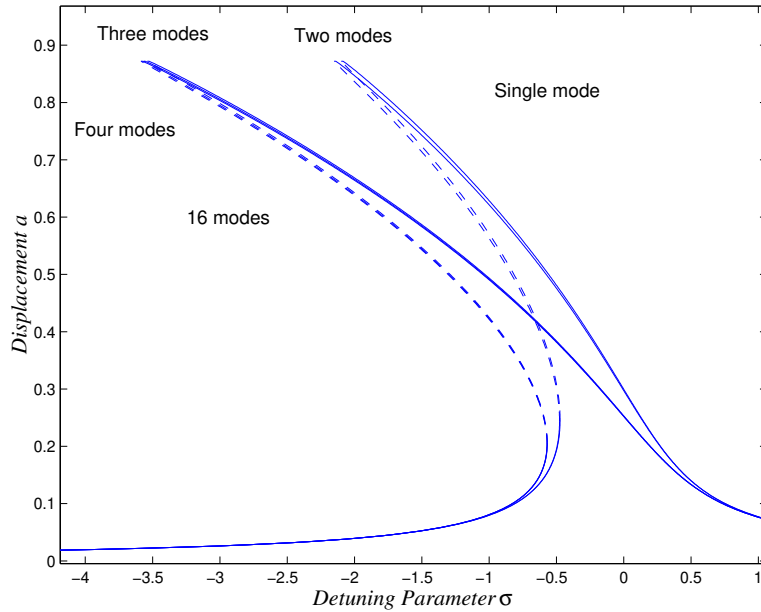
Figure 3.13: Frequency-response curves of a single-layered spherical shell when $k_x = 0.1$ and $k_y = 0.1$.

3.3.3   Multi-Layered Shells

In the analysis of single-layered shells, we can see a large change in the effective nonlinearity by increasing the number of retained modes from 2 to 3, Figs 3.13-3.18, while increasing the number of retained modes in isotropic shells from 1 to 2 and from 2 to 3 have a similar effect due to symmetry, Figs 3.3 and 3.4. This large change in the behavior of single-layered shells is due to the different stiffnesses along the x and y directions caused by the laminated composite. In Fig. 3.23, we plot the effective nonlinearity for a 13-layerd spherical shell with $k_x = k_y = 1$. We can see that increasing the number of modes retained from 1 to 2 and from 2 to 3 produce similar changes in the effective nonlinearty. These results show that increasing the number of layers reduces the effect of the third mode because of the difference between the stiffnesses along the x and y directions is reduced as the number of layers increases.

Next, we study the effect of changing the number of layers on the shell dynamics. In Fig. 3.24, we show the variation of ω_{11} with the curvature k_x when $k_y = 0$. We can see
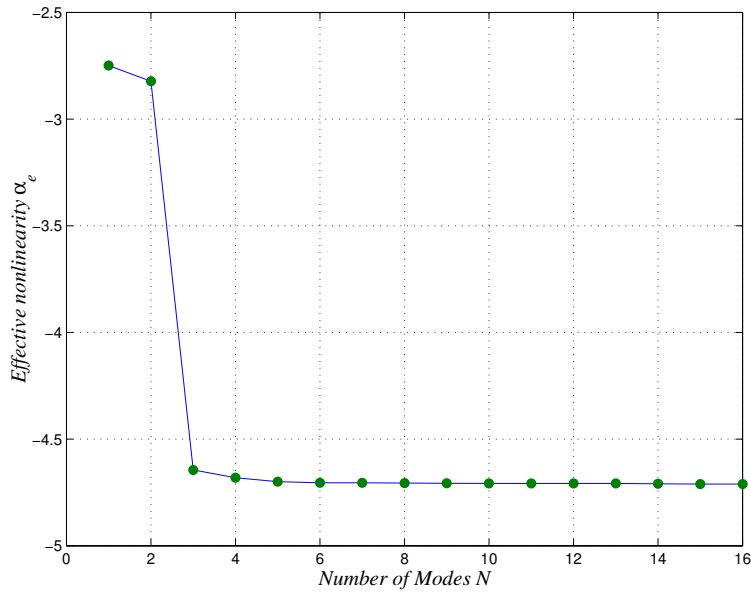
Figure 3.14: Effective nonlinearity for a single-layered spherical when $k_x = 0.1$ and $k_y = 0.1$.
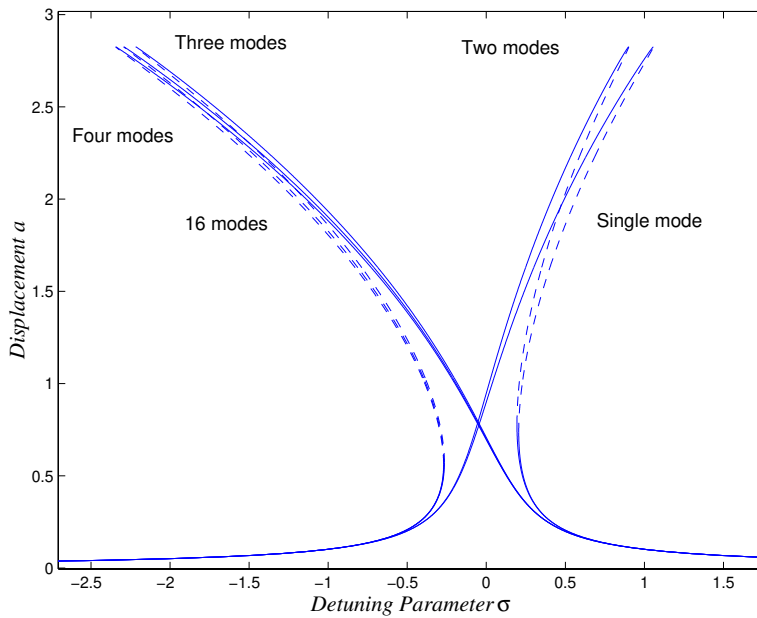
Figure 3.15: Frequency-response curves of a single-layered cylindrical shell when $k_x = 0.0$ and $k_y = 0.0935$.
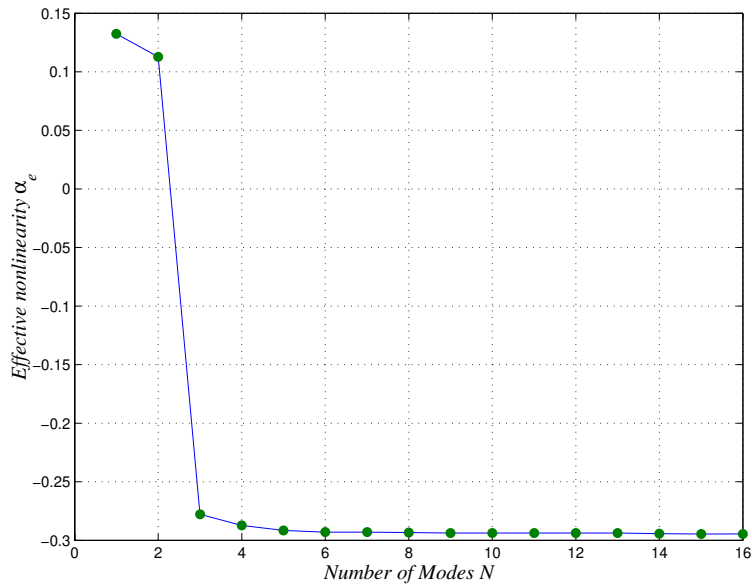
Figure 3.16: Effective nonlinearity for a single-layered cylindrical shell when $k_x = 0.0$ and $k_y = 0.0935$.
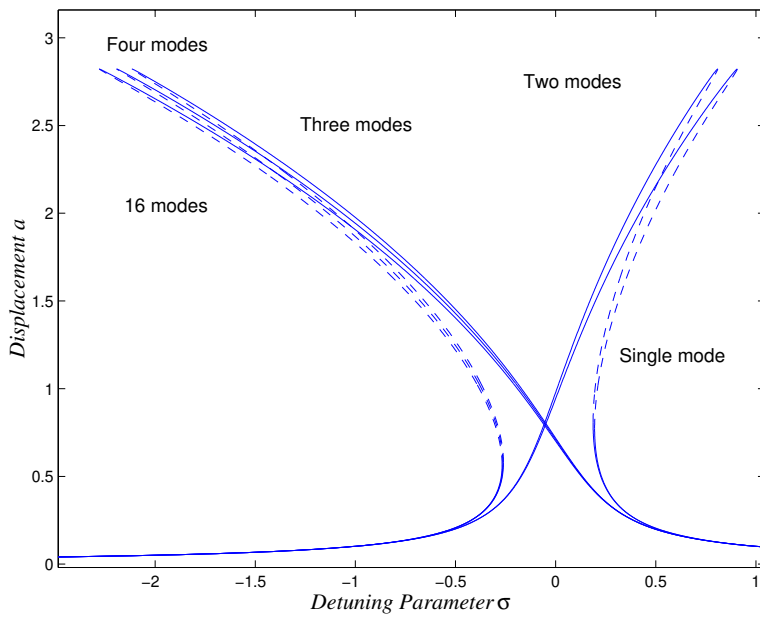
Figure 3.17: Frequency-response curves of a single-layered doubly-curved shell when $k_x = -0.194$ and $k_y = 0.1$.
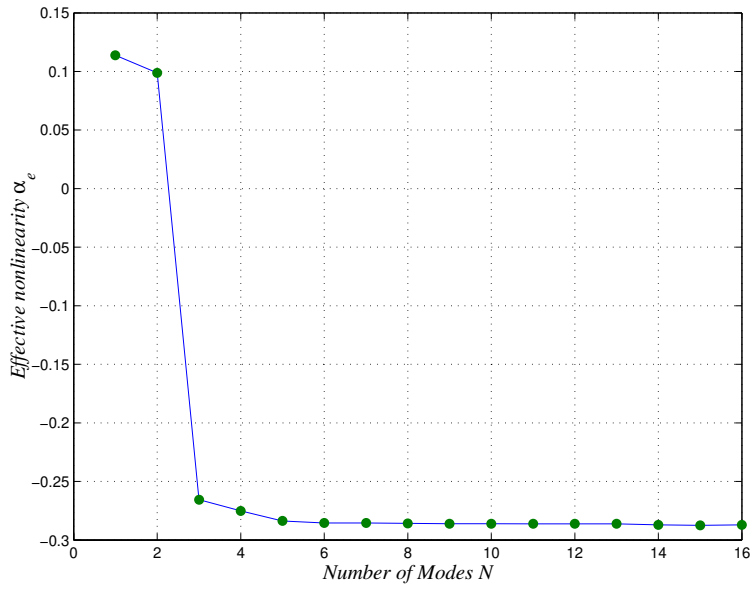
Figure 3.18: Effective nonlinearity for a single-layered doubly-curved shell when $k_x = -0.194$ and $k_y = 0.1$.
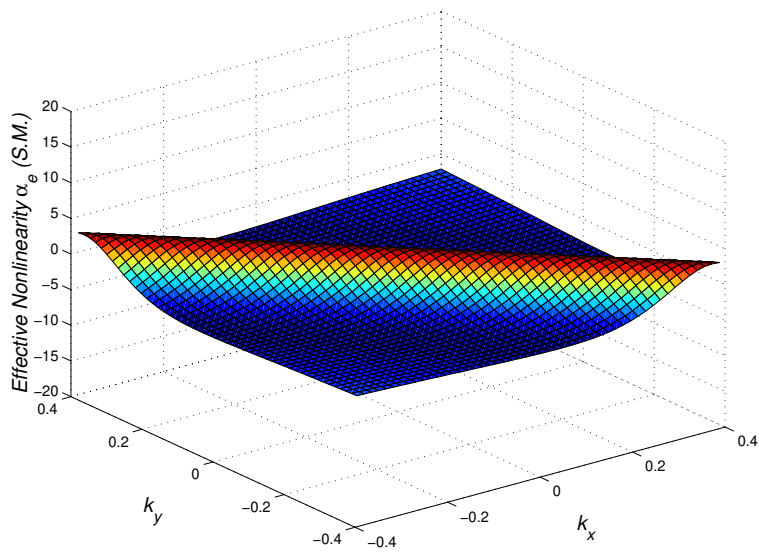
Figure 3.19: Effective nonlinearity for a single-layered shell using a single-mode approximation.
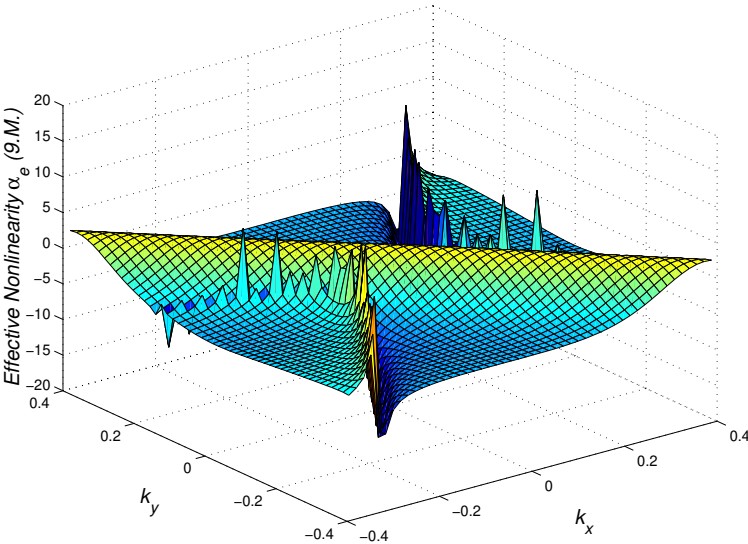
Figure 3.20: Effective nonlinearity for a single-layered shell using a nine-mode approximation.
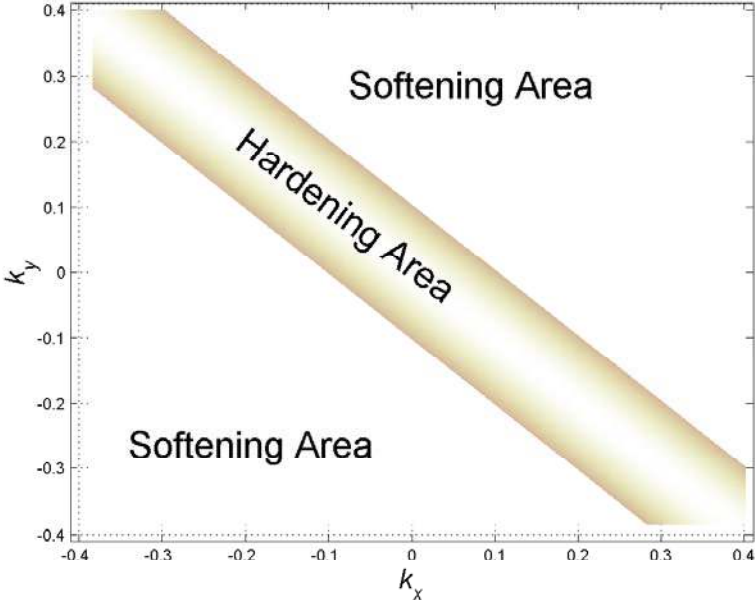
Figure 3.21: The softening and hardening regions in a single-layered shell using a nine-mode approximation.
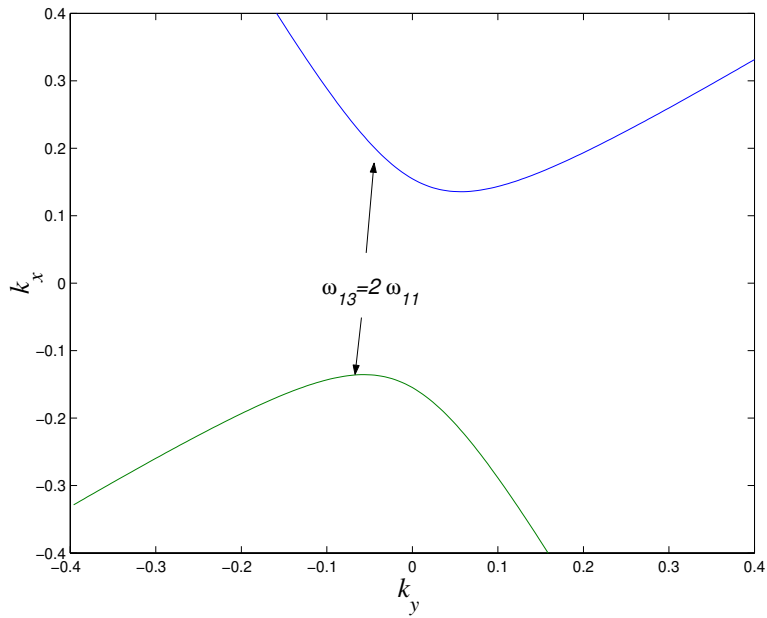
Figure 3.22: Conditions for the activation of a two-to-one internal resonance between the second and first modes of a single-layered shell.
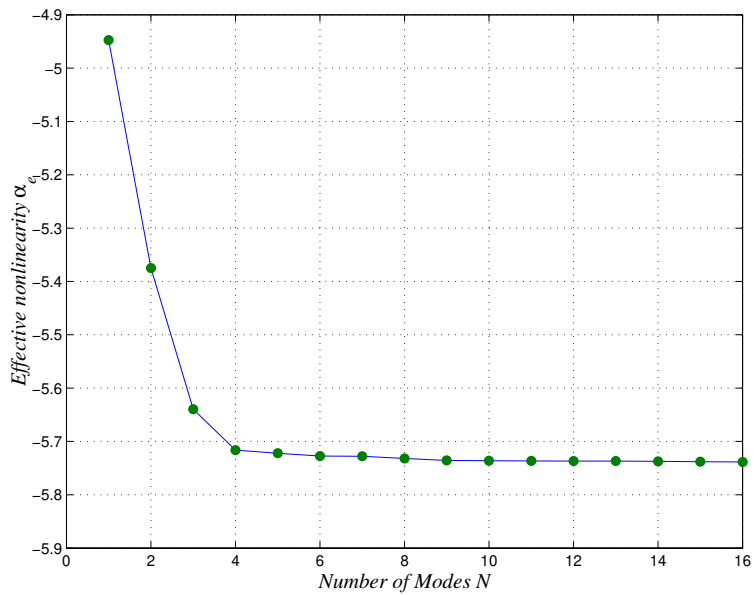
Figure 3.23: Effective nonlinearity for a 13-layered shell when $k_x = 0.1$ and $k_y = 0.1$.

that changing the number of layers from 1 to 3 leads to a relatively large change in ω_{11}, while increasing the number of layers more (to 5,7, or 9) has a negligible effect on ω_{11}. Also, increasing the absolute value of k_x results in a large influence on ω_{11}. In Fig. 3.25, we can see that changing the number of layers from 1 to 3 reduces the value of ω_{31} from approximately 355 to 349. Increasing the number of layers from 3 to 5 results in a relatively large change in ω_{31} from 349 to 320. Increasing the number of layers to 7 and 9 reduces ω_{31} to 305 and 298. Thus, we conclude that increasing the number of layers reduces ω_{31}. In Fig. 3.26, we show the effect of changing the number of layers on ω_{13}. Increasing the number of layers from 1 to 3 results in increasing ω_{13} when $-0.28 < k_x < 0.28$ and decreasing ω_{13} when $|k_x| > 0.28$. Increasing the number of layers beyond 3 increases ω_{13}. In Fig. 3.27, we show the effect of increasing the number of layers on ω_{33}. Increasing the number of layers from 1 to 3 results in a recognizable change in ω_{33}, while increasing the number of layers beyond 3 results in a very small change in ω_{33}.

In Fig. 3.28, we show the influence of changing the number of layers on the possible two-to-one internal-resonance curves. It is clear that increasing the number of layers from 1 to 3 changes qualitativaly the internal resonance curves, while increasing the number of layers beyond 3 results only in a quantitative change, causing the internal-resonance curves to move away from the center.

In Fig. 3.29, we show variation of the effective nonlinearity with k_x by using a nine-mode approximation when $k_y = 0$. Increasing the number of layers from 1 to 3 results in a relativily large change in the effective nonlinearity. The effective nonlinearity for a multi-layered shell has a larger value compared with the single-layered shell when $-0.063 < k_x < 0.063$ and a smaller value elsewhere. Increasing the number of layers beyond 3 has a small effect on the effective nonlinearity. In all of the results, we can see a recognizable change in the natural frequencies and the effective nonlinearity when the number of layers increases from 1 to 3 due to the change in the modulus of elasticity along the y direction.
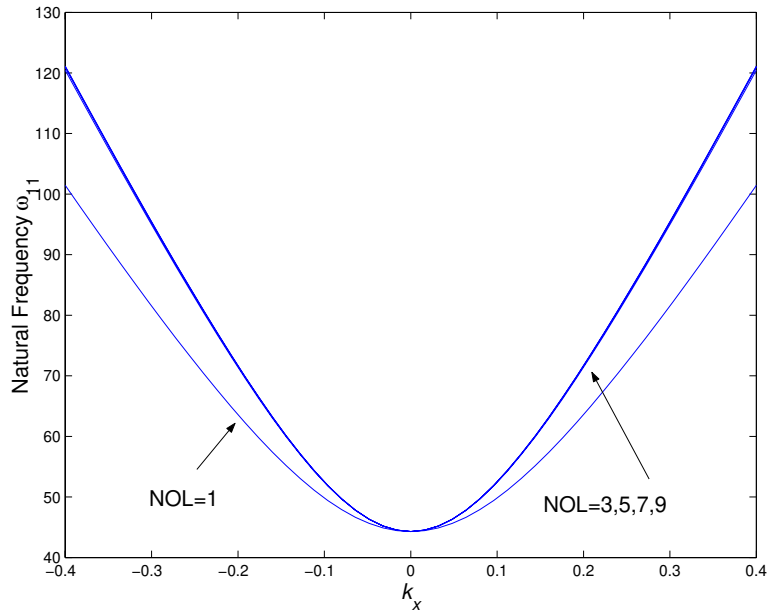
Figure 3.24: Variation of the natural frequency ω_{11} with k_x when $k_y = 0$.
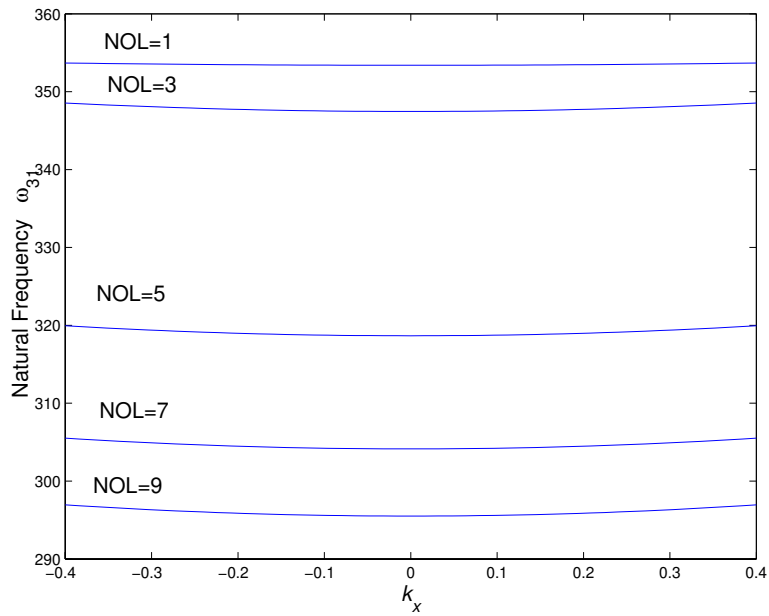
Figure 3.25: Variation of the natural frequency ω_{31} with k_x when $k_y = 0$.
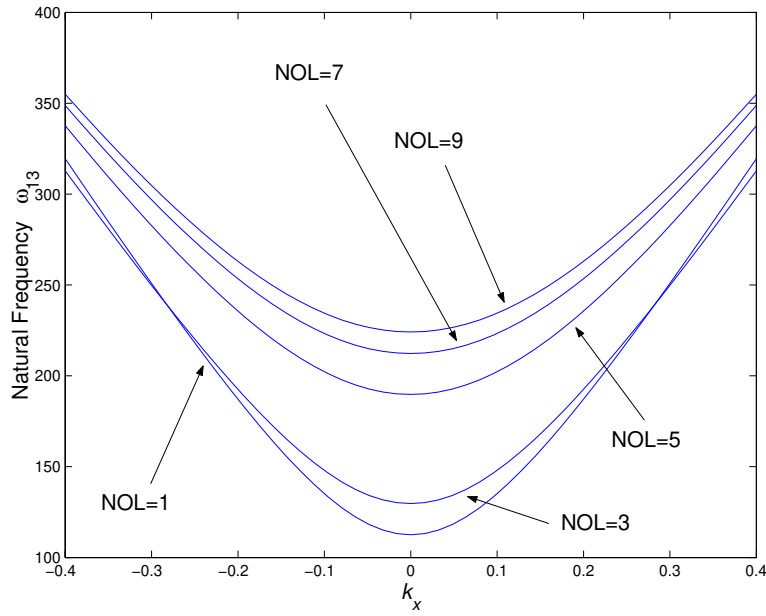
Figure 3.26: Variation of the natural frequency ω_{13} with k_x when $k_y = 0$.
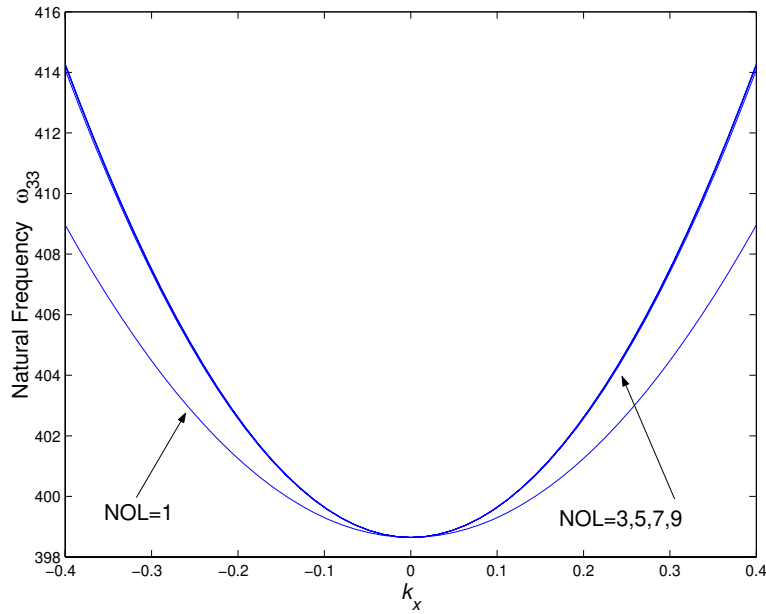
Figure 3.27: Variation of the natural frequency ω_{33} with k_x when $k_y = 0$.
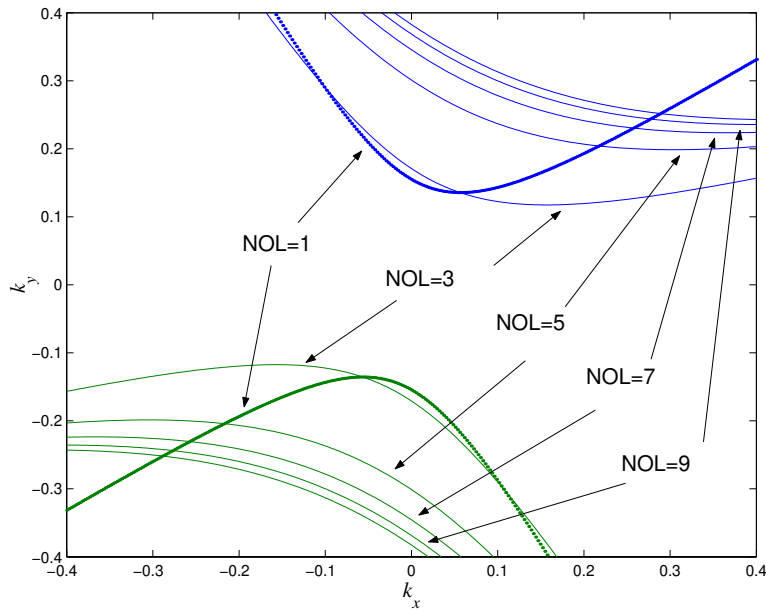
Figure 3.28: Two-to-one internal resonance conditions for a multi-layerd shell.
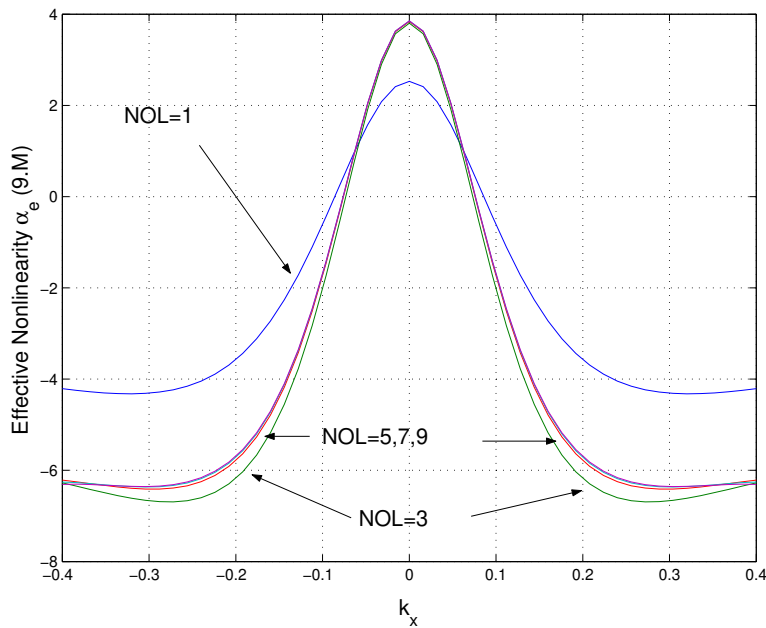
Figure 3.29: Variation of the effective nonlinearity for a cylindrical shell with k_x when $k_y = 0$ using a nine-mode approximation.

3.4   Global Dynamics

In this section, we use a multi-mode Galerkin discretization to calculate periodic responses of doubly curve cross-ply shallow shells to a primary-resonance excitation and determine their stability and bifurcations. A combination of a shooting technique and Floquet theory is used to locate periodic solutions and investigate their bifurcations. Numerical results are shown for single-mode and four-mode approximations. We show that, for certain shell parameters, a single-mode approximation misses some important dynamics, such as period-doubling bifurcations.

3.4.1   Numerical Results

In the preceding section, we used the method of multiple scales to determine a second-order uniform expansion of the solution of Eqs. (3.16) when the excitation frequency Ω is close to the natural frequency of the fundamental mode of the shell. We investigated how the effective nonlinearity depends on the number of modes retained in the discretization. We found out that the results obtained with a single-mode discretization may lead to an incorrect characterization of the effective nonlinearity. We presented cases in which a single-mode discretization predicts a hardening-type effective nonlinearity, whereas a multi-mode discretization predicts a softening-type effective nonlinearity and vice versa.

In this section, we investigate the influence of the number of modes retained in the discretization on the predicted periodic motions and their bifurcations for the case in which the excitation frequency Ω is close to the fundamental natural frequency of the shell. We consider a graphite/epoxy shell with the following parameters:

$$\nu_{12} = 0.3, \quad l_x = 1, \quad l_y = 1, \quad \frac{E_1}{E_2} = 15.4,$$

$$\frac{G_{12}}{E_2} = 0.79, \quad \frac{G_{23}}{E_2} = 0.5, \quad \mu_{11} = 0.30 \tag{3.34}$$
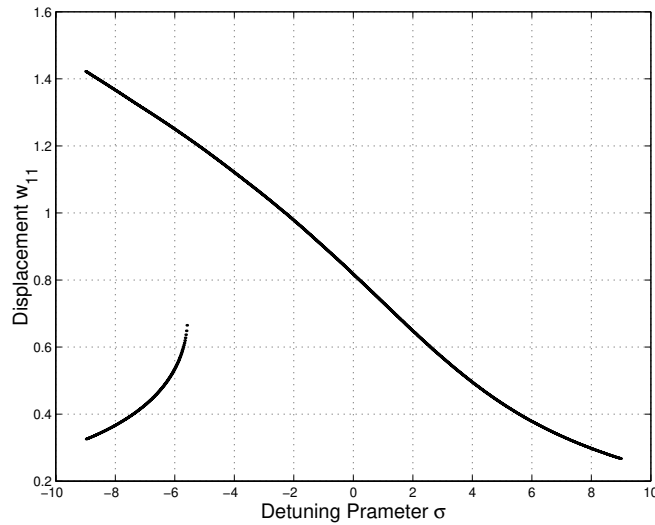
Figure 3.30: Frequency-response curve for a single-layer shell obtained using a single-mode discretization when $k_x = 0.129$, $k_y = 0.129$, and $F_{11} = 405$.

With these parameters, the lowest six antisymmetric natural frequencies are

$$\omega_{11} = 73.66, \quad \omega_{13} = 155.38, \quad \omega_{15} = 300.10,$$

$$\omega_{31} = 356.42, \quad \omega_{33} = 402.96, \quad \omega_{51} = 974.07 \tag{3.35}$$

Using a perturbation method, such as the method of multiple scales or averaging, one can derive the equations describing the modulation of the amplitude and phase of the shell on a slow time scale. Using the modulation equations to determine the stability of periodic motions yields their stability to a special class of disturbances, which have the same period as the predicted motions. Consequently, such an approach would not be able to predict period-doubling bifurcations of periodic motions of the shell because the period of the disturbances would be twice that of the predicted motions. Furthermore, the perturbation solution is valid only for small but finite-amplitude motions.

To investigate the influence of the truncation on the periodic motions of the shell and
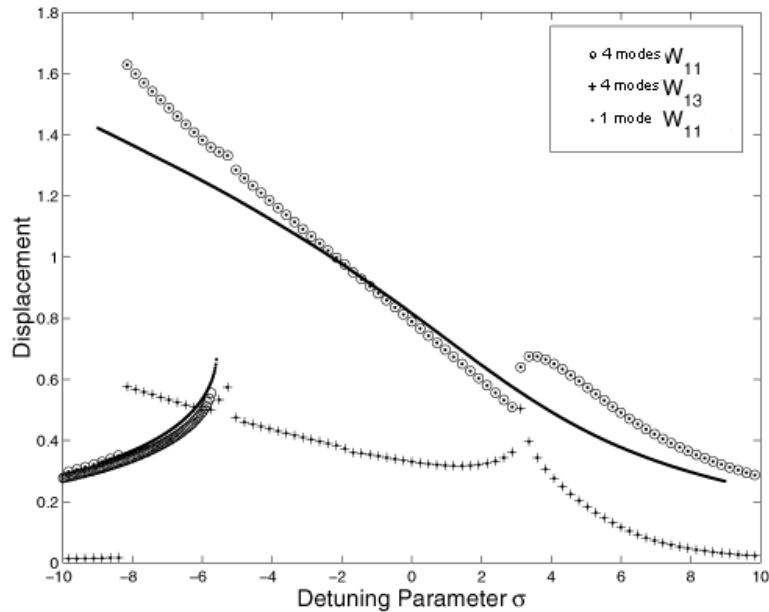
Figure 3.31: Frequency-response curves for a single-layered spherical shell obtained by using a four-mode discretization when $k_x = 0.129$, $k_y = 0.129$, and $F_{11} = 405$.

their stability and hence their bifurcations, we use a combination of a shooting technique and Floquet theory. To this end, we truncate equations (3.16) and write the resulting equations in state-space form as

$$\dot{\eta} = f\left(\eta; F, \Omega\right) \tag{3.36}$$

where η and f are $2n \times 1$ vectors and N is the number of modes retained in the discretization. For a given F and Ω, we seek an initial condition vector η_0 such that

$$\eta\left(\frac{2\pi}{\Omega}; \eta_0\right) = \eta_0 \tag{3.37}$$

The procedure is detailed by Nayfeh and Balachandran (1995). We start with a single-mode discretization. For a given F and Ω, once a periodic motion is calculated, we determine the maximum of W_{11} as a function of Ω. Then, we keep F fixed, vary Ω slightly, and repeat
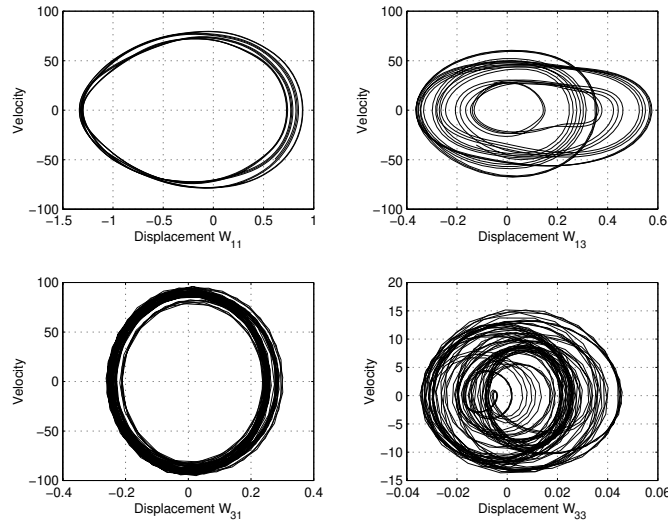
Figure 3.32: Phase portrails of chaotic motions of a single-layered spherical shell for the first, second, third, and fourth modes, when $k_x = k_y = 0.129$, $\sigma = -5.18$, and $F_{11} = 405$.
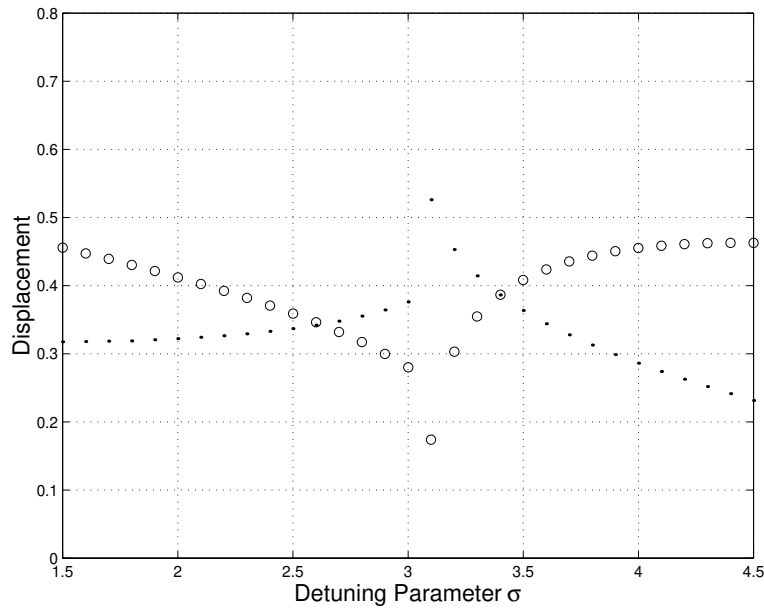
Figure 3.33: Frequency-response curves for a single-layered shell near the two-to-one internal resonance.
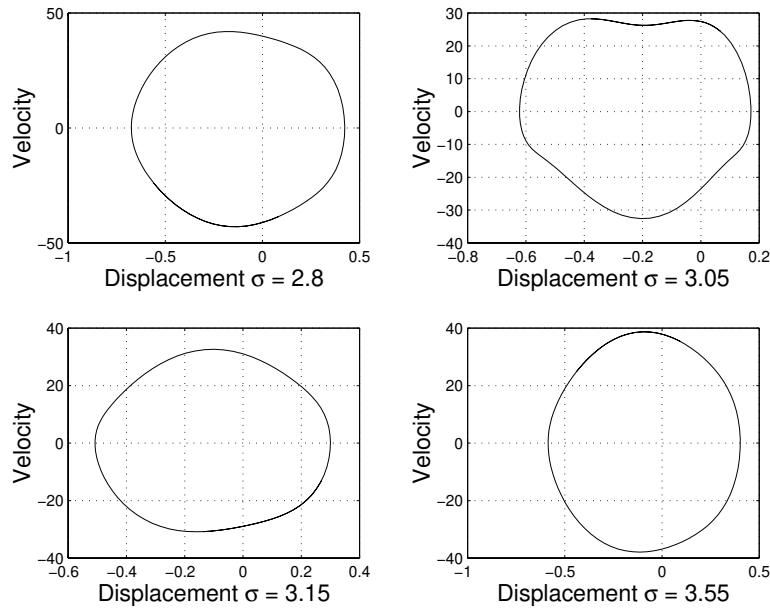
Figure 3.34: Limit cycles near the two-to-one internal resonance.

the process. In Fig. 3.30, we show the results obtained for a single-layer shell. Starting with a $\sigma = \Omega - \omega_{11} = -9.0$ and increasing it, we find that the periodic motion (limit cycle) deforms smoothly and increases in size, with all of the Floquet multipliers being inside the unit circle and one of them increasing towards unity. As σ increases beyond -5.8, the limit cycle loses stability through a cycle-fold bifurcation as a consequence of one of the Floquet multipliers exiting the unit circle through $+1$. The post-bifurcation is a jump to a larger limit cycle. Increasing σ further leads to a decrease in the size of the limit cycle. Starting from $\sigma = 9$ and decreasing it, we find that the limit cycle increases in size and remains stable with all of the Floquet multipliers being inside the unit circle until $\sigma = -8.9$. As σ decreases further, the limit-cycle loses stability through a cyclic-fold bifurcation as a result of one Floquet multiplier exiting the unit circle through $+1$. Consequently, the response jumps down to a small limit cycle. As σ decreases further, the limit cycle deforms smoothly and decreases in size.

Next, we increase the number retained modes to four so that Eqs. (3.16) represent an 8-degree-of-freedom dynamical system and repeat the process of calculating the limit cycles

and investigating their stability and bifurcations. The calculation and stability investigation of a limit cycles using the shooting method requires the integration of a system of 72 first-order equations. The results are shown in Fig. 3.31. Starting with $\sigma = -10$ and increasing it, we find that the limit cycle increases slightly in size until σ reaches -5.2 where it suffers a cyclic-fold bifurcation, leading to a jump to a larger limit cycle. Comparing these results with those in Fig. 3.30 obtained with a one-mode discretization, we conclude that the latter may overpredict or underpredict the size of the limit cycles and underpredicts the cyclic-fold bifurcation frequency. Starting from $\sigma = -8.9$ on the higher curve and decreasing it, we find that the limit cycle smoothly decreases in size until $\sigma = -5.63$, where the limit cycle loses stability through a period-doubling bifurcation, with a Floquet multiplier leaving the unit circle through -1. Decreasing the value of σ further results in a sequence of period-doubling bifurcations leading to chaos, as shown in Fig. 3.32. Chaos bifurcates to a stable limit cycle at $\sigma = 5.02$ through a reverse sequence of period-doubling bifurcations. After that, all of the limit cycles remain stable until $\sigma = 3.08$, where they lose stability when one of the Floquet multipliers leaves the unit circle through $+1$. Finally, the limit cycle remains stable, but initially it increases slightly in size and then smoothly decreases in size.

In Fig. 3.33, we show that the amplitude of the second mode, which is usually neglected, is larger than the amplitude of the first mode at $\sigma = 3.05$. In Fig. 3.34, we show the distortion in the limit cycles near the bifurcation point. Increasing the number of modes retained over four, in this case, did not influence the qualitative or quantitative dynamic behavior of the shell. We used six modes and nine modes in checking for convergence.

3.5   Direct Approach

In this section, we use the method of multiple scales and directly attack the governing partial-differential equations, Eqs. (3.8) and (3.9), and associated simply supported boundary conditions. We repeat these equations below for convenience:

$$D_{11}w_{xxxx} + 2(D_{12} + 2D_{66})w_{xxyy} + D_{22}w_{yyyy} + k_x\Phi_{yy} + k_y\Phi_{xx} + Cw_t + \rho h w_{tt}$$

$$= \Phi_{yy}w_{xx} + \Phi_{xx}w_{yy} - 2\Phi_{xy}w_{xy} + F\cos(\omega t) \tag{3.38}$$

$$-K_{11}\Phi_{xxxx} - (2K_{12} + K_{66})\Phi_{xxyy} - K_{22}\Phi_{yyyy} + k_x w_{yy} + k_y w_{xx} = w_{yy}w_{xx} - w_{xy}^2 \tag{3.39}$$

As in the preceding section, we nondimensionalize the governing system using the following parameters:

$$\hat{w} = \frac{w}{h} \ , \ \hat{x} = \frac{x}{l_x} \ , \ \hat{y} = \frac{y}{l_y} \ , \ \hat{\Omega} = l_x^2\sqrt{\frac{\rho h}{D^*}}\Omega \ , D^* = \frac{E_2 h^3}{12(1 - \nu_{12}\nu_{21})} \ ,$$

$$\hat{\Phi} = D^*\Phi \ , \ \hat{F} = \frac{l_x^4}{D^* h}F \ , \ C = \frac{l_x^4}{D^* h}c \ , \hat{t} = \frac{1}{l_x^2}\sqrt{\frac{D^*}{\rho h}}t \tag{3.40}$$

In what follows, we drop the hat for convenience.

We use the method of multiple scales to obtain a second-order uniform approximate solution of Eqs. (3.38) and (3.39) in the case of simply supported boundary conditions. Accordingly, we express the solution in terms of the two time scales $T_0 = t$ and $T_2 = \epsilon^2 t$ as

$$w(x, y, T_0, T_2; \epsilon) = \epsilon w^{(1)}(x, y, T_0, T_2) + \epsilon^2 w^{(2)}(x, y, T_0, T_2)$$

$$+ \epsilon^3 w^{(3)}(x, y, T_0, T_2) + \cdots \tag{3.41}$$

$$\Phi(x, y, T_0, T_2; \epsilon) = \epsilon\Phi^{(1)}(x, y, T_0, T_2) + \epsilon^2\Phi^{(2)}(x, y, T_0, T_2)$$

$$+ \epsilon^3\Phi^{(3)}(x, y, T_0, T_2) + \cdots \tag{3.42}$$

where ϵ is a small nondimensional bookkeeping parameter. To express the nearness of the excitation frequency Ω to the fundamental natural frequency ω_{11}, we introduce the detuning

parameter σ defined as

$$\Omega = \omega_{11} + \epsilon^2 \sigma \tag{3.43}$$

We scale the damping and the excitation amplitude as

$$C = \epsilon^2 \overline{C} \text{ and } f = \epsilon^2 \overline{f} \tag{3.44}$$

Substituting Eqs. (3.41)-(3.44) into Eqs. (3.38) and (3.39) and equating coefficients of like powers of ϵ, we obtain

<u>Order ϵ^1</u>

$$\frac{D_{11}h}{l_x^2}w^{(1)}_{xxxx} + \frac{2(D_{12}+2D_{66})h}{l_x^2 l_y^2}w^{(1)}_{xxyy} + \frac{D_{22}h}{l_y^4}w^{(1)}_{yyyy} + \frac{k_x D^*}{l_x l_y^2}\Phi^{(1)}_{yy} + \frac{k_y D^*}{l_x^3}\Phi^{(1)}_{xx} + \frac{D^* h}{l_x^4}w^{(1)}_{T_0 T_0} = 0$$

$$\tag{3.45}$$

$$-\frac{K_{11}D^*}{l_x^4}\Phi^{(1)}_{xxxx} - \frac{(2K_{12}+K_{66})D^*}{l_x^2 l_y^2}\Phi^{(1)}_{xxyy} - \frac{K_{22}D^*}{l_y^4}\Phi^{(1)}_{yyyy} + \frac{k_x h}{l_y^2 l_x}w^{(1)}_{yy} + \frac{k_y h}{l_x^3}w^{(1)}_{xx} = 0 \tag{3.46}$$

<u>Order ϵ^2</u>

$$\frac{D_{11}h}{l_x^2}w^{(2)}_{xxxx} + \frac{2(D_{12}+2D_{66})h}{l_x^2 l_y^2}w^{(2)}_{xxyy} + \frac{D_{22}h}{l_y^4}w^{(2)}_{yyyy} + \frac{k_x D^*}{l_x l_y^2}\Phi^{(2)}_{yy} + \frac{k_y D^*}{l_x^3}\Phi^{(2)}_{xx} + \frac{D^* h}{l_x^4}w^{(2)}_{T_0 T_0}$$

$$= \frac{D^* h}{l_y^2 l_x^2}(\Phi^{(1)}_{yy}w^{(1)}_{xx} + \Phi^{(1)}_{xx}w^{(1)}_{yy} - 2\Phi^{(1)}_{xy}w^{(1)}_{xy}) \tag{3.47}$$

$$-\frac{K_{11}D^*}{l_x^4}\Phi^{(2)}_{xxxx} - \frac{(2K_{12}+K_{66})D^*}{l_x^2 l_y^2}\Phi^{(2)}_{xxyy} - \frac{K_{22}D^*}{l_y^4}\Phi^{(2)}_{yyyy} + \frac{k_x h}{l_y^2 l_x}w^{(2)}_{yy} + \frac{k_y h}{l_x^3}w^{(2)}_{xx}$$

$$= \frac{h^2}{l_x^2 l_y^2}\left[w^{(1)}_{yy}w^{(1)}_{xx} - (w^{(1)}_{xy})^2\right] \tag{3.48}$$

Order ϵ^3

$$\frac{D_{11}h}{l_x^2}w_{xxxx}^{(3)} + \frac{2(D_{12}+2D_{66})h}{l_x^2 l_y^2}w_{xxyy}^{(3)} + \frac{D_{22}h}{l_y^4}w_{yyyy}^{(3)} + \frac{k_x D^*}{l_x l_y^2}\Phi_{yy}^{(3)} + \frac{k_y D^*}{l_x^3}\Phi_{xx}^{(3)}$$

$$+ \frac{D^*h}{l_x^4}w_{T_0 T_0}^{(3)} + l_x\sqrt{\frac{1}{\rho h D^*}}Cw_{T_0} = 2\frac{D^*h}{l_x^4}w_{T_0 T_2}$$

$$+ \frac{D^*h}{l_y^2 l_x^2}(\Phi_{yy}^{(1)}w_{xx}^{(2)} + \Phi_{yy}^{(2)}w_{xx}^{(1)} + \Phi_{xx}^{(1)}w_{yy}^{(2)} + \Phi_{xx}^{(2)}w_{yy}^{(1)} - 2\Phi_{xy}^{(1)}w_{xy}^{(2)} - 2\Phi_{xy}^{(2)}w_{xy}^{(1)})$$

$$+ F\cos(\omega_{11}T_0 + \sigma T_2) \tag{3.49}$$

$$-\frac{K_{11}D^*}{l_x^4}\Phi_{xxxx}^{(3)} - \frac{(2K_{12}+K_{66})D^*}{l_x^2 l_y^2}\Phi_{xxyy}^{(3)} - \frac{K_{22}D^*}{l_y^4}\Phi_{yyyy}^{(3)} + \frac{k_x h}{l_y^2 l_x}w_{yy}^{(3)} + \frac{k_y h}{l_x^3}w_{xx}^{(3)}$$

$$= \frac{h^2}{l_x^2 l_y^2}\left(w_{yy}^{(1)}w_{xx}^{(2)} + w_{yy}^{(2)}w_{xx}^{(1)} - 2w_{xy}^{(2)}w_{xy}^{(1)}\right) \tag{3.50}$$

The solutions of Eqs. (3.45) and (3.46) can be expressed as

$$w^{(1)} = a_1(T_2)\sin(\pi x)\sin(\pi y)\cos\left[\omega_{11}T_0 + \beta(T_2)\right] \tag{3.51}$$

$$\Phi^{(1)} = a_2(T_2)\sin(\pi x)\sin(\pi y)\cos\left[\omega_{11}T_0 + \beta(T_2)\right] \tag{3.52}$$

Substituting Eqs. (3.51) and (3.52) into Eqs. (3.45) and (3.46), we solve for ω_{11} and express $a_2(T_2)$ as a function of $a_1(T_2)$ as

$$a_2(T_2) = \zeta a_1(T_2) \tag{3.53}$$

$$\omega_{11}^2 = -\pi^2(-D_{11}\,h\,\pi^2\,l_y^4 - 2\,h\,\pi^2\,l_x^2\,l_y^2\,D_{12} - 4\,h\,\pi^2\,l_x^2\,l_y^2\,D_{66} - D_{22}\,h\,\pi^2\,l_x^4 \tag{3.54}$$

$$+ l_y^2\,l_x^3\,\zeta\,D^*\,k_x + l_y^4\,l_x\,\zeta\,D^*\,k_y)\Big/(D^*\,h\,l_y^4) \tag{3.55}$$

where

$$\zeta = -\frac{h\, l_x\, l_y^2\, (k_x\, l_x^2 + k_y\, l_y^2)}{D^*\, \pi^2\, (K_{11}\, l_y^4 + 2\, l_x^2\, l_y^2\, K_{12} + l_x^2\, l_y^2\, K_{66} + K_{22}\, l_x^4)} \tag{3.56}$$

Next, we substitute Eqs. (3.51)-(3.53) into Eqs. (3.47) and (3.48) and obtain

$$\frac{D_{11}h}{l_x^2} w^{(2)}_{xxxx} + \frac{2(D_{12} + 2D_{66})h}{l_x^2 l_y^2} w^{(2)}_{xxyy} + \frac{D_{22}h}{l_y^4} w^{(2)}_{yyyy} + \frac{k_x D^*}{l_x l_y^2} \Phi^{(2)}_{yy} + \frac{k_y D^*}{l_x^3} \Phi^{(2)}_{xx} + \frac{D^* h}{l_x^4} w^{(2)}_{T_0 T_0}$$

$$= \frac{\pi^4 a_1^2 \zeta D^* h}{l_y^2 l_x^2} \left[\sin^2(\pi x)\sin^2(\pi y) - \cos^2(\pi x)\cos^2(\pi y)\right]$$

$$\times \left[\cos(2\omega_{11} T_0 + 2\beta) + 1\right] \tag{3.57}$$

$$-\frac{K_{11} D^*}{l_x^4} \Phi^{(2)}_{xxxx} - \frac{(2K_{12} + K_{66})D^*}{l_x^2 l_y^2} \Phi^{(2)}_{xxyy} - \frac{K_{22} D^*}{l_y^4} \Phi^{(2)}_{yyyy} + \frac{k_x h}{l_y^2 l_x} w^{(2)}_{yy} + \frac{k_y h}{l_x^3} w^{(2)}_{xx}$$

$$= \frac{a_1^2 \pi^4 h^2}{2 l_x^2 l_y^2} \left[\sin^2(\pi x)\sin^2(\pi y) - \cos^2(\pi x)\cos^2(\pi y)\right]$$

$$\times \left[\cos(2\omega_{11} T_0 + 2\beta) + 1\right] \tag{3.58}$$

The solution of Eqs. (3.57) and (3.58) can be expressed in the form

$$w^{(2)} = a_1^2(T_2) U_1(x,y) \cos\left[2\omega_{nm} T_0 + 2\beta(T_2)\right] + a_1^2(T_2) U_2(x,y) \tag{3.59}$$

$$\Phi^{(2)} = a_1^2(T_2) P_1(x,y) \cos\left[2\omega_{nm} T_0 + 2\beta(T_2)\right] + a_1^2(T_2) P_2(x,y) \tag{3.60}$$

where the U_i and P_i are expanded in Fourier series as

$$U_1(x,y) = \sum_{n=1}^{\infty} \sum_{m=1}^{\infty} Q_{nm} \sin(n\pi x)\sin(m\pi y) \tag{3.61}$$

$$P_1(x,y) = \sum_{n=1}^{\infty} \sum_{m=1}^{\infty} L_{nm} \sin(n\pi x)\sin(m\pi y) \tag{3.62}$$

$$U_2(x, y) = \sum_{n=1}^{\infty} \sum_{m=1}^{\infty} Q1_{nm} \sin(n\pi x) \sin(m\pi y) \tag{3.63}$$

$$P_2(x, y) = \sum_{n=1}^{\infty} \sum_{m=1}^{\infty} L1_{nm} \sin(n\pi x) \sin(m\pi y) \tag{3.64}$$

We note that $w^{(2)}$ and $\Phi^{(2)}$ satisfy the boundary conditions. Next, we substitute Eqs. (3.59)-(3.64) into Eqs. (3.57) and (3.58) and obtain

$$\sum_{m=1}^{\infty} \sum_{n=1}^{\infty} \left\{ \left(C1_{nm}Q_{nm} + C2_{nm}L_{nm} - 4C4\omega_{11}^2 Q_{nm} \right) \cos(2\omega_{nm}T_0 + 2\beta(T_2)) \right.$$

$$+ \left. (C1_{nm}Q1_{nm} + C2_{nm}L_{nm}) \right\} \sin(n\pi x) \sin(m\pi y)$$

$$= -\frac{\zeta C5}{2} \left[\sin^2(\pi x) \sin^2(\pi y) - \cos^2(\pi x) \cos^2(\pi y) \right] \left[\cos(2\omega_{11}T_0 + 2\beta) + 1 \right] \tag{3.65}$$

$$\sum_{m=1}^{\infty} \sum_{n=1}^{\infty} \left\{ \left[-A1_{nm}L_{nm} + A2_{nm}Q_{nm} \right] \left[\cos(2\omega_{nm}T_0 + 2\beta(T_2)) \right] - A1_{nm}L1_{nm} + A2_{nm}Q1_{nm} \right\}$$

$$\times \sin(n\pi x) \sin(m\pi y) = \frac{A3}{2} \left[\sin^2(\pi x) \sin^2(\pi y) - \cos^2(\pi x) \cos^2(\pi y) \right]$$

$$\times \left[\cos(2\omega_{11}T_0 + 2\beta) + 1 \right] \tag{3.66}$$

Multiplying Eqs. (3.65) and (3.66) by $\sin(n\pi x) \sin(m\pi y)$, integrating over the domain, and solving for Q_{nm}, L_{nm}, $Q1_{nm}$, and $L1_{nm}$, we find

$$Q_{nm} = -\frac{1}{\omega_{nm}^2 - 4\omega_{11}^2} \left[\frac{1}{2} \frac{C2_{nm}A3(\bar{G}_{nm1111} - G_{nm1111})}{A1_{nm}C4} + \frac{\zeta C5(G_{nm1111} - \bar{G}_{nm1111})}{C4} \right] \tag{3.67}$$

$$L_{nm} = \frac{A2_{nm}}{A1_{nm}}Q_{nm} + \frac{A3(\bar{G}_{nm1111} - G_{nm1111})}{2A1_{nm}} \tag{3.68}$$

$$Q1_{nm} = -\frac{1}{\omega_{nm}^2} \left[\frac{1}{2} \frac{C2_{nm}A3(\bar{G}_{nm1111} - G_{nm1111})}{A1_{nm}C4} + \frac{\zeta C5(G_{nm1111} - \bar{G}_{nm1111})}{C4} \right] \tag{3.69}$$

$$L1_{nm} = \frac{A2_{nm}}{A1_{nm}}Q1_{nm} + \frac{A3(\bar{G}_{nm1111} - G_{nm1111})}{2A1_{nm}} \tag{3.70}$$

where the A's, C's and the G's are defined in Appendix A.

Substituting Eqs. (3.51), (3.52), (3.59), and (3.64) into Eqs. (3.49) and (3.50) and applying the solvability conditions, we find that the modulation equations governing the amplitude and phase can be expressed as

$$a' = -\frac{1}{2}Ca + \frac{F}{2\omega_{11}}\sin(\gamma) \tag{3.71}$$

$$a\gamma' = \sigma a + \alpha_e a^3 + \frac{F}{2\omega_{11}}\cos\gamma \tag{3.72}$$

where

$$\gamma = \sigma T_2 - \beta \tag{3.73}$$

and

$$\alpha_e = \frac{1}{2\omega_{11}}\sum_{lj}^{NM}\left\{\frac{A3C2_{11}}{A1_{11}C_4}\left[(l^2+j^2)G_{11lj11} - lj\bar{G}_{11lj11}\right]\left(\frac{Q_{lj}}{2}+Q1_{lj}\right)\right.$$
$$-\frac{C5\zeta}{C4}\left[((l^2+j^2)G_{11lj11} - 2lj\bar{G}_{11lj11})\left(\frac{Q_{nm}}{2}+Q1_{nm}\right)\right]$$
$$\left.-\frac{C5}{C4}\left[((l^2+j^2)G_{11lj11} - 2lj\bar{G}_{11lj11})\left(\frac{L_{nm}}{2}+L1_{nm}\right)\right]\right\} \tag{3.74}$$

3.6   Numerical Results

Next, we use Eqs. (3.71)-(3.73) to compare the results obtained by the direct approach with the single-mode and multi-mode Galerkin approximations obtained in Section 3.3.2. In Fig. 3.35, we consider a cylindrical single-layered shell with the curvatures $k_x = 0.0$ and $k_y = 0.0935$. Clearly, retaining one or two modes in the approximation predicts harding-type nonlinear response, whereas using the direct approach or 16 modes in the approximation predicts a softening-type nonlinear response. It is also shown that the results of the 16-mode Galerkin approximation is in excellent agreement with that obtained with the direct approach.
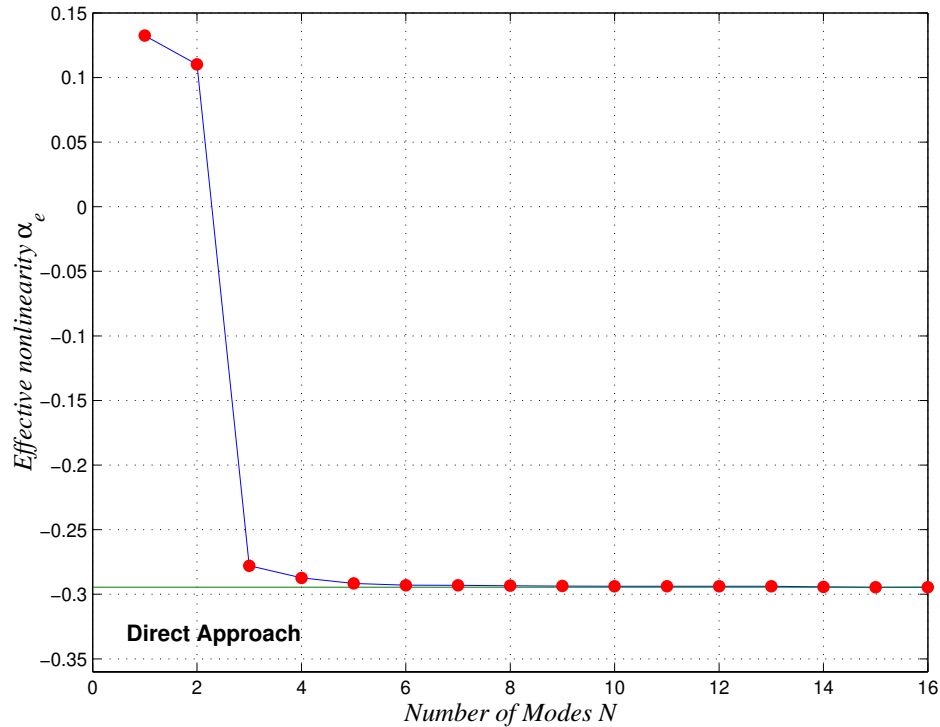
Figure 3.35: Comparison between the effective nonlinearity predicted for cylindrical single-layered shell by using the direct approach with that predicted by using a multi-mode Galerkin approximation when $k_x = 0.0$ and $k_y = 0.0935$.

In another example, we compare in Fig. 3.36 the effective nonlinearity of a doubly cureved single-layered shell with $k_x = 0.1$ and $k_y = -0.194$ obtained by using a multi-mode discretization approximation with the one obtained by using the direct approach. It is clear that, as the number of modes retained in the approximation increases, the difference between the two predicted values decreases.
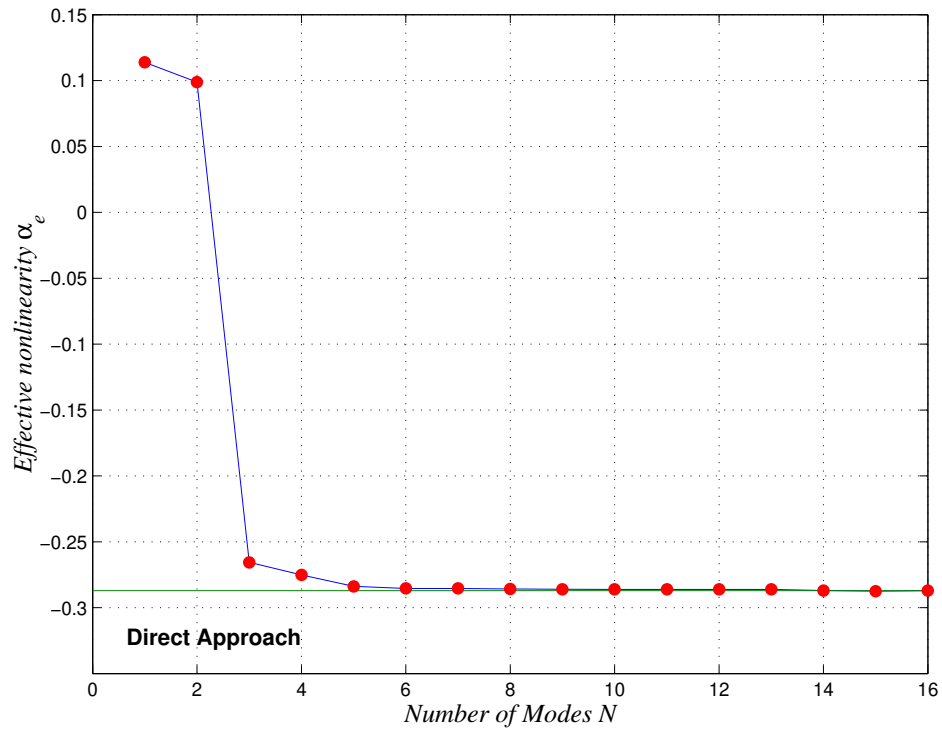
Figure 3.36: Comparison between the effective nonlinearity predicted for a doubly curved single-layered shell by using the direct approach with that predicted by using a multi-mode Galerkin approximation when $k_x = 0.1$ and $k_y = -0.194$.

Chapter 4

Response of a Shallow Shell to a Subharmonic Resonance Excitation

We consider the nonlinear forced vibrations of a doubly curved cross-ply laminated shallow shell with simply supported boundary conditions. We investigate its responses to a subharmonic resonance (i.e., $\Omega \approx 2\omega_{11}$). The nonlinear partial-differential equations governing the motion of the shell are based on the von Kármán-type geometric nonlinear theory and the first-order shear-deformation theory. An approximation based on the Galerkin method is used to reduce the partial-differential equations of motion to an infinite system of nonlinearly coupled second-order ordinary-differential equations. These equations are solved by using the method of multiple scales. Numerical results for isotropic, single-layered, and multi-layered shells are obtained. The influence of the number of modes retained in the discretization and the number of layers on the shell response to a subharmonic resonance excitation is investigated.

4.1 Analysis

The discritized equations of motion for simply supported shallow shells can be expressed as

$$\ddot{W}_{\nu\zeta} + 2\mu_{\nu\zeta}\dot{W}_{\nu\zeta} + \omega_{\nu\zeta}^2 W_{\nu\zeta} + \sum_{n,m}^{\infty}\sum_{l,j}^{\infty} P_{\nu\zeta nmlj} W_{nm}W_{lj} + \sum_{n,m}^{\infty}\sum_{l,j}^{\infty}\sum_{o,p}^{\infty} S_{\nu\zeta nmljop} W_{nm}W_{lj}W_{op}$$

$$= F_{\nu\zeta}\cos(\Omega t)$$

(4.1)

where $P_{\nu\zeta nmlj}$ and $S_{\nu\zeta nmljop}$ are defined in Appendix A. To examine the subharmonic resonance $\Omega \approx 2\omega_{11}$, we need to order the response of the first mode W_{11} as

$$W_{11} = \epsilon W_{11}^{(1)}(T_0, T_1, T_2) + \epsilon^2 W_{11}^{(2)}(T_0, T_1, T_2) + \epsilon^3 W_{11}^{(3)}(T_0, T_1, T_2) + \cdots \qquad (4.2)$$

where ϵ is a bookkeeping parameter, $T_0 = t$ is a fast time scale, and $T_1 = \epsilon t$ and $T_2 = \epsilon^2 t$ are slow time scales describing the time evolution of the amplitudes and phases of the response. The derivatives with respect to time can be expressed as

$$\frac{\partial}{\partial t} = D_0 + \epsilon D_1 + \epsilon^2 D_2 + \cdots \qquad (4.3)$$

$$\frac{\partial^2}{\partial t^2} = D_0^2 + 2\epsilon D_0 D_1 + \epsilon^2(D_1^2 + 2D_0 D_2) + \cdots \qquad (4.4)$$

where $D_i = \frac{\partial}{\partial T_i}$. Since no other mode is assumed to be excited, either directly or indirectly through an internal resonance, the contributions of all of the other modes are of higher order, so we scale them as

$$W_{\nu\zeta} = \epsilon^2 W_{\nu\zeta}^{(2)}(T_0, T_2) + \epsilon^3 W_{\nu\zeta}^{(3)}(T_0, T_2) + \cdots \qquad \nu \text{ and } \zeta \neq 1 \qquad (4.5)$$

In addition, we scale the damping and the forcing such that their influence balances the influence of the nonlinearities, and thus we let

$$\mu_{\nu\zeta} = \epsilon^2 \mu_{\nu\zeta} \qquad (4.6)$$

$$F_{\nu\zeta} = \epsilon^3 f_{\nu\zeta} \tag{4.7}$$

Substituting Eqs. (4.2)-(4.7) into Eq. (4.1) and equating coefficients of like powers of ϵ leads to

Order ϵ

$$D_0^2 W_{11}^{(1)} + \omega_{11}^2 W_{11}^{(1)} = 0 \tag{4.8}$$

Order ϵ^2

$$D_0^2 W_{\nu\zeta}^{(2)} + \omega_{\nu\zeta}^2 W_{\nu\zeta}^{(2)} = -P_{\nu\zeta 1111}\left(W_{11}^{(1)}\right)^2 + f_{\nu\zeta}\cos\left(\Omega T_0\right) \tag{4.9}$$

Order ϵ^3

$$D_0^2 W_{11}^{(3)} + \omega_{11}^2 W_{11}^{(3)} = -2D_0 D_2 W_{11}^{(1)} - 2\mu_{\nu\zeta} D_0 W_{11}^{(1)}$$
$$- \sum_{nm}^{\infty} P_{1111nm} W_{11}^{(1)} W_{nm}^{(2)} - \sum_{nm}^{\infty} P_{11nm11} W_{11}^{(1)} W_{nm}^{(2)} - S_{11111111}\left(W_{11}^{(1)}\right)^3 \tag{4.10}$$

The solution of equation (4.8) can be expressed as

$$W_{11}^{(1)} = A(T_1, T_2)e^{i\omega_{11}T_0} + cc \tag{4.11}$$

where cc stands for the complex conjugate of the preceding terms and $A(T_1, T_2)$ is a complex-valued function determined by eliminating the secular terms from the higher approximations. Substituting Eq. (4.11) into Eq. (4.9) yields

$$D_0^2 W_{\nu\zeta}^{(2)} + \omega_{\nu\zeta}^2 W_{\nu\zeta}^{(2)} = -P_{\nu\zeta 1111}\left(A^2 e^{2i\omega_{11}T_0} + A\bar{A} + cc\right) + f_{\nu\zeta}\cos\left(\Omega T_0\right) \tag{4.12}$$

Since there are no secular terms at this level of approximation, the complex-valued amplitude $A(T_1, T_2)$ is a function of T_2 only.

Solving Eq. (4.12) for $W_{\nu\zeta}^{(2)}$ leads to

$$W_{\nu\zeta}^{(2)} = -P_{\nu\zeta 1111}\left(\frac{A^2 e^{2i\omega_{11}T_0}}{\omega_{\nu\zeta}^2 - 4\omega_{11}^2} + \frac{A\bar{A}}{\omega_{\nu\zeta}^2}\right) + \frac{f_{\nu\zeta}e^{i\Omega T_0}}{2(\omega_{\nu\zeta}^2 - \Omega^2)} + cc \tag{4.13}$$

To describe the nearness of Ω to $2\omega_{11}$, we introduce the detuning parameter σ defined by

$$\Omega = 2\omega_{11} + \epsilon^2\sigma \tag{4.14}$$

Substituting Eqs. (4.11), (4.13) and (4.14) into (4.10) and eliminating the terms that lead to secular terms, we obtain

$$2i\omega_{11}(A' + \mu_{11}A) + \sum_{nm}^{\infty}(P_{1111nm} + P_{11nm11})\left[-P_{nm1111}A^2\bar{A}\left(\frac{1}{\omega_{nm}^2 - 4\omega_{11}^2} + \frac{2}{\omega_{nm}^2}\right)\right.$$
$$\left. + \frac{f_{nm}\bar{A}e^{i\sigma T_2}}{2(\omega_{nm}^2 - 4\omega_{11}^2)}\right] + 3S_{11111111}A^2\bar{A} = 0 \tag{4.15}$$

Next, we express $A(T_2)$ in polar form as

$$A = \frac{1}{2}a(T_2)e^{i\beta(T_2)} \tag{4.16}$$

where $a(T_2)$ is the amplitude and $\beta(T_2)$ is the phase of the response. Differentiating $A(T_2)$ with respect to T_2 leads to

$$A' = \frac{1}{2}a'(T_2)e^{i\beta(T_2)} + \frac{1}{2}ia(T_2)\beta'(T_2)e^{i\beta(T_2)} \tag{4.17}$$

Substituting Eqs. (4.16) and (4.17) into Eq. (4.15) yields

$$(ia' - a\beta' + i\mu_{11}a) + \alpha_e a^3 + f_e a e^{i(\sigma T_2 - 2\beta)} = 0 \tag{4.18}$$

where

$$\alpha_e = \sum_{nm}^{\infty}\frac{1}{8\omega_{11}}(P_{1111nm} + P_{11nm11})\left[P_{nm1111}\left(\frac{1}{\omega_{nm}^2 - 4\omega_{11}^2} + \frac{2}{\omega_{nm}^2}\right)\right] - \frac{3}{8\omega_{11}}S_{11111111} \tag{4.19}$$

$$f_e = \sum_{nm}^{\infty}(P_{1111nm} + P_{11nm11})\left[\frac{f_{nm}}{4\omega_{11}(\omega_{nm}^2 - 4\omega_{11}^2)}\right] \tag{4.20}$$

Next, we let

$$\gamma = \sigma T_2 - 2\beta \tag{4.21}$$

Substituting Eq. (4.21) into Eq. (4.18) and separating real and imaginary parts yields

$$a' = -\mu a + f_e a \sin(\gamma) \tag{4.22}$$

$$\frac{1}{2}a\gamma' = \frac{1}{2}\sigma a + \alpha_e a^3 + f_e a \cos(\gamma) \tag{4.23}$$

4.2   Numerical Results

The effective nonlinearity, Eq. (4.19), is the same as Eq. (3.29) obtained in the case of primary resonance. The effect of the number of retained modes and the number of layers is discussed in the preceding chapter. Next, we use Eq. (4.20) to investigate the influence of the number of terms retained in the Galerkin approximation on the accuracy of the calculated effective forcing.

4.2.1   Effective Forcing

We consider an isotropic shell with the following parameters:

$$\nu_{12} = 0.3, \quad l_x = 1, \quad l_y = 1,$$
$$E_1 = 21 \times 10^9, \quad \frac{G_{12}}{E_1} = 0.79 \tag{4.24}$$

In Fig. 4.1, we show the normalized effective forcing, $\bar{f}_e = f_e(multi-mode)/f_e(single-mode)$, for an isotropic shell with $k_y = 0$. It is clear that the contribution of the second mode is very small when $|k_x| < 0.1$. This contribution increases as $|k_x|$ increases above 0.1. In fact the value of the normalized effective forcing is almost 1.3 when $|k_x| = 0.24$, which indicates that using a single mode underestimates the forcing by about 30%. Increasing $|k_x|$ further results in a larger contribution of the second mode. Due to the singularity resulting from the two-to-one internal resonance, shown in Fig. 3.12, the effective forcing increases very rapidly near $|k_x| = 0.35$. Increasing the number of modes retained in the approximation to three and four, plotted in * and $\cdots$, respectively, we find that the normalized effective forcing remains below 1.3 when $|k_x| < 0.16$. Increasing $|k_x|$ beyond 0.16 increases $\bar{f}_e$ further. These solutions have another singularity near $k_x = 0.23$ because of the $\omega_{31} = 2\omega_{11}$ internal resonance.

Now, we investigate the effect of the number of modes on the effective forcing for a single-

Figure 4.1: Normalized effective forcing for an isotropic shell with $k_y = 0$ using two, three, and four modes.

Figure 4.2: Normalized effective forcing for a single-layered shell with $k_y = 0$ using two, three, and four modes.

layered shell with the following parameters:

$$\frac{E_1}{E_2} = 15.4, \quad \frac{G_{12}}{E_2} = 0.79, \quad \frac{G_{23}}{E_2} = 0.5 \tag{4.25}$$

In Fig. 4.2, we plot the normalized effective forcing for a single-layered shell as a function of k_x with $k_y = 0$ using two, three, and four modes in the approximation. Using two modes produces a very small change in the effective forcing. This change in the effective forcing increases slowly as $|k_x|$ increases and reaches a maximum value of 1.06 when $k_x = 0.4$ and -0.4. Increasing the number of modes retained in the approximation to three produces a large jump in the effective forcing. The normalized effective forcing has a value of 1.32 when $k_x = 0$, which indicates that using a single-mode approximation underestimates the effective forcing by 32.5%. Increasing $|k_x|$ reduces the normalized effective forcing to a minimum value of 1.175 at $|k_x| = 0.28$. Increasing $|k_x|$ further leads to an increase of $\bar{f}_e$ to 1.95 at $|k_x| = 0.4$. Increasing the number of modes retained to four modes has a small effect on the value predicted using three modes. This difference is negligible when $|k_x| < 0.22$. Increasing the number of modes beyond four has a negligible effect.

Since a single-layered shell is asymmetric due to the difference in the stiffnesses in the x and y directions, we plot the normalized effective forcing for a single-layered shell as a function of k_y with $k_x = 0$ using two, three, and four modes, Fig. 4.3. It is clear that using two modes in the approximation, as in the previous case, produces a very small change in the predicted effective forcing. The value of the effective forcing increases slightly as the value of $|k_y|$ increases until it reaches 1.05 when $k_x = 0.4$ and -0.4. Increasing the number of modes retained in the approximation further produces a recognizable difference in the behavior. The normalized effective forcing equals approximately 1.3 when $k_y = 0$. Increasing the absolute value of k_y increases the normalized effective forcing until $k_y = 0.16$, where a singularity occurs due to an internal resonance. When $|k_y| = 0.4$, the value of the normalized effective forcing is 0.86. Reducing $|k_y|$ decreases the normalized effective forcing. We can see that a single-mode approximation may underestimate or overestimate the effective forcing. As in the previous case, increasing the number of modes beyond four has a negligible effect.
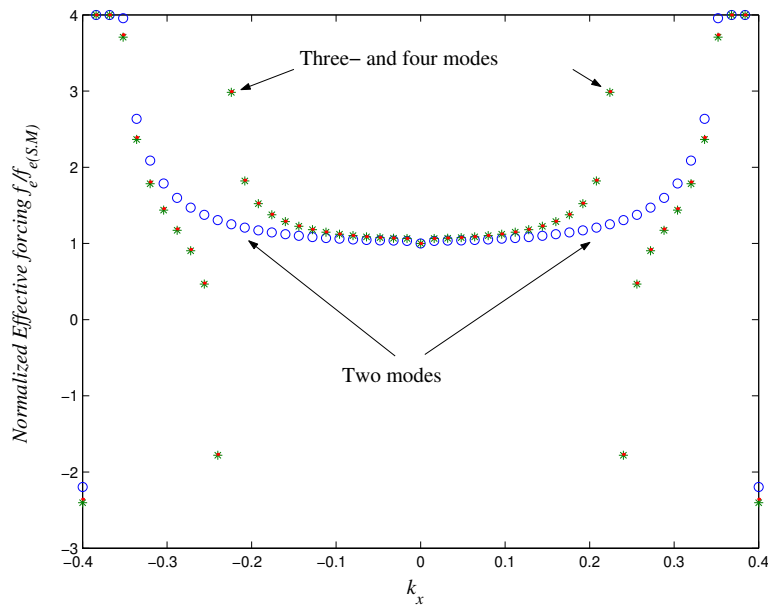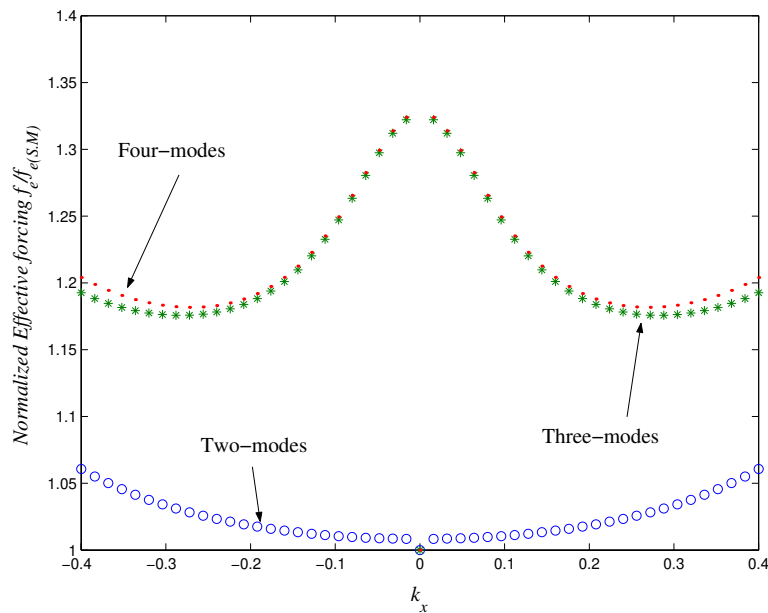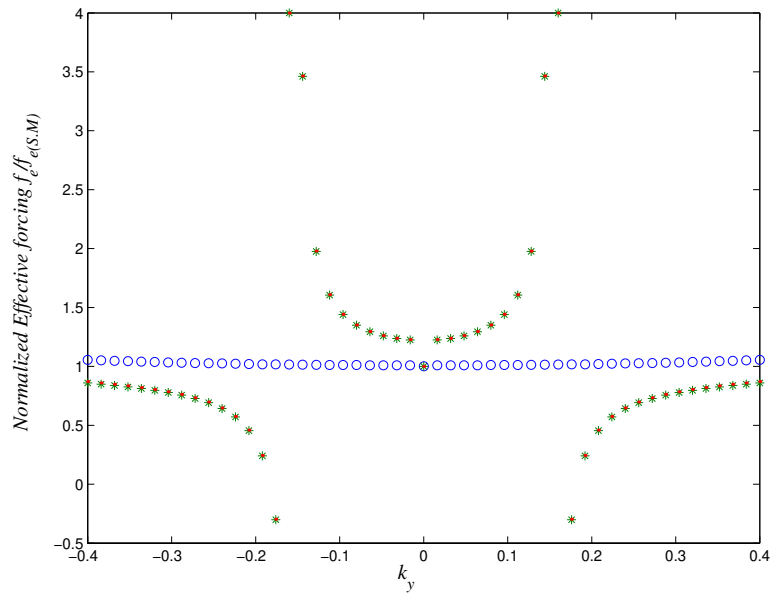
Figure 4.3: Normalized effective forcing for a single-layered shell with $k_x = 0$ using two, three, and four modes.
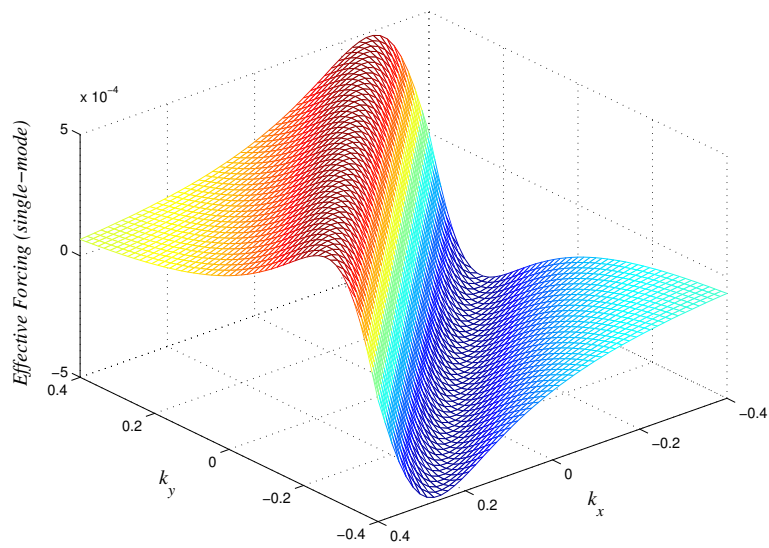
Figure 4.4: Effective forcing of a single-layered shell using a single-mode approximation.
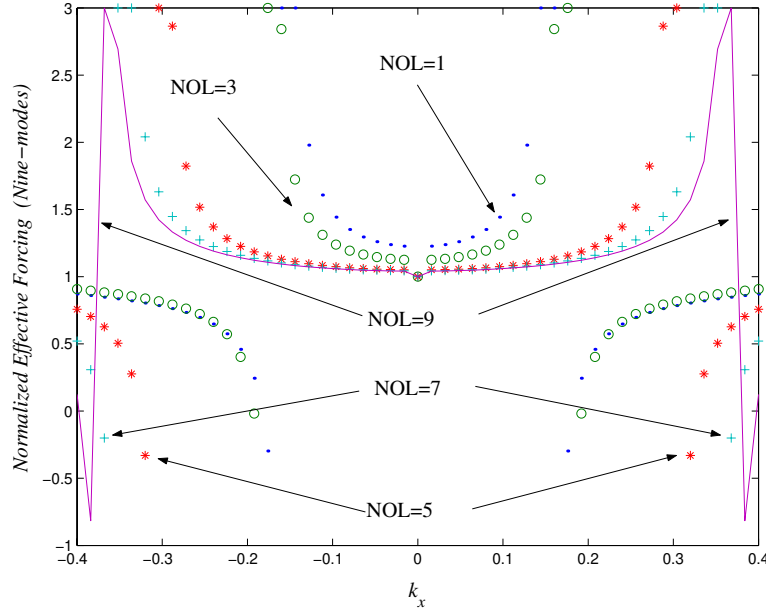
Figure 4.5: Normalized effective forcing obtained using a nine-mode approximation for a multi-layered shell with $k_y = 0$.

To have a better understanding of the behavior of the effective forcing, we plot in Fig. 4.4 the effective forcing for a single-layered shell obtained by using a single-mode approximation in terms of both curvatures, k_x and k_y. It is clear from the figure that the effective forcing depends on the values of the curvatures. The value of the effective forcing is equal to zero along the line $k_x/k_y = -1$. Moving along the line $k_x/k_y = 1$ away from zero results in an increase in f_e to a maximum value of 5×10^{-4} and then a decrease in f_e until it reaches 2×10^{-5}.

Next, we study the effect of changing the number of layers on the calculated effective forcing as a function of k_x when $k_y = 0$. In Fig. 4.5, we plot the normalized effective forcing using nine modes for a shell with 1,3,5,7, and 9 layers. We can see from Fig. 3.28 that increasing the number of layers shifts the internal-resonance singularity. For a single-layered shell, the normalized effective forcing increases as $|k_x|$ increases until it encounters the singularity at $k_x \approx 0.16$. Starting from $|k_x| = 0.4$, we find that the normalized effective forcing decreases as $|k_x|$ is decreased. Increasing the number of layers to 3 shifts the singularity to
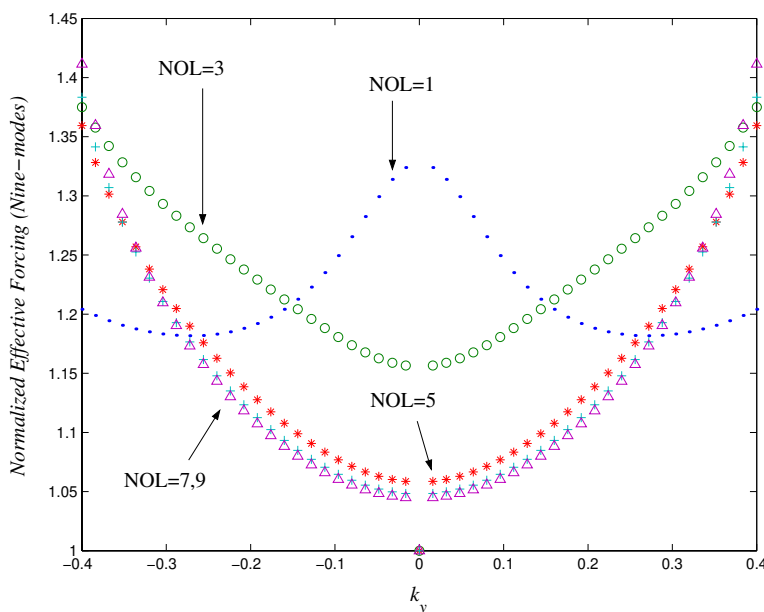
Figure 4.6: Normalized effective forcing obtained using a nine-mode approximation for a multi-layered shell with $k_x = 0$.

$k_x = 0.172$ while the behavior stays the same. Increasing the number of layers further does not change the general behavior of the normalized effective forcing.

Now, we plot in Fig. 4.6 the normalized effective forcing obtained by using nine modes in terms of k_y when $k_x = 0$. For a single-layered shell, the normalized effective forcing has a maximum value of 1.32 at $k_y = 0$. Increasing the value of $|k_y|$ reduces $\bar{f}_e$ until it reaches 1.175 at $|k_y| = 0.28$, where it starts to increase once again. Increasing the number of layers to 3 changes the behavior of the normalized effective forcing. The value of the normalized effective forcing has a minimum value of 1.15 when $k_y = 0$. As $|k_y|$ increases, the normalized effective forcing increases and reaches 1.37 when $k_y = 0.4$ and -0.4. Increasing the number of layers to 5 does not change the behavior, but it reduces the minimum value of $\bar{f}_e$ to 1.06 when $k_y = 0$. As $|k_y|$ increases, $\bar{f}_e$ increases and reaches 1.36 at $k_y = 0.4$ and -0.4. Increasing the number of layers to 7 and 9 slightly changes $\bar{f}_e$ while its behavior remains the same. We can see a change in $\bar{f}_e$ as the number of layers increases from 1 to 3. This change is due to the large change in the stiffness.

(a)

(b)
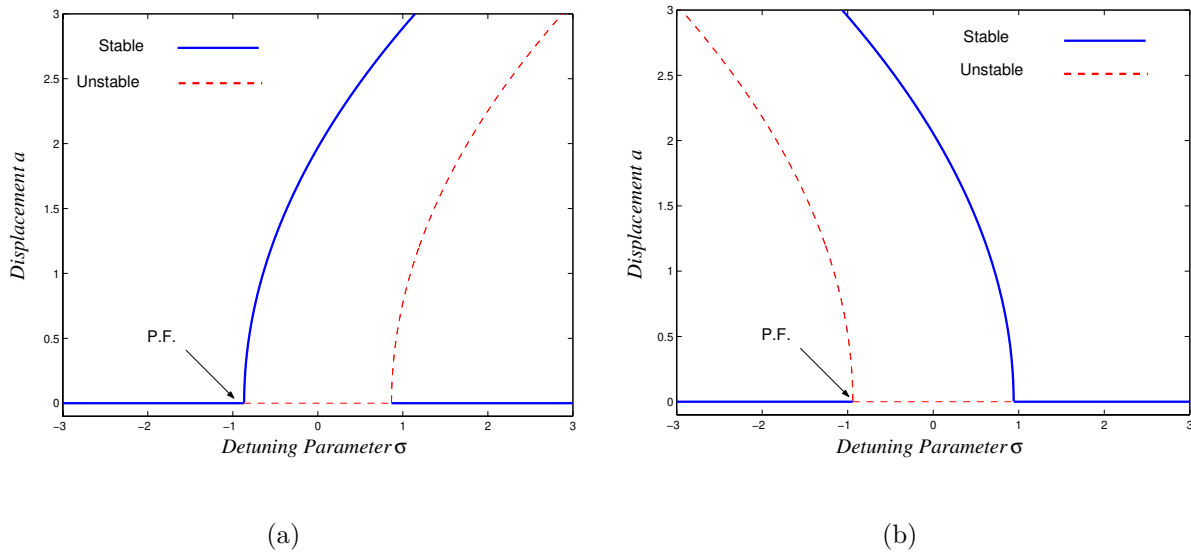
Figure 4.7: Frequency-response curves of a single-layered shell when : (a) single-mode approximation and (b) nine-mode approximation.

4.2.2 Shell Dynamics

Next, we use Eqs. (4.19), (4.20), (4.22), and (4.23) to investigate influence of the number of modes on the predicted shell dynamics. We consider an isotropic shell with the following parameters:

$$\nu_{12} = 0.3, \quad l_x = 1, \quad l_y = 1, \quad f_{11} = 300,$$

$$E_1 = 21 \times 10^9, \quad \frac{G_{12}}{E_1} = 0.79, \quad k_x = 0.0, \quad k_y = 0.05588 \tag{4.26}$$

In Fig. 4.7(a), we plot the frequency-response curves obtained by using a single-mode approximation. The curves are bent to the right, indicating a hardening-type behavior. The solid lines in the figure represent stable solutions, while the dashed lines indicate unstable solutions. When $\sigma < -0.94$, there is only one solution, the trivial solution, which is stable.

(a)   (b)
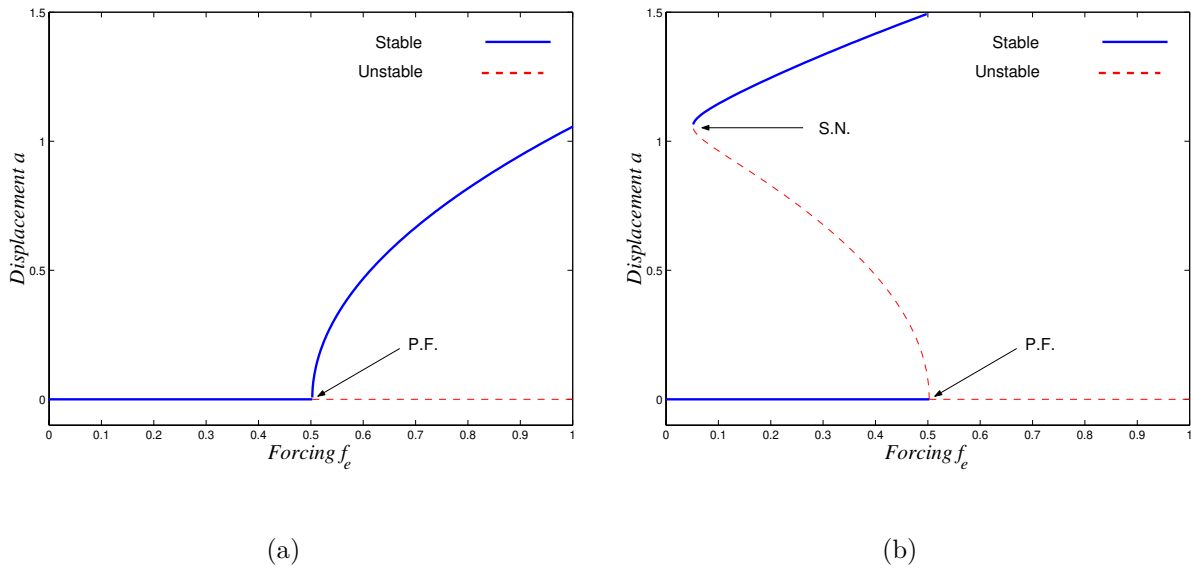
Figure 4.8: Force-response curves of a single-layered shell when $k_x = 0.0$ and $k_y = 0.05588$ using a single-mode approximation: (a) $\sigma = -1$ and (b) $\sigma = 1$.

When $-0.94 < \sigma < 0.94$, there are two possible solutions, the trivial solution, which is unstable, and a nontrivial solution, which is stable,. When $\sigma > 0.94$, there are three possible solutions: a trivial, which is stable, and two nontrivial solutions, the larger of which is stable and the smaller is unstable. In this interval, the response may be trivial or nontrivial, depending on the initial conditions. At large values of σ, the response homes on the trivial solution for small initial conditions. Decreasing σ below the subcritical pitchfork bifurcation at $\sigma = 0.94$ results in a jump in the response to the upper stable solution. A further decrease in σ results in a decrease in the response amplitude a until the left bifurcation point (a supercritical pitchfork bifurcation) is reached , where a homes on the trivial solution.

In Fig. 4.7(b), we increase the number of modes retained in the approximation to 9. Now, the frequency-response curves are bent to left, indicating a softening-type behavior. As in the case of primary resonance, the low-order discretization approach produces erroneous qualitative and quantitative frequency-response curves in the case of subharmonic resonance.

(a)

(b)
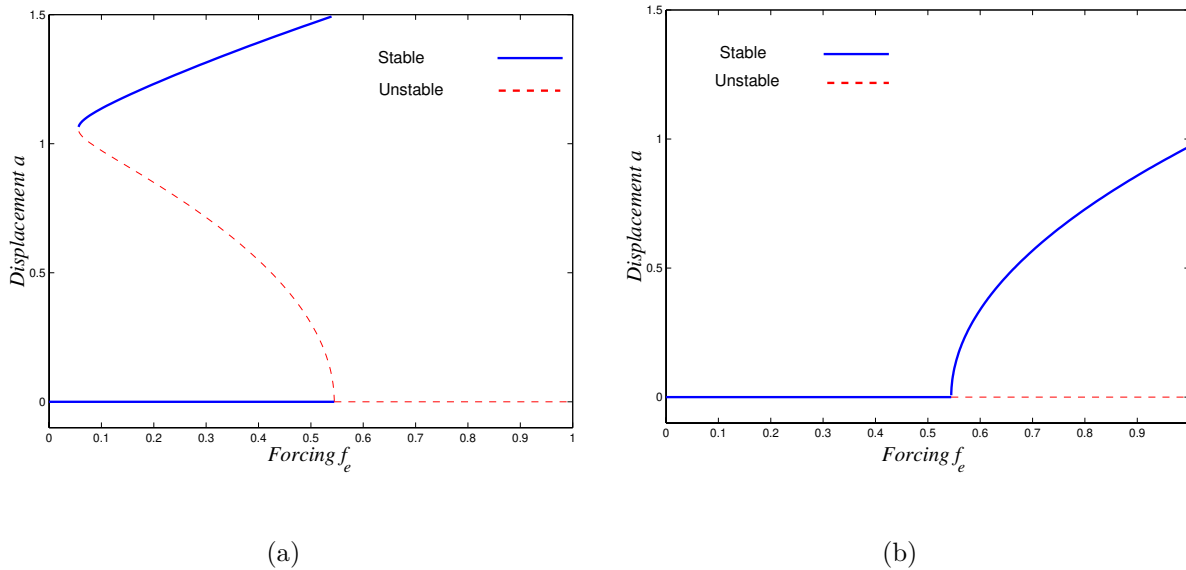
Figure 4.9: Force-response curves of a single-layered shell when $k_x = 0.0$ and $k_y = 0.05588$ using a nine-mode approximation: (a) $\sigma = -1$ and (b) $\sigma = 1$.

Next, we show in Fig. 4.8(a) typical force-response curves for the same shell using a single-mode approximation when $\sigma = 1$. There are two bifurcations: a saddle-node bifurcation at $f_e = 0.05$ and a subcritical pitchfork bifurcation at $f_e = 0.5$. In the interval $0.05 < f_e < 0.5$, there are three solutions: a trivial, which is stable and two nontrivial solutions, the larger of which is stable. In this interval, the response may be trivial or nontrivial, depending on the initial conditions. When $f_e > 0.5$, there are two solutions, the trivial solution, which is unstable and a nontrivial solution, which is stable. when $f_e < 0.05$, the response is always trivial.

Now, we plot in Fig. 4.8(b) the force-response curve when $\sigma = -1$. There are two branches of solutions: trivial and nontrivial. The trivial solution is stable when $f_e < 0.5$ and unstable when $f_e > 0.5$. The nontrivial solution starts from the supercritical pitchfork bifurcation at $\sigma = 0.5$. When $f_e < 0.5$, the response homes on the trivial solution. Increasing f_e beyond the bifurcation point results in a smooth increase in the amplitude a. When $f_e > 0.5$, the response homes on the nontrivial solution. Decreasing f_e results in a decrease in a. At the
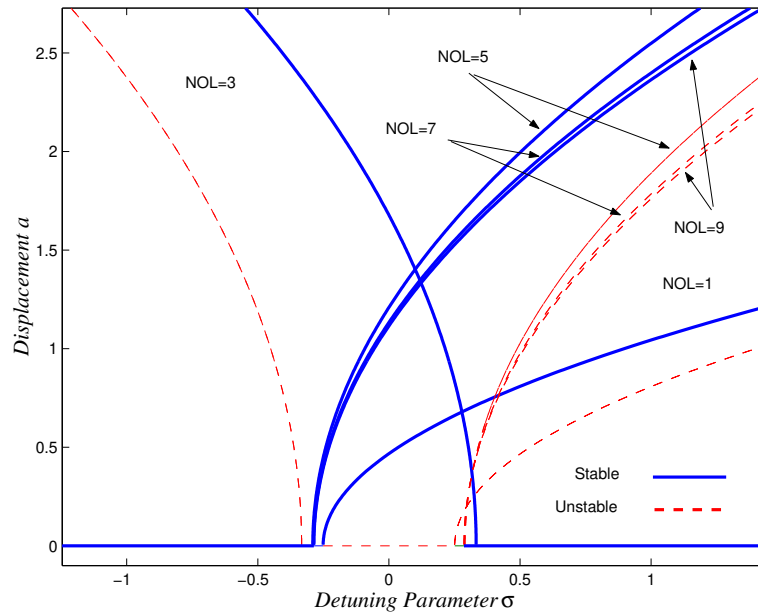
Figure 4.10: Frequency-response curves for a multi-layered shell when $k_x = 0$ and $k_y = 0.075$.

bifurcation point, the response transfers smoothly to the trivial solution. In this case, the system does not experience any jumps in either the backward or forward sweeps of f_e.

In Figs. 4.9(a) and 4.9(b), we plot the force-response curves obtained using nine modes in the approximation. These figures are qualitatively similar to Figs. 4.8(a) and 4.8(b) except that the curve with negative detuning is similar to the curve with negative detuning. In Fig. 4.9, the pitchfork bifurcation occurs at $f_e = 0.544$ and the saddle-node bifurcation occurs at $f_e = 0.055$. This shift in the position of the bifurcation points is the result of the predicted effective forcing.

Next, we study the effect of the number of layers on the shell dynamics obtained using nine-mode approximation. In Fig. 4.10, we plot the frequency-response curves for a multi-layered shell when $k_x = 0$ and $k_y = 0.075$ with 1, 3, 5, 7, and 9 layers. The single-layered frequency response curve is bent to the left, indicating a hardening-type behavior. Increasing the number of layers to 3 results in a quantitative change in the behavior. Increasing the number of layers to 5, 7, 9 results in another quantitative change in the behavior. This

quantitative change in the behavior is due to the change in the stiffness.

Chapter 5

Two-to-One Internal Resonance

In this chapter, we consider the nonlinear vibrations of a doubly curved cross-ply shallow shell with simply supported boundary conditions in the case of two-to-one internal resonance $\omega_{13} \approx 2\omega_{11}$. We investigate its responses for two cases of primary resonance: $\Omega \approx \omega_{13}$ and $\Omega \approx \omega_{11}$. We use the Galerkin procedure to discretize the governing nonlinear partial-differential equations of motion and obtain a reduced-order system of coupled nonlinear ordinary-differential equations. We apply the method of multiple scales to the discretized system to obtain the modulation equations governing the slow dynamics of the shell. A pseudo-arclength scheme is used to determine the fixed points of the modulation equations and then determine the stability of these points. We investigate the effect of the number of modes retained in the approximation on the predicted responses. A combination of a shooting technique and Floquet theory is used to determine the detailed solution branches and their stability. We found that, in some cases, the fixed points undergo Hopf bifurcations, which result in dynamic solutions. We use long-time integration to calculate chaotic solutions. The limit cycles may undergo symmetry-breaking, saddle-node, and period-doubling bifurcations. Furthermore, we found that neglecting the effect of the modes not involved in the internal resonance may produce erroneous dynamic responses.

5.1   Analysis

The discretized equations of motion for a simply supported shell can be expressed as

$$\ddot{W}_{\eta\nu} + 2\mu_{\eta\nu}\dot{W}_{\eta\nu} + \omega_{\eta\nu}^2 W_{\eta\nu} + \sum_{n,m}^{\infty}\sum_{l,j}^{\infty} P_{\eta\nu nmlj}W_{nm}W_{lj} + \sum_{n,m}^{\infty}\sum_{l,j}^{\infty}\sum_{o,p}^{\infty} S_{\eta\nu nmliop}W_{nm}W_{lj}W_{op}$$

$$= F_{\eta\nu}\cos(\Omega t)$$

$$(5.1)$$

Because of the presence of a two-to-one internal resonance, we need to carry out the expansion to second order to account for the nonlinear shifts in the frequencies. Applying the method of multiple scales to the second-order system, such as Eq. (5.1), can lead to modulation equations not derivable from a Lagrangian in the absence of damping and excitation. This problem can be overcome by transforming the system to a first-order form and then treating it with the method of multiple scales (Nayfeh, 2000). Then, the method of reconstitution (Nayfeh, 1985) is used to derive the modulation equations. Thus, we let

$$\dot{W}_{ij} = v_{ij} \tag{5.2}$$

Substituting Eq. (5.2) into Eq. (5.1) gives

$$v_{\eta\nu} - \dot{W}_{\eta\nu} = 0 \tag{5.3}$$

$$\dot{v}_{\eta\nu} + 2\mu_{\eta\nu}v_{\eta\nu} + \omega_{\eta\nu}^2 W_{\eta\nu} + \sum_{n,m}^{\infty}\sum_{l,j}^{\infty} P_{\eta\nu nmlj}W_{nm}W_{lj} + \sum_{n,m}^{\infty}\sum_{l,j}^{\infty}\sum_{o,p}^{\infty} S_{\eta\nu nmliop}W_{nm}W_{lj}W_{op}$$

$$= F_{\eta\nu}\cos(\Omega t) \quad (5.4)$$

To examine the two-to-one internal resonance $\omega_{13} \approx 2\omega_{11}$, we seek an approximation of the interacting modes W_{11} and W_{13} and the noninteracting modes (modes not involved in the internal resonance) as

$$W_{11} = \epsilon W_{11}^{(1)}(T_0, T_1, T_2) + \epsilon^2 W_{11}^{(2)}(T_0, T_1, T_2) + \epsilon^3 W_{11}^{(3)}(T_0, T_1, T_2) + \cdots \tag{5.5}$$

$$v_{11} = \epsilon v_{11}^{(1)}(T_0, T_1, T_2) + \epsilon^2 v_{11}^{(2)}(T_0, T_1, T_2) + \epsilon^3 v_{11}^{(3)}(T_0, T_1, T_2) + \cdots \tag{5.6}$$

$$W_{13} = \epsilon W_{13}^{(1)}(T_0, T_1, T_2) + \epsilon^2 W_{13}^{(2)}(T_0, T_1, T_2) + \epsilon^3 W_{13}^{(3)}(T_0, T_1, T_2) + \cdots \tag{5.7}$$

$$v_{13} = \epsilon v_{13}^{(1)}(T_0, T_1, T_2) + \epsilon^2 v_{13}^{(2)}(T_0, T_1, T_2) + \epsilon^3 v_{13}^{(2)}(T_0, T_1, T_2) + \cdots \tag{5.8}$$

$$W_{\eta\nu} = \epsilon^2 W_{\eta\nu}^{(2)}(T_0, T_1, T_2) + \epsilon^3 W_{\eta\nu}^{(3)}(T_0, T_1, T_2) + \cdots \qquad \eta \neq 1, \nu \neq 1, 3 \tag{5.9}$$

$$v_{\eta\nu} = \epsilon^2 v_{\eta\nu}^{(2)}(T_0, T_1, T_2) + \epsilon^3 v_{\eta\nu}^{(2)}(T_0, T_1, T_2) + \cdots \qquad \eta \neq 1, \nu \neq 1, 3 \tag{5.10}$$

where ϵ is a bookkeeping parameter, $T_0 = t$ is a fast time scale, and $T_1 = \epsilon t$ and $T_2 = \epsilon^2 t$ are slow time scales describing the time evolution of the amplitudes and phases of the response. The derivative with respect to time can be expressed as

$$\frac{\partial}{\partial t} = D_0 + \epsilon D_1 + \epsilon^2 D_2 + \cdots \tag{5.11}$$

where $D_i = \frac{\partial}{\partial T_i}$. We scale the forcing and damping terms as

$$\mu_{\eta\nu} = \epsilon^2 \mu_{\eta\nu} \tag{5.12}$$

$$F_{11} = \epsilon^2 f_{11} \tag{5.13}$$

$$F_{13} = \epsilon^2 f_{13} \tag{5.14}$$

$$F_{\eta\nu} = \epsilon^3 f_{\eta\nu} \qquad \eta \neq 1, \nu \neq 1, 3 \tag{5.15}$$

Substituting Eqs. (5.5)-(5.15) into Eqs. (5.3) and (5.4) and equating coefficients of like powers of ϵ leads to

Order ϵ

$$D_0 W_{11}^{(1)} - v_{11}^{(1)} = 0 \tag{5.16}$$

$$D_0 v_{11}^{(1)} - \omega_{11}^2 W_{11}^{(1)} = 0 \tag{5.17}$$

$$D_0 W_{13}^{(1)} - v_{13}^{(1)} = 0 \tag{5.18}$$

$$D_0 v_{13}^{(1)} - \omega_{13}^2 W_{13}^{(1)} = 0 \tag{5.19}$$

Order ϵ^2

$$D_0 W_{11}^{(2)} - v_{11}^{(2)} = -D_1 W_{11}^{(1)} \tag{5.20}$$

$$D_0 v_{11}^{(2)} - \omega_{11}^2 W_{11}^{(2)} = -D_1 v_{11}^{(1)} - \sum_{m,j=1}^{3} P_{111m1j} W_{1m}^{(1)} W_{1j}^{(1)} + f_{11} \cos(\Omega T_0) \tag{5.21}$$

$$D_0 W_{13}^{(2)} - v_{13}^{(2)} = -D_1 W_{13}^{(1)} \tag{5.22}$$

$$D_0 v_{13}^{(2)} - \omega_{13}^2 W_{13}^{(2)} = -D_1 v_{13}^{(1)} - \sum_{m,j=1}^{3} P_{131m1j} W_{1m}^{(1)} W_{1j}^{(1)} + f_{13} \cos(\Omega T_0) \tag{5.23}$$

$$D_0 W_{\eta\nu}^{(2)} - v_{\eta\nu}^{(2)} = 0 \tag{5.24}$$

$$D_0 v_{\eta\nu}^{(2)} - \omega_{\eta\nu}^2 W_{\eta\nu}^{(2)} = - \sum_{n,m=1}^{\infty} \sum_{l,j=1}^{\infty} P_{\eta\nu nmlj} W_{nm}^{(1)} W_{lj}^{(1)} \qquad \eta \neq 1, \nu \neq 1,3 \tag{5.25}$$

Order ϵ^3

$$D_0 W_{11}^{(3)} - v_{11}^{(3)} = - D_1 W_{11}^{(2)} - D_2 W_{11}^{(1)} \tag{5.26}$$

$$D_0 v_{11}^{(3)} - \omega_{11}^2 W_{11}^{(3)} = - D_1 v_{11}^{(2)} - D_2 v_{11}^{(1)} - 2\mu_{11} D_0 v_{11}^{(1)}$$
$$- \sum_{m=1}^{3} \sum_{l,j=1}^{\infty} P_{111mlj} W_{1m}^{(1)} W_{lj}^{(2)} - \sum_{m=1}^{3} \sum_{j=1}^{3} \sum_{p=1}^{3} S_{111m1j1p} W_{1m}^{(1)} W_{1j}^{(1)} W_{1p}^{(1)}$$
$$\tag{5.27}$$

$$D_0 W_{13}^{(3)} - v_{13}^{(3)} = - D_1 W_{13}^{(2)} - D_2 W_{13}^{(1)} \tag{5.28}$$

$$D_0 v_{13}^{(3)} - \omega_{13}^2 W_{13}^{(3)} = - D_1 v_{13}^{(2)} - D_2 v_{13}^{(1)} - 2\mu_{13} D_0 v_{13}^{(1)}$$
$$- \sum_{m=1}^{3} \sum_{l,j=1}^{\infty} P_{131mlj} W_{1m}^{(1)} W_{lj}^{(2)} - \sum_{m=1}^{3} \sum_{j=1}^{3} \sum_{p=1}^{3} S_{131m1j1p} W_{1m}^{(1)} W_{1j}^{(1)} W_{1p}^{(1)}$$
$$\tag{5.29}$$

The solution of Eqs. (5.16)-(5.19) can be expressed as

$$W_{11}^{(1)} = A_{11}(T_1, T_2) e^{i\omega_{11} T_0} + cc \tag{5.30}$$

$$W_{13}^{(1)} = A_{13}(T_1, T_2) e^{i\omega_{13} T_0} + cc \tag{5.31}$$

$$v_{11}^{(1)} = i\omega_{11}A_{11}(T_1, T_2)e^{i\omega_{11}T_0} + cc \tag{5.32}$$

$$v_{13}^{(1)} = i\omega_{13}A_{13}(T_1, T_2)e^{i\omega_{13}T_0} + cc \tag{5.33}$$

where cc stands for the complex conjugate of the preceding terms and $A_1(T_1, T_2)$ and $A_2(T_1, T_2)$ are complex-valued functions determined by eliminating the secular terms at the higher levels of approximation.

Substituting Eqs. (5.30)-(5.33) into Eqs. (5.20)-(5.25) yields

$$D_0 W_{11}^{(2)} - v_{11}^{(2)} = - D_1 A_{11}e^{i\omega_{11}T_0} + cc \tag{5.34}$$

$$D_0 v_{11}^{(2)} - \omega_{11}^2 W_{11}^{(2)} = - i\omega_{11}D_1 A_{11}e^{i\omega_{11}T_0}$$
$$- \sum_{m,j=1}^{3} P_{111m1j}\left[A_{1m}A_{1j}e^{i(\omega_{1m}+\omega_{1j})T_0} + A_{1m}\bar{A}_{1j}e^{i(\omega_{1m}-\omega_{1j})T_0}\right]$$
$$+ \frac{f_{11}}{2}e^{i\Omega T_0} + cc \tag{5.35}$$

$$D_0 W_{13}^{(2)} - v_{13}^{(2)} = - D_1 A_{11}e^{i\omega_{13}T_0} + cc \tag{5.36}$$

$$D_0 v_{13}^{(2)} - \omega_{13}^2 W_{13}^{(2)} = - i\omega_{13}D_1 A_{13}e^{i\omega_{13}T_0}$$
$$- \sum_{m,j=1}^{3} P_{131m1j}\left[A_{1m}A_{1j}e^{i(\omega_{1m}+\omega_{1j})T_0} + A_{1m}\bar{A}_{1j}e^{i(\omega_{1m}-\omega_{1j})T_0}\right]$$
$$+ \frac{f_{13}}{2}e^{i\Omega T_0} + cc \tag{5.37}$$

$$D_0 W_{\eta\nu}^{(2)} - v_{\eta\nu}^{(2)} = 0 \tag{5.38}$$

$$D_0 v_{\eta\nu}^{(2)} - \omega_{\eta\nu}^2 W_{\eta\nu}^{(2)} = - \sum_{n,m=1}^{\infty}\sum_{l,j=1}^{\infty} P_{\eta\nu nmlj}\left[A_{nm}A_{lj}e^{i(\omega_{nm}+\omega_{lj})T_0} + A_{nm}\bar{A}_{lj}e^{i(\omega_{nm}-\omega_{lj})T_0}\right]$$
$$+ cc \qquad \eta \neq 1, \nu \neq 1, 3 \tag{5.39}$$

Next, we consider two cases: $\Omega \approx \omega_{13}$ and $\Omega \approx \omega_{11}$.

5.2   Primary Resonance of the Higher-Frequency Mode

We introduce the detuning parameters σ_1 and σ_2 defined by

$$\omega_{13} = 2\omega_{11} + \epsilon\sigma_1 \tag{5.40}$$

$$\Omega = \omega_{13} + \epsilon\sigma_2 \tag{5.41}$$

Substituting Eqs. (5.40) and (5.41) into Eqs. (5.34)-(5.39) and eliminating the terms that produce secular terms, we obtain

$$2i\omega_{11}D_1A_{11} = -(P_{111113} + P_{111311})\bar{A}_{11}A_{13}e^{i\sigma_1 T_1} \tag{5.42}$$

$$2i\omega_{13}D_1A_{13} = -P_{131111}A_{11}^2 e^{-i\sigma_1 T_1} + \frac{f_{13}}{2}e^{i\sigma_2 T_1} \tag{5.43}$$

Then, the solution of the second-order equations (5.20)-(5.25) can be written as

$$
\begin{aligned}
W_{11}^{(2)} = \frac{1}{\omega_{11}^2}\Bigg[&-\frac{1}{4}\bar{A}_{13}A_{11}P_{111113}e^{i(\omega_{11}-\omega_{13})T_0} - \frac{1}{4}\bar{A}_{13}A_{11}P_{111311}e^{-i(\omega_{13}-\omega_{11})T_0} \\
&+\frac{1}{8}A_{13}A_{11}P_{111113}e^{i(\omega_{13}+\omega_{11})T_0} + \frac{1}{8}A_{13}A_{11}P_{111311}e^{i(\omega_{13}+\omega_{11})T_0} - \frac{1}{6}f_{13}e^{i\Omega T_0} - \frac{1}{6}e^{-i\Omega T_0}f_{11} \\
&- 2P_{111111}\bar{A}_{11}A_{11} + \frac{1}{3}e^{2i\omega_{11}T_0}P_{111111}A_{11}^2 + \frac{1}{15}e^{-2i\omega_{13}T_0}P_{111313}\bar{A}_{13}^2 + \frac{1}{15}e^{2i\omega_{13}T_0}P_{111313}A_{13}^2 \\
&+\frac{1}{3}e^{-2i\omega_{11}T_0}P_{111111}\bar{A}_{11}^2 + \frac{1}{8}\bar{A}_{13}\bar{A}_1 P_{111113}e^{-i(\omega_{13}+\omega_{11})T_0} + \frac{1}{8}\bar{A}_{13}\bar{A}_{11}P_{111311}e^{-i(\omega_{13}-\omega_{11})T_0} \\
&- 2P_{111313}\bar{A}_{13}A_{13} - \frac{1}{4}A_{13}\bar{A}_{11}P_{111113}e^{i(\omega_{13}-\omega_{11})T_0} - \frac{1}{4}A_{13}\bar{A}_{11}P_{111311}e^{i(\omega_{13}-\omega_{11})T_0}\Bigg] \tag{5.44}
\end{aligned}
$$

$$
\begin{aligned}
v_{11}^{(2)} = \frac{i}{\omega_{11}}\Bigg[&-\frac{2}{3}e^{-2i\omega_{11}T_0}P_{111111}\bar{A}_{11}^2 + \frac{1}{3}e^{-i\Omega T_0}f_{13} + \frac{1}{4}A_{13}\bar{A}_{11}P_{111113}e^{i(\omega_{13}-\omega_{11})T_0} \\
&+\frac{1}{4}A_{13}\bar{A}_{11}P_{111311}e^{i(\omega_{13}-\omega_1)T_0} - \frac{1}{3}f_{13}e^{i\Omega T_0} - \frac{4}{15}e^{-2i\omega_{13}T_0}P_{111313}\bar{A}_{13}^2 \\
&-\frac{1}{4}\bar{A}_{13}A_{11}P_{111113}e^{-i(\omega_{13}+\omega_{11})T_0} - \frac{1}{4}\bar{A}_{13}A_{11}P_{111311}e^{-i(\omega_{13}-\omega_{11})T_0} + \frac{4}{15}e^{2i\omega_{13}T_0}P_{111313}A_{13}^2 \\
&+\frac{3}{8}A_{13}A_{11}P_{111113}e^{i(\omega_{13}+\omega_{11})T_0} + \frac{3}{8}A_{13}A_{11}P_{111311}e^{i(\omega_{13}+\omega_{11})T_0} + \frac{2}{3}e^{2i\omega_{11}T_0}P_{111111}A_{11}^2 \\
&-\frac{3}{8}\bar{A}_{13}\bar{A}_{11}P_{111113}e^{-i(\omega_{13}+\omega_{11})T_0} - \frac{3}{8}\bar{A}_{13}\bar{A}_{11}P_{111311}e^{-i(\omega_{13}+\omega_{11})T_0}\Bigg] \tag{5.45}
\end{aligned}
$$

$$W_{13}^{(2)} = \frac{1}{\omega_{11}^2} \Bigg[-\frac{1}{16} e^{2i\omega_{11}T_0} P_{131111} A_{11}{}^2 - \frac{1}{16} e^{-2i\omega_{11}T_0} P_{131111} \bar{A}_{11}^2 + \frac{1}{12} e^{-2i\omega_{13}T_0} P_{131313} \bar{A}_{13}^2$$

$$+ \frac{1}{12} e^{2i\omega_2 T_0} P_{131313} A_{13}{}^2 + \frac{1}{5} A_{13} A_{11} P_{131311} e^{i(\omega_{13}+\omega_{11})T_0} + \frac{1}{5} A_{13} A_{11} P_{131113} e^{i(\omega_{13}+\omega_{11})T_0}$$

$$- \frac{1}{3} A_{13} \bar{A}_{11} P_{131311} e^{i(\omega_{13}-\omega_{11})T_0} - \frac{1}{3} A_{13} \bar{A}_{11} P_{131113} e^{i(\omega_{13}-\omega_{11})T_0} + \frac{1}{5} \bar{A}_{13} \bar{A}_{11} P_{131311} e^{-i(\omega_{13}+\omega_{11})T_0}$$

$$+ \frac{1}{5} \bar{A}_{13} \bar{A}_{11} P_{131113} e^{-i(\omega_{13}+\omega_{11})T_0} - \frac{1}{2} P_{131111} \bar{A}_{11} A_{11} - \frac{1}{2} P_{131313} \bar{A}_{13} A_{13}$$

$$- \frac{1}{3} \bar{A}_{13} A_{11} P_{131311} e^{-i(\omega_{13}-\omega_{11})T_0} - \frac{1}{3} \bar{A}_{13} A_{11} P_{131113} e^{-i(\omega_{13}-\omega_{11})T_0} + \frac{1}{32} f_{13} e^{i\Omega T_0}$$

$$+ \frac{1}{32} f_{13} e^{-i\Omega T_0} \Bigg] \tag{5.46}$$

$$v_{13}^{(2)} = \frac{i}{\omega_{11}} \Bigg[\frac{1}{3} \bar{A}_{13} A_{11} P_{131311} e^{-i(\omega_{13}-\omega_{11})T_0} + \frac{1}{3} \bar{A}_{13} A_{11} P_{131113} e^{-i(\omega_{13}-\omega_{11})T_0}$$

$$+ \frac{1}{3} e^{2i\omega_{13}T_0} P_{131313} A_{13}^2 - \frac{1}{3} A_{13} \bar{A}_{11} P_{131113} e^{i(\omega_{13}-\omega_{11})T_0} - \frac{3}{5} \bar{A}_{13} \bar{A}_{11} P_{131311} e^{-i(\omega_{13}+\omega_{11})T_0}$$

$$- \frac{3}{5} \bar{A}_{13} \bar{A}_{11} P_{131113} e^{-i(\omega_{13}+\omega_{11})T_0} - \frac{1}{3} e^{-2i\omega_{13}T_0} P_{131313} \bar{A}_{13}^2 + \frac{3}{5} A_{13} A_{11} P_{131311} e^{i(\omega_{13}+\omega_1)T_0}$$

$$+ \frac{3}{5} A_{13} A_{11} P_{131113} e^{i(\omega_{13}+\omega_{11})T_0} - \frac{1}{3} A_{13} \bar{A}_{11} P_{131311} e^{i(\omega_{13}-\omega_{11})T_0} \Bigg] +$$

$$\frac{i}{\omega_{11}^2} \Bigg[\frac{1}{16} e^{2i\omega_{11}T_0} \omega_{13} P_{131111} A_{11}{}^2 - \frac{1}{32} \omega_{13} f_{13} e^{i\Omega T_0} + \frac{1}{32} f_{13} \omega_{13} e^{-i\Omega T_0}$$

$$- \frac{1}{16} e^{-2i\omega_{11}T_0} \omega_{13} P_{131111} \bar{A}_{11}^2 \Bigg] \tag{5.47}$$

$$W_{\eta\nu}^{(2)} = - \sum_{n,m=1}^{3} \sum_{l,j=1}^{3} P_{\eta\nu nmlj} \Bigg[\frac{A_{nm} A_{lj} e^{i(\omega_{nm}+\omega_{lj})T_0}}{\omega_{\eta\nu}^2 - (\omega_{nm}+\omega_{lj})^2} + \frac{A_{nm} \bar{A}_{lj} e^{i(\omega_{nm}-\omega_{lj})T_0}}{\omega_{\eta\nu}^2 - (\omega_{nm}-\omega_{lj})^2} \Bigg]$$

$$+ cc \qquad \eta \neq 1, \nu \neq 1,3 \tag{5.48}$$

Substituting Eqs. (5.30)- (5.33) and (5.44)-(5.48) into Eqs. (5.26)-(5.29) and eliminating the terms that produce secular terms, we obtain

$$2i\omega_{11} D_2 A_{11} = i\Xi_1 A_{11} + \Xi_2 A_{11}{}^2 \bar{A}_{11} + \Xi_3 A_1 A_{13} \bar{A}_{13} + \Xi_4 e^{i(\sigma_1+\sigma_2)T_1} \bar{A}_{11} \tag{5.49}$$

$$2i\omega_{13} D_2 A_{13} = \xi_1 A_{11} \bar{A}_{11} A_{13} + i\xi_2 A_{13} + \xi_3 A_{13}^2 \bar{A}_{13} \tag{5.50}$$

where the ξ_i and Ξ_j are defined as

$$\xi_1 = \frac{1}{15\omega_{13}^2}\varepsilon^2(60P_{131313}P_{131111} + 15P_{111311}P_{131111} + 15P_{111113}P_{131111} + 120P_{131311}P_{111111}$$

$$+ 8P_{131311}^2 - 30S_{13131111}\omega_{13}^2 - 30S_{2112}\omega_{13}^2 - 30S_{13111311}\omega_{13}^2 + 8P_{131113}^2$$

$$+ 16P_{131311}P_{131113} + 120P_{131113}P_{111111})$$

$$- \sum_{n,m}^{\infty}\left[\frac{2P_{nm1111}(P_{13nm11} + P_{1311nm})}{\omega_{nm}^2} + \frac{(P_{13nm11} + P_{1311nm})(P_{nm1113} + P_{nm1311})}{\omega_{nm}^2 + (\omega_{11} - \omega_{13})^2}\right.$$

$$\left. + \frac{(P_{13nm13} + P_{1313nm})(P_{nm1113} + P_{nm1311})}{\omega_{nm}^2 - (\omega_{11} + \omega_{13})^2}\right] \tag{5.51}$$

$$\xi_2 = -2\omega_{13}\mu_2\varepsilon^2 \tag{5.52}$$

$$\xi_3 = \frac{1}{15\omega_{13}^2}\varepsilon^2(116P_{111313}P_{131311} - 45S_{13131313}\omega_{13}^2 + 50P_{131313}^2 + 116P_{111313}P_{131113})$$

$$+ \sum_{nm}^{\infty}(P_{13nm13} + P_{1313nm})\left[- P_{nm1313}\left(\frac{2}{\omega_{nm}^2} + \frac{1}{\omega_{nm}^2 - 4\omega_{11}^2}\right)\right] \tag{5.53}$$

$$\Xi_1 = -2\omega_{11}\mu_1\varepsilon^2 \tag{5.54}$$

$$\Xi_2 = \frac{1}{48\omega_{11}^2}\varepsilon^2(-144S_{11111111}\omega_{11}^2 + 27P_{111311}P_{131111} + 27P_{111113}P_{131111} + 160P_{111111}^2)$$

$$+ \sum_{n,m}^{\infty}(P_{11nm11} + P_{1111nm})\left[- P_{nm1111}\left(\frac{2}{\omega_{nm}^2} + \frac{1}{\omega_{nm}^2 - 4\omega_{11}^2}\right)\right] \tag{5.55}$$

$$\Xi_3 = \frac{1}{120\omega_{11}^2}\varepsilon^2(32P_{111313}P_{131113} - 240S_{11131311}\omega_{11}^2 + 60P_{111113}P_{131313} + 32P_{111313}P_{131311}$$

$$+ 480P_{111111}P_{111313} + 60P_{111311}P_{131313} + 15P_{111311}^2 - 240S_{13131113}\omega_{11}^2$$

$$- 240S_{11111313}\omega_{11}^2 + 30P_{111311}P_{111113} + 15P_{111113}^2)$$

$$- \sum_{n,m}^{\infty}\left[\frac{2(P_{11nm13} + P_{1113nm})P_{nm1313}}{\omega_{nm}^2} + \frac{(P_{11nm13} + P_{1113nm})(P_{nm1113} + P_{nm1311})}{\omega_{nm}^2 - (\omega_{11} - \omega_{13})^2}\right.$$

$$\left. + \frac{(P_{11nm13} + P_{1113nm})(P_{nm1113} + P_{nm1311})}{\omega_{nm}^2 - (\omega_{11} + \omega_{13})^2}\right] \tag{5.56}$$

$$\Xi_4 = -\frac{1}{96\omega_{11}^2}\varepsilon^2(3P_{111113}f_{13} - 32P_{111111}f_{13} + 3P_{111311}f_{13}) \tag{5.57}$$

Now, we use the method of reconstitution (Nayfeh, 1985) to derive the modulation equations. We combine Eqs. (5.42) and (5.43) with (5.49) and (5.50) as

$$\dot{A}_{11} = \varepsilon D_1 A_{11} + \varepsilon^2 D_2 A_{11} \tag{5.58}$$

$$\dot{A}_{13} = \varepsilon D_1 A_{13} + \varepsilon^2 D_2 A_{13} \tag{5.59}$$

Hence,

$$2i\omega_{11}\dot{A}_{11} = i\Xi_1 A_{11} + \Xi_2 A_{11}^2\bar{A}_{11} + \Xi_3 A_{11}A_{13}\bar{A}_{13} + \Xi_4 e^{i(\sigma_1+\sigma_2)\varepsilon t}\bar{A}_{11} + \Xi_5 e^{i\sigma_1\varepsilon t}\bar{A}_{11}A_{13} \tag{5.60}$$

$$2i\omega_{13}\dot{A}_{13} = \xi_4 e^{i\sigma_2\varepsilon t} + \xi_5 e^{-i\sigma_1\varepsilon t}A_{11}^2 + \xi_1 A_{11}\bar{A}_{11}A_{13} + i\xi_2 A_{13} + \xi_3 A_{13}^2\bar{A}_{13} \tag{5.61}$$

where

$$\Xi_5 = -\varepsilon(P_{111113} + P_{111311}) \tag{5.62}$$

$$\xi_4 = \frac{1}{2}\varepsilon f_{13} \tag{5.63}$$

$$\xi_5 = -\varepsilon P_{131111} \tag{5.64}$$

To express the modulation equations in polar form, we substitute

$$A_{11} = \frac{1}{2}a_1 e^{i\beta_1} \tag{5.65}$$

$$A_{13} = \frac{1}{2}a_2 e^{i\beta_2} \tag{5.66}$$

into Eqs. (5.60) and (5.61), separate real and imaginary parts, and obtain

$$\dot{a}_1 = \frac{1}{4\omega_{11}}\left[a_1\Xi_5\sin(\gamma_1 - \gamma_2)a_2 + 2a_1\Xi_1 + 2a_1\Xi_4\sin(\gamma_1)\right] \tag{5.67}$$

$$\dot{a}_2 = \frac{1}{4\omega_{13}}\left[-\xi_5\sin(\gamma_1 - \gamma_2)a_1^2 + 4\xi_4\sin(\gamma_2) + 2\xi_2 a_2\right] \tag{5.68}$$

$$\dot{\gamma}_1 = \frac{1}{4\omega_{11}}\left[a_1^2\Xi_2 + \Xi_3 a_2^2 + 2\Xi_5\cos(\gamma_1 - \gamma_2)a_2 + 4\sigma_1\omega_{11} + 4\sigma_2\omega_{11} + 4\Xi_4\cos(\gamma_1)\right] \tag{5.69}$$

$$\dot{\gamma}_2 = \frac{1}{8\omega_{13}a_2}\left[\xi_1 a_1^2 a_2 + 2a_1^2\xi_5\cos(\gamma_1 - \gamma_2) + \xi_3 a_2^3 + 8a_2\sigma_2\omega_{13} + 8\xi_4\cos(\gamma_2)\right] \tag{5.70}$$

where

$$\gamma_1 = \sigma_2\varepsilon t - 2\beta_1 + \sigma_1\varepsilon t \tag{5.71}$$

$$\gamma_2 = -\beta_2 + \sigma_2\varepsilon t \tag{5.72}$$

The Cartesian form of the modulation equations can be obtained by expressing the A_{ij} as

$$A_{11} = \frac{1}{2}(p_1 - iq_1)e^{i\lambda_1(t;\varepsilon)} \tag{5.73}$$

$$A_{13} = \frac{1}{2}(p_2 - iq_2)e^{i\lambda_2(t;\varepsilon)} \tag{5.74}$$

where

$$\lambda_1 = \frac{1}{2}\sigma_1\varepsilon t + \frac{1}{2}\sigma_2\varepsilon t - n\pi \tag{5.75}$$

$$\lambda_2 = \sigma_2\varepsilon t - 2n\pi + 2m\pi \tag{5.76}$$

Substituting Eqs. (5.73)-(5.76) into Eqs. (5.60) and (5.61) and letting $\varepsilon = 1$ leads to

$$\dot{p}_1 = -\frac{1}{8\omega_{11}}(4q_1\omega_{11}\sigma_1 + 4q_1\omega_{11}\sigma_2 - 4\Xi_1 p_1 + \Xi_2 p_1^2 q_1 + \Xi_2 q_1^3 + \Xi_3 q_1 p_2^2$$
$$+ \Xi_3 q_1 q_2^2 - 4\Xi_4 q_1 + 2\Xi_5 p_1 q_2 - 2\Xi_5 q_1 p_2) \tag{5.77}$$

$$\dot{q}_1 = \frac{1}{8\omega_{11}}(4p_1\sigma_1\omega_{11} + 4p_1\sigma_2\omega_{11} + 4\Xi_1 q_1 + \Xi_2 p_1^3 + \Xi_2 p_1 q_1^2 + \Xi_3 p_1 p_2^2$$
$$+ \Xi_3 p_1 q_2^2 + 4\Xi_4 p_1 + 2\Xi_5 p_1 p_2 + 2\Xi_5 q_1 q_2) \tag{5.78}$$

$$\dot{p}_2 = -\frac{1}{8\omega_{13}}(8\sigma_2 q_2 \omega_{13} + 4\xi_5 p_1 q_1 + q_2 p_1^2 \xi_1 + q_2 q_1^2 \xi_1 - 4p_2 \xi_2$$

$$+ q_2 p_2^2 \xi_3 + q_2^3 \xi_3) \tag{5.79}$$

$$\dot{q}_2 = \frac{1}{8\omega_{13}}(8\sigma_2 p_2 \omega_{13} + 8\xi_4 + 2\xi_5 p_1^2 - 2\xi_5 q_1^2 + \xi_1 p_1^2 p_2 + \xi_1 q_1^2 p_2$$

$$+ 4\xi_2 q_2 + \xi_3 p_2^3 + \xi_3 p_2 q_2^2) \tag{5.80}$$

We note that the modulation equations, Eqs. (5.77)-(5.80), are invariant under the transformation $(p_1, q_1, p_2, q_2) \Longleftrightarrow (-p_1, -q_1, p_2, q_2)$. This implies that the projection of a solution of the modulation equations onto the $p_1 - q_1$ plane remains unaffected by rotation through 180° around the origin. Hence, the fixed points, trajectories, limit cycles, and attractors occur in duplicate if they are not transformed onto themselves by the symmetry.

The fixed points of the modulation equations can be obtained by setting the $\dot{a}_i$ and $\dot{\gamma}_i = 0$ in Eqs. (5.67)-(5.70) or the $\dot{p}_i$ and $\dot{q}_i = 0$ in Eqs. (5.77)-(5.80) and then solving for the roots. These roots correspond to periodic vibrations of the shell. The stability of these fixed points depend on the real parts of the eigenvalues of the Jacobian matrix of Eqs. (5.67)-(5.70) or Eqs. (5.77)-(5.80). A given fixed point is asymptotically stable if and only if all of the eigenvalues lie in the left-half of the complex plane and unstable if at least one eigenvalue lies in the right-half of the complex plane. When $a_1 = 0$ and $a_2 \neq 0$, the shell vibrates periodically with only one frequency (single-mode response). On the other hand, when $a_1 \neq 0$ and $a_2 \neq 0$ the shell vibrates with two frequencies (two-mode response). For stability analysis, the polar form is not convenient whenever one or more of the state variables of the system have a zero value. This condition causes the corresponding fixed-point equations to become identities. In such case, it is not straightforward to determine the stability of the fixed point from the polar form of the modulation equations (Nayfeh and Mook, 1979). For this reason, it is more convenient to determine the stability of such a fixed point from the Cartesian form of the modulation equations.
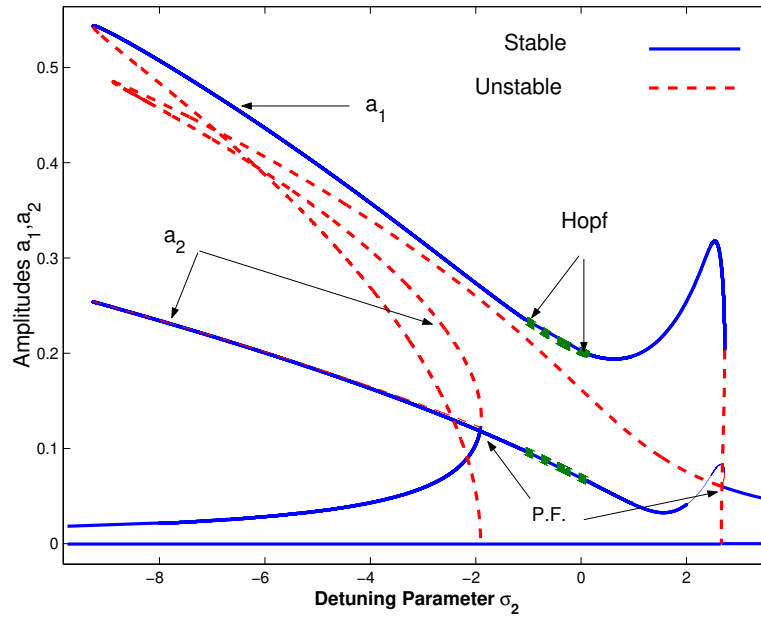
Figure 5.1: Frequency-response curves for a single-layered shell when $k_x = 0.33, k_y = 0.398,$ $\sigma_1 = -1.8,$ and $f_{11} = 350$ for the case $\Omega \approx \omega_{13}.$
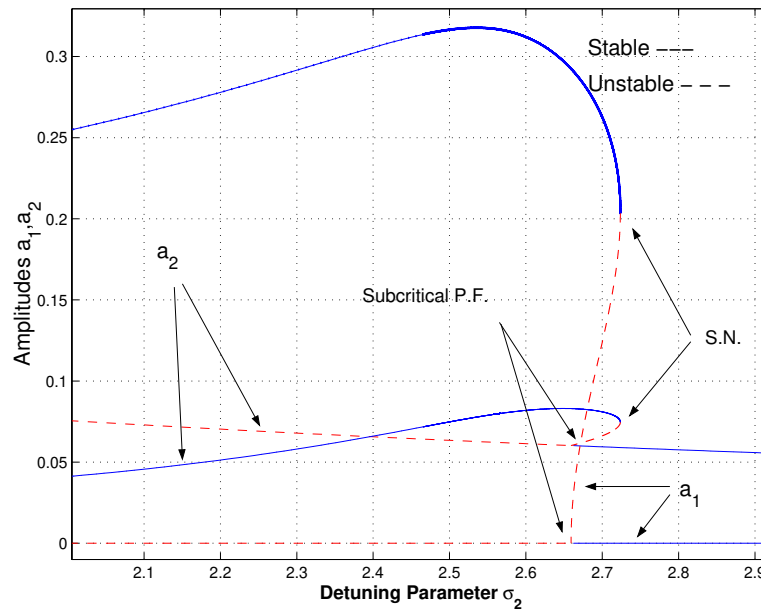
Figure 5.2: An enlargement of the frequency-response curves in Fig. 5.1 near the subcritical pitchfork bifurcation at $\sigma_2 = 2.66.$
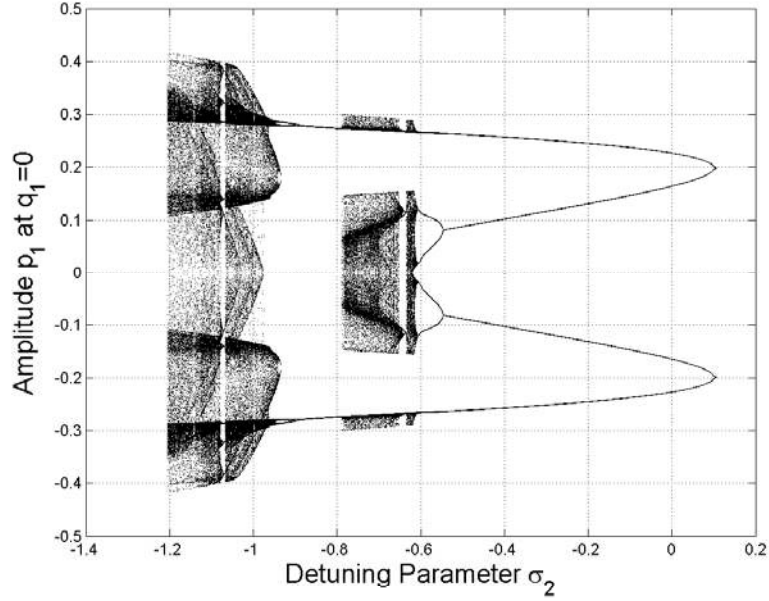
Figure 5.3: Bifurcation diagram for p_1 corresponding to $q_1 = 0$ when $k_x = 0.33, k_y = 0.398$, $\sigma_1 = -1.8$, and $f_{11} = 350$ for the case $\Omega \approx \omega_{13}$.

5.2.1 Two-Mode Case

In this section, we investigate the two-to-one internal resonance by considering only the interacting modes W_{11} and W_{13}. We consider a single-layered graphite/epoxy shell with the following parameters:

$$\nu_{12} = 0.3, \quad l_x = 1, \quad l_y = 1, \quad \frac{E_1}{E_2} = 15.4,$$

$$\frac{G_{12}}{E_2} = 0.79, \quad \frac{G_{23}}{E_2} = 0.5, \quad \mu_1 = 0.35,$$

$$k_x = 0.33, \quad k_y = 0.398, \quad f_1 = 350 \tag{5.81}$$

With these parameters, the lowest four anti-symmetric nondimensional natural frequencies are

$$\omega_{11} = 171.909, \quad \omega_{13} = 343.818,$$

$$\omega_{31} = 373.601, \quad \omega_{33} = 431.868 \tag{5.82}$$

and $\omega_{13} \approx 2\omega_{11}$. Next, we use the detuning parameter σ_2 as a bifurcation parameter to study the behavior of the fixed points and dynamic solutions of the modulation equations.

Typical frequency-response curves are shown in Fig. 5.1. There are two possible equilibrium solutions: single-mode and two-mode solutions. In the first solution, the driven second mode responds with an amplitude a_2, whereas the first-mode amplitude a_1 is zero. This solution is stable for large positive and negative values of σ_2. In addition, it is bent to the left, indicating a softening-type effective nonlinearity. Starting on the stable single-mode branch and decreasing σ_2, we find that one of the eigenvalues of the Jacobian matrix of Eqs. (5.77)-(5.80) crosses the imaginary axis along the real axis at $\sigma_2 = 2.66$, resulting in a jump to the two-mode solution through a subcritical pitchfork bifurcation, as shown in greater detail in Fig. 5.2. The single-mode solution loses stability and its amplitude increases as σ_2 decreases until $\sigma_2 = -8.875$. At that point, a turning point occurs and the amplitude of the single-mode solution starts to decrease as σ_2 increases until $\sigma_2 = -1.896$, where it encounters another pitchfork bifurcation and regains stability. Moreover, unstable two-mode solutions are born at that point.

Starting near the first pitchfork bifurcation and tracking the two-mode solution as we decrease σ_2, we find that the two-mode solution loses stability through a Hopf bifurcation at $\sigma_2 = 0.106$ (as a result of two complex conjugate eigenvalues crossing the imaginary axis transversely from the left to the right half of the complex plane), resulting in the creation of dynamic solutions. To predict the dynamic behavior of the system, we integrate the modulation equations numerically and calculate the values of p_1 corresponding to $q_1 = 0$. The result is the bifurcation diagram shown in Fig. 5.3. Another Hopf bifurcation occurs at $\sigma_2 = -1.2$, leading to a stable two-mode equilibrium solution. The stable fixed points continue until $\sigma_2 = -9.26$, where the system suffers a saddle-node bifurcation, resulting in a jump to the lower branch of stable single-mode solutions.

To analyze the dynamic solutions, we use a combination of a shooting technique and Floquet theory to locate periodic solutions and investigate their stability. We start at $\sigma_2 = 0.106$,

Figure 5.4: The symmetric period-one limit cycle obtained at $\sigma_2 = 0.1$: (a) phase portrait and (b) frequency spectrum.

Figure 5.5: The unsymmeric period-one limit cycle obtained at $\sigma_2 = -0.2$: (a) phase portrait and (b) frequency spectrum.

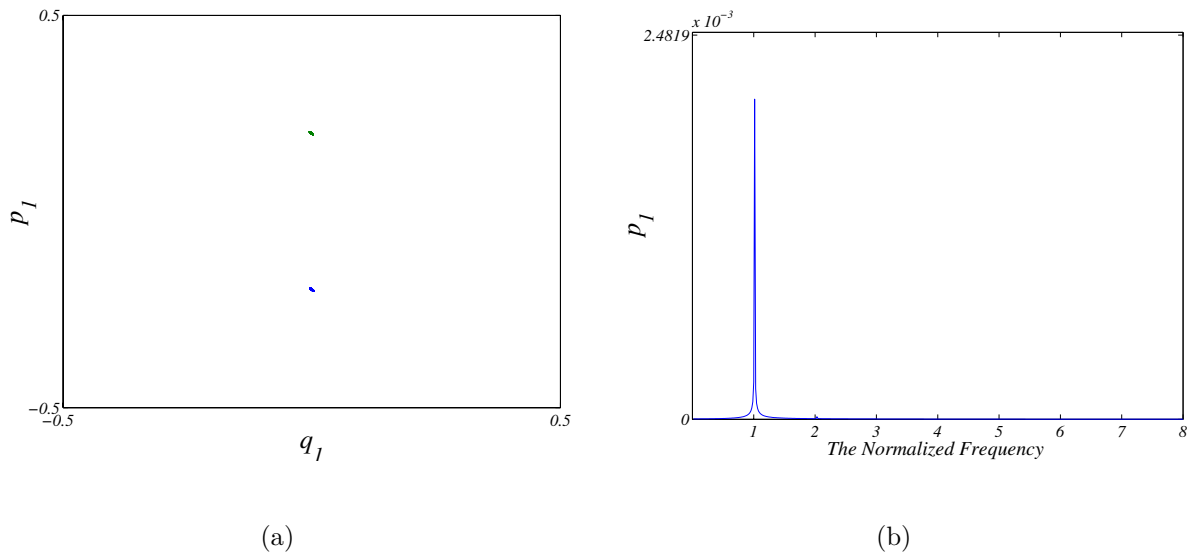(a)   (b)
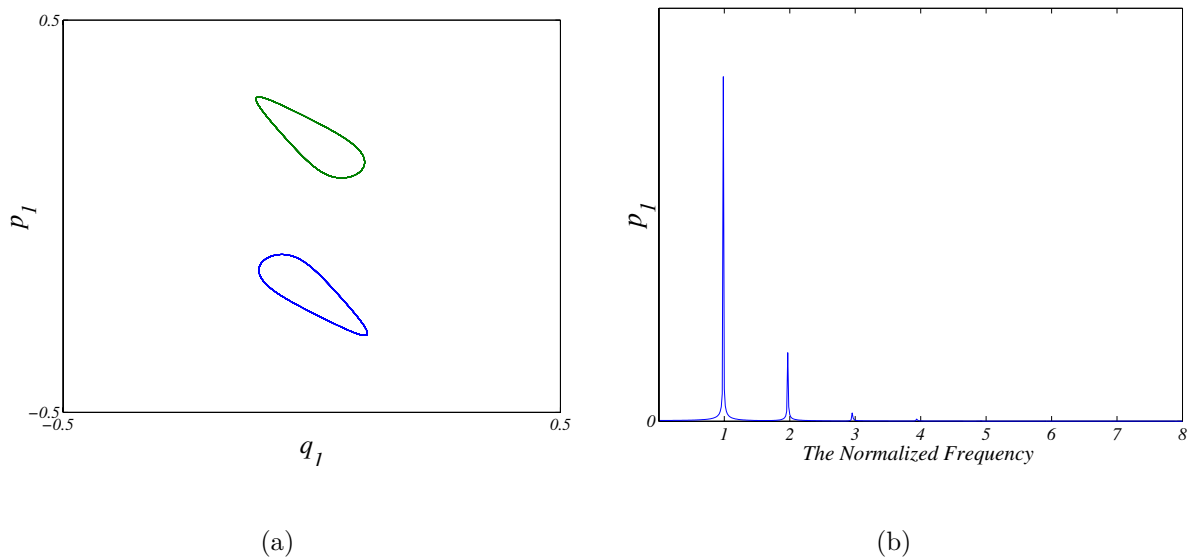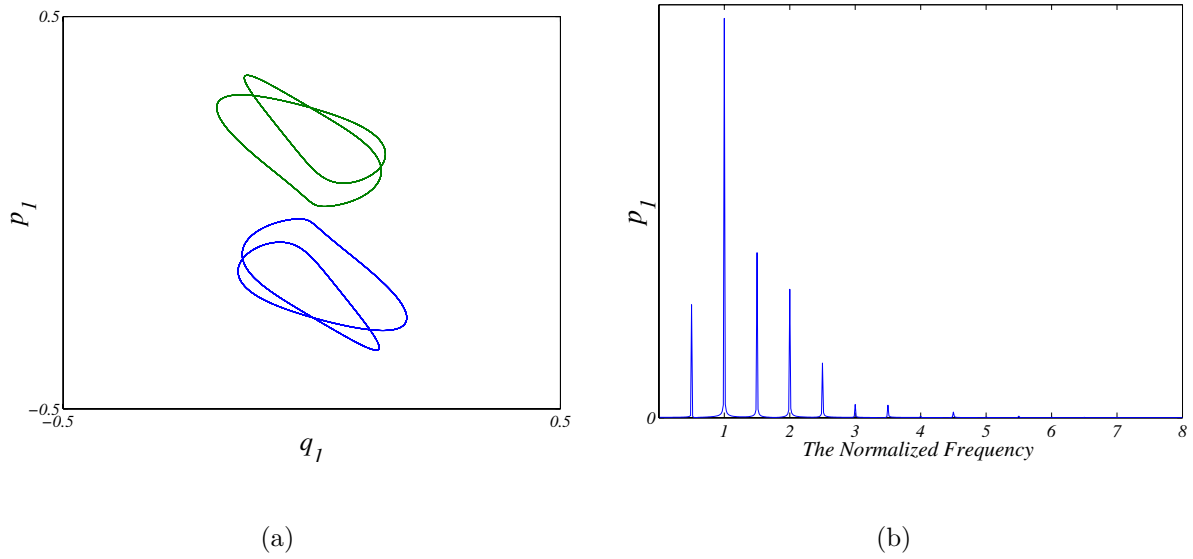
Figure 5.6: The period-two limit cycle obtained at $\sigma_2 = -0.6$: (a) phase portrait and (b) frequency spectrum.

(a)   (b)

Figure 5.7: The period-four limit cycle obtained at $\sigma_2 = -0.608$: (a) phase portrait and (b) frequency spectrum.

where a small symmetric period-one limit cycle is born due to the right Hopf bifurcation, as shown in Fig. 5.4(a). The FFT for this limit cycle in Fig. 5.4(b) shows a spike at the normalized frequency 1. The presence of only odd peaks is an indication of a symmetric limit cycle. As σ_2 decreases, the limit cycle increases smoothly in size and then loses symmetry as a consequence of one of the Floquet multipliers exiting the unit circle through $+1$. The limit cycle is shown in Fig. 5.5(a) and the FFT is shown in Fig. 5.5(b). The presence of spikes at 1 and 2, both odd and even harmonics, indicates an unsymmetric limit cycle. This unsymmetric limit cycle increases in size until $\sigma_2 = 0.56$, where a period-doubling bifurcation occurs as a consequence of one of the Floquet multiplies exiting the unit circle through -1. In Fig. 5.6(a), we show the period-two limit cycle obtained at $\sigma_2 = -0.6$. The FFT for this limit cycle is shown in Fig. 5.6(b) and the period-two motion is indicated by the presence of peaks at the normalized frequencies $1/2$, $3/2$, $5/2$, and $7/2$. This limit cycle smoothly increases in size as σ_2 decreases until -0.607, where another period-doubling bifurcation occurs. The phase portrait and FFT of a period-four limit cycle are shown in Figs. 5.7(a) and 5.7(b). The FFT shows the presence of peaks at $1/4$, $3/4$, $5/4$, and $(2n - 1)/4$, which affirms that attractor is a period-four. Shortly after the second period-doubling bifurcation, the system goes into a chaotic motion. At $\sigma_2 = -0.634$, a window of symmetric period-one limit cycle appears within the chaos. The corresponding phase portrait and FFT are shown in Figs. 5.8(a) and 5.8(b). After this window, the chaos, shown in Fig. 5.9, resumes until it undergoes an interior crisis, resulting in its disappearance and the creation of a new period-one solution at $\sigma_2 = -0.79$, as illustrated by the Poincaré map in Fig. 5.3. The presence of a broadband spectrum in the FFT in Fig. 5.9(b) is a mark of a chaotic response.

The new period-one solution, shown in Fig. 5.10(a), has a new shape and period. It is clear from the FFT in Fig. 5.10(b) that the motion is symmetric. This solution loses symmetry and then suffers a period-doubling bifurcation at $\sigma_2 = -0.92$, Figs. 5.11(a) and 5.11(b). Another period-doubling bifurcation occurs at $\sigma_2 = -0.938$, Fig. 5.12, and shortly after this period-doubling sequence, a chaotic solution appears. Inside this chaotic solution, one can find multiple windows of limit cycles. At $\sigma_2 = -1.029$ and $\sigma_2 = -1.07$, symmetric period-

(a)   (b)
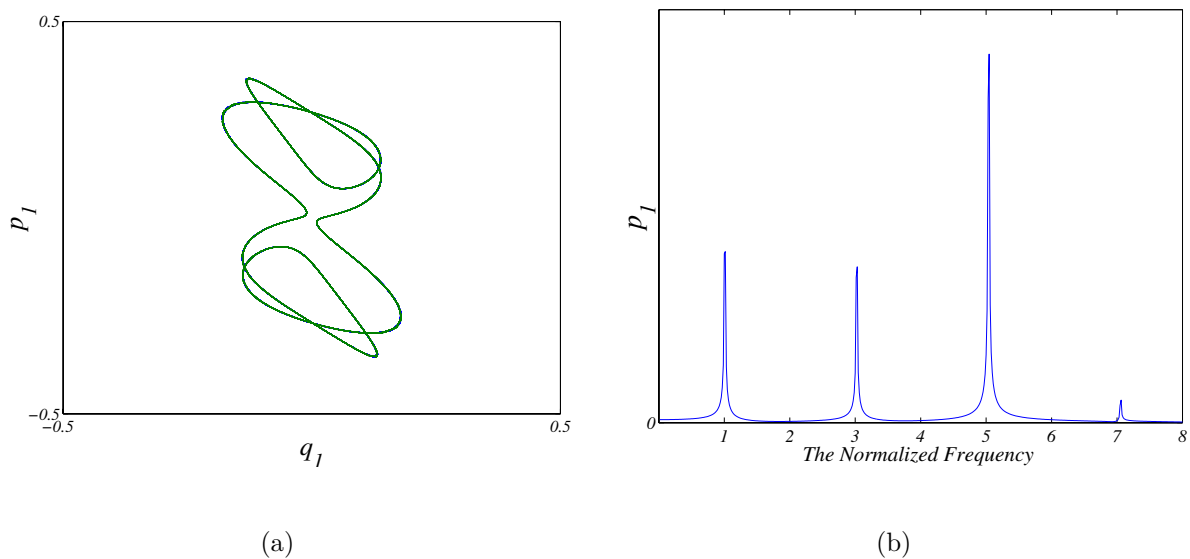
Figure 5.8: The period-one limit cycle obtained at $\sigma_2 = -0.636$: (a) phase portrait and (b) frequency spectrum.

one solutions are found, as shown in Figs. 5.13 and 5.14. At $\sigma_2 = -1.088$, an unsymmetric limit cycle appears, as shown in Fig. 5.15. Lastly, a window of symmetric limit cycles exists at $\sigma_2 = -1.141$, as shown in Fig. 5.16.

To enhance our understanding of the system dynamics, we plot in Fig. 5.17 the force-response curves obtained for $\sigma_1 = -1.8$ and $\sigma_2 = 0.0$. We can see that, as the forcing increases, a_2 increases while a_1 remains zero, a single-mode solution. At $f_{11} = 59.8$, the system suffers a supercritical pitchfork bifurcation, which causes the single-mode solution to lose stability and generates a new stable two-mode solution. As we increase the forcing further, a_1 starts to increase while a_2 remains almost constant at 0.72. This phenomenon is known as saturation (Nayfeh and Mook, 1979). This two-mode solution suffers a Hopf bifurcation at $f_{11} = 144$, leading to dynamic solutions. These solutions terminate through a reverse Hopf bifurcation at $f_{11} = 447$.

Next, we plot in Fig. 5.18 the force-response curves obtained for $\sigma_1 = -1.8$ and $\sigma_2 = -1.8$. Starting from zero, we can see that, as we increase the forcing f_{11}, a_2 increases while a_1

(a)   (b)
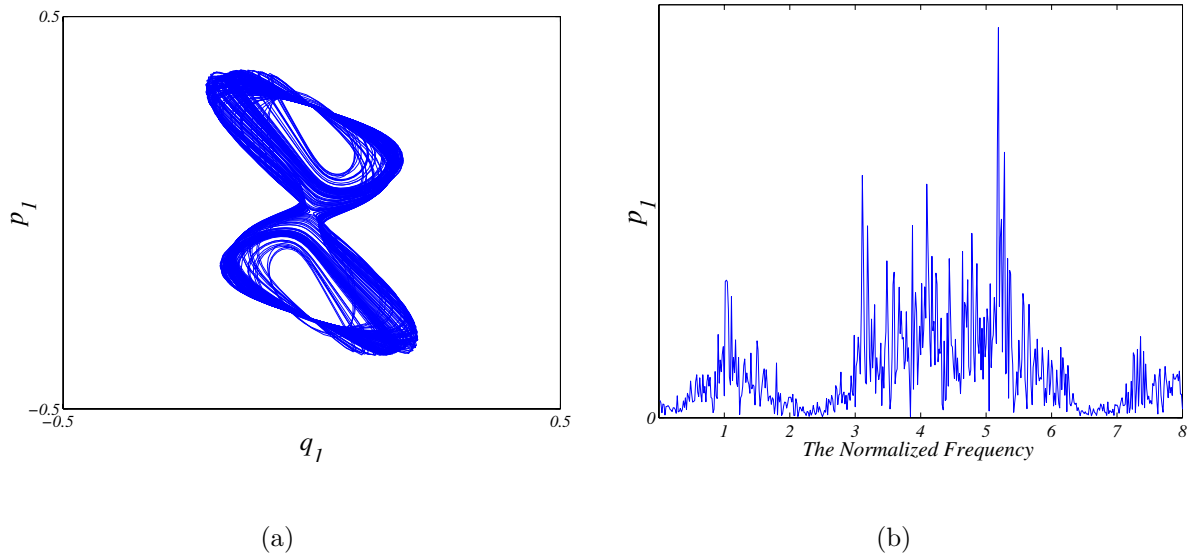
Figure 5.9: Chaotic solution obtained at $\sigma_2 = -0.7$: (a) phase portrait and (b) frequency spectrum.

(a)   (b)
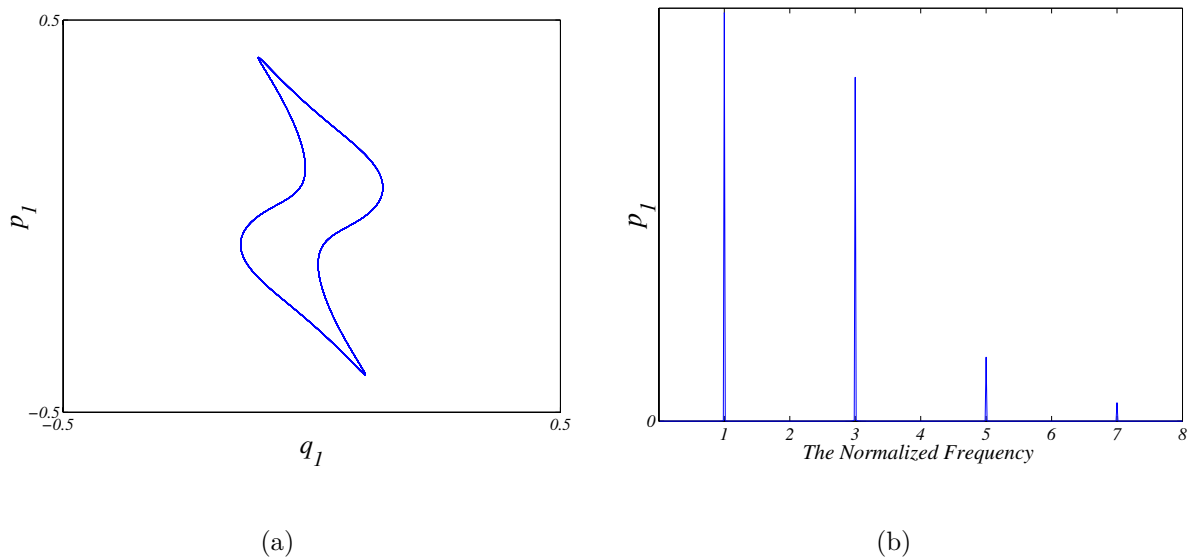
Figure 5.10: The period-one limit cycle obtained at $\sigma_2 = -0.8$: (a) phase portrait and (b) frequency spectrum.
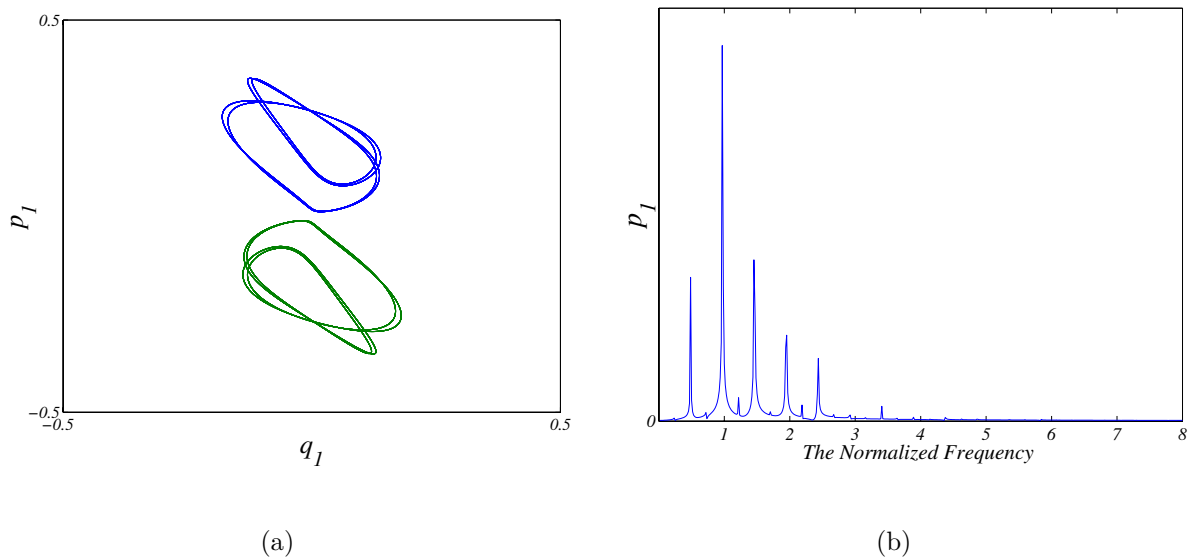
(a)   (b)
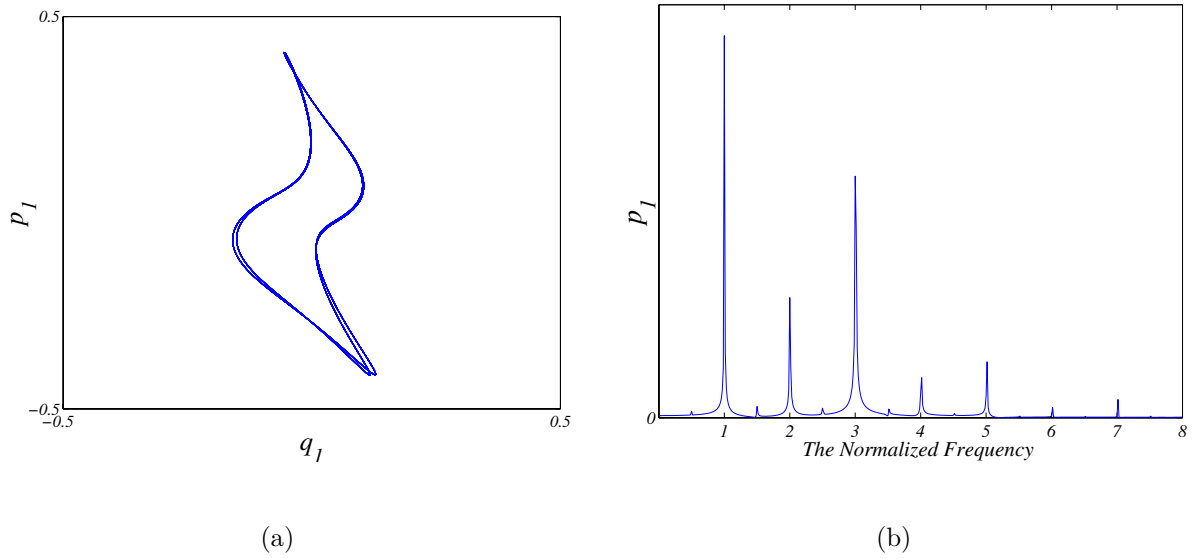
Figure 5.11: The period-two limit cycle obtained at $\sigma_2 = -0.93$: (a) phase portrait and (b) frequency spectrum.

(a)   (b)
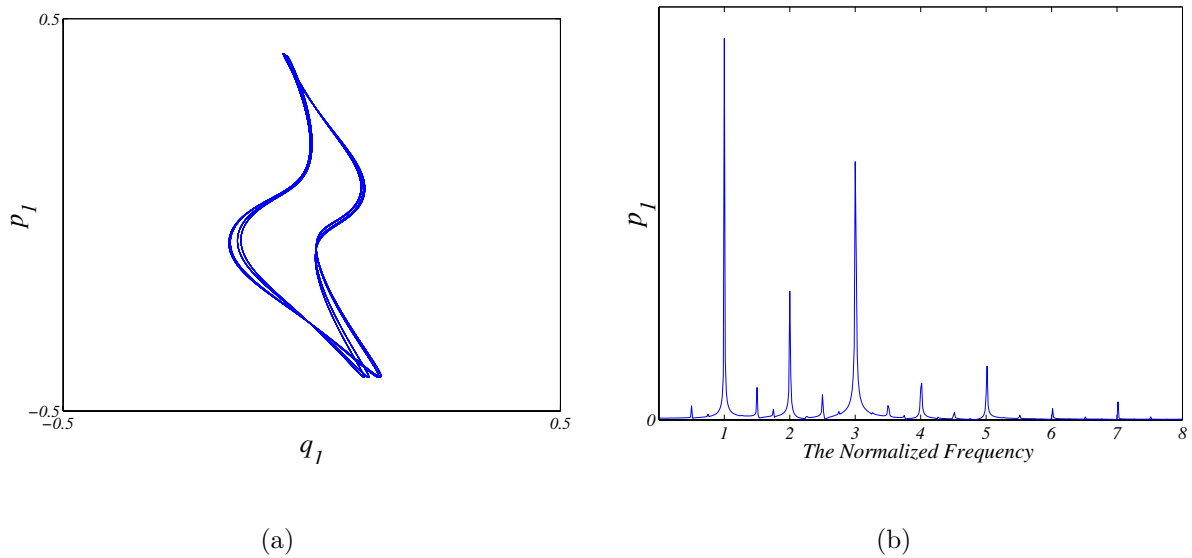
Figure 5.12: The period-four limit cycle obtained at $\sigma_2 = -0.939$: (a) phase portrait and (b) frequency spectrum.

(a)   (b)
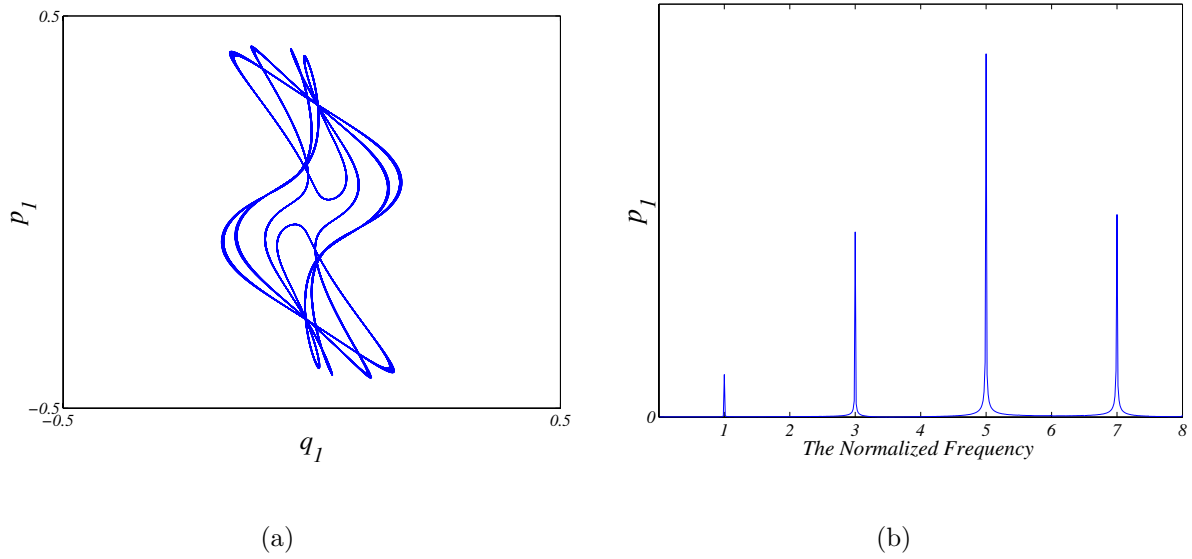
Figure 5.13: A symmetric period-one limit cycle within chaos obtained at $\sigma_2 = -1.029$: (a) phase portrait and (b) frequency spectrum.

(a)   (b)
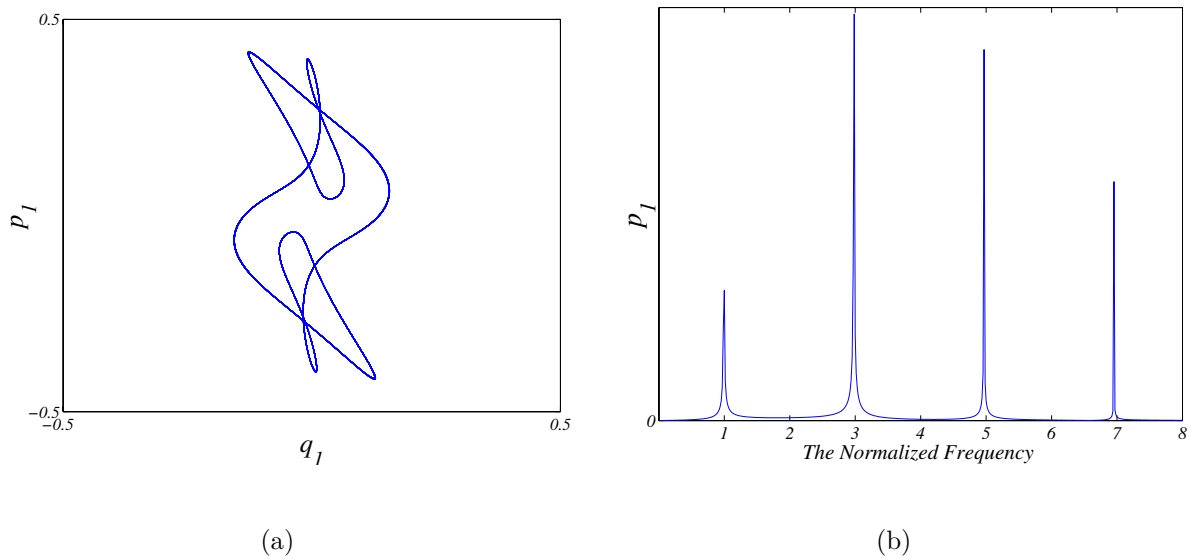
Figure 5.14: A symmetric period-one limit cycle within chaos obtained at $\sigma_2 = -1.07$: (a) phase portrait and (b) frequency spectrum.
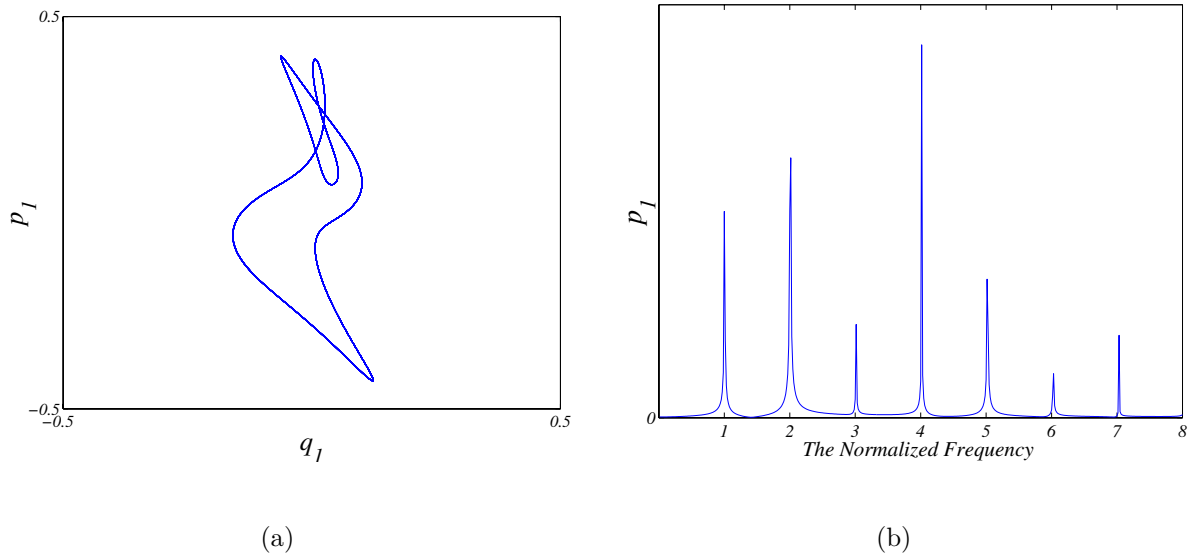
Figure 5.15: An unsymmetric period-one limit cycle within chaos obtained at $\sigma_2 = -1.088$: (a) phase portrait and (b) frequency spectrum.
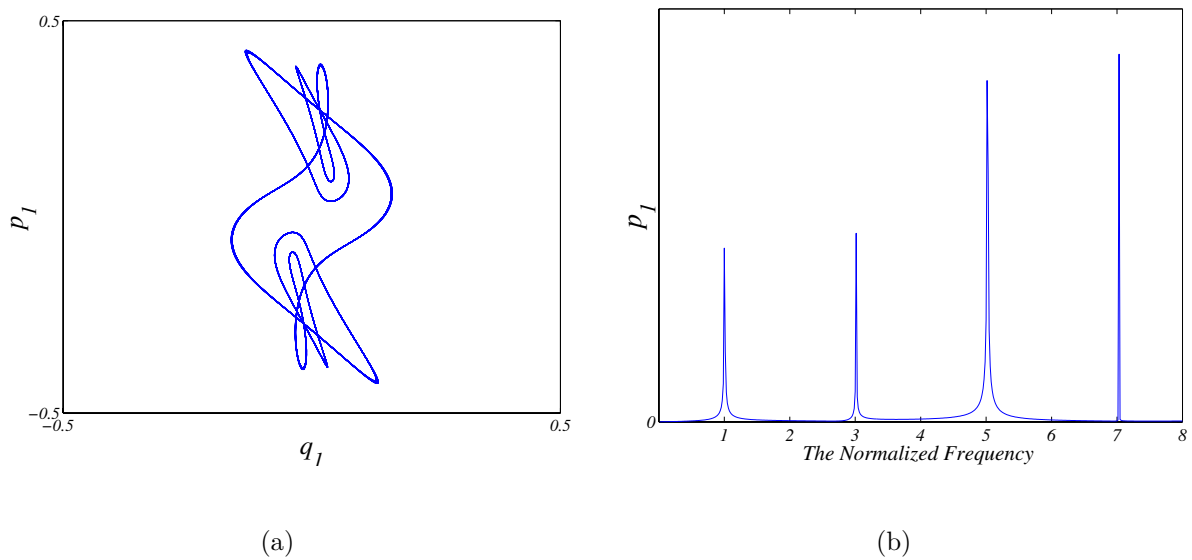
Figure 5.16: A symmetric period-one limit cycle within chaos obtained at $\sigma_2 = -1.141$: (a) phase portrait and (b) frequency spectrum.
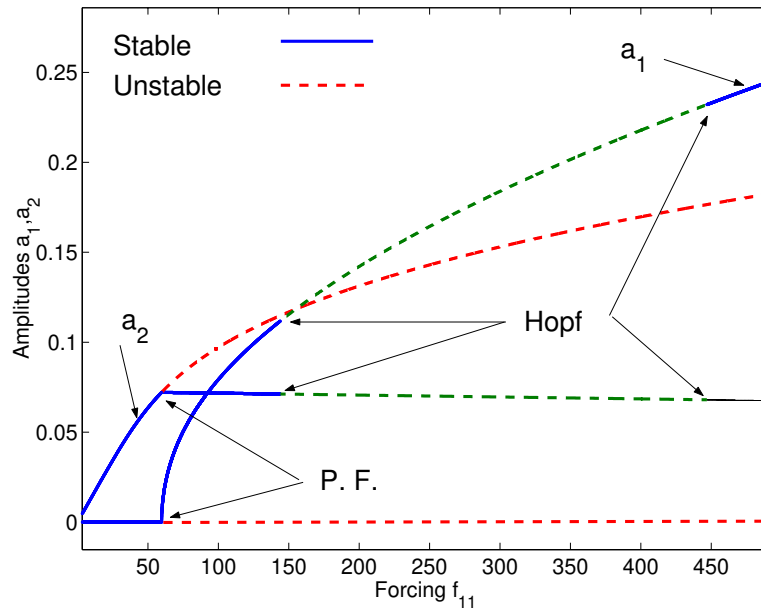
Figure 5.17: Force-response curves for a single-layered shell using two-mode approximation when $k_x = 0.33$, $k_y = 0.398$, $\sigma_1 = -1.8$, and $\sigma_2 = 0$ for the case $\Omega \approx \omega_{13}$.

remains zero. This persists until $f_{11} = 322.5$, where a subcritical pitchfork bifurcation occurs. The single-mode solution loses stability through this bifurcation and a new unstable two-mode solution is created. At this point, the system response jumps to another coexisting branch of stable two-mode solutions. Increasing the forcing to 540, the two-mode solution loses stability through a Hopf bifurcation. On the other hand, decreasing the forcing leads to a saddle-node bifurcation at $f_{11} = 133.7$, which results in a jump to the single-mode solution.

We can see from Figs. 5.17 and 5.18 that changing one of the parameters, such as σ_2, can induce a new dynamic behavior. In the shell problem, we have a relatively large number of parameters, which may produce different dynamic behaviors.

Figure 5.18: Force-response curves for a single-layered shell using a two-mode approximation when $k_x = 0.33, k_y = 0.398, \sigma_1 = -1.8$, and $\sigma_2 = -1.8$ for the case $\Omega \approx \omega_{13}$.

5.2.2 Multi-Mode Case

In this section, we investigate the effect of the noninteracting modes on the predicted shell dynamics. We include seven noninteracting modes. We consider the same shell parameters defined in (5.81). Again, we use the detuning parameter σ_2 as a bifurcation parameter to generate the frequency-response curves. The frequency-response curves are shown in Fig. 5.19. We can see that, the effect of the noninteracting modes on the two-mode response is small. However, their effect on the single-mode response is relatively large. To demonstrate this, we plot a_1 and a_2 in Figs. 5.20 and 5.21, respectively. We can see clearly in Fig. 5.20 that using only the interacting modes W_{11} and W_{13} shifts the bifurcation points and dynamic solutions and underestimates or overestimates the response amplitude. Furthermore, using only the interacting modes may miss some of the dynamics and bifurcations, such as the stable single-mode solution in $-0.828 < \sigma_2 < -1.65$, as shown in Fig 5.21.

In another example, we plot in Fig. 5.22 the force-response curves when $\sigma_1 = -1.8$ and

Figure 5.19: Frequency-response curves for a single-layered shell generated by using a nine-mode approximation when $k_x = 0.33, k_y = 0.398, \sigma_1 = -1.8$, and $f_{13} = 350$ for the case $\Omega \approx \omega_{13}$.

$\sigma_2 = -1.8$. Compared with Fig. 5.18, we can see that using nine modes in the approximation shifts the subcritical pitchfork bifurcation to $f_{11} = 370$ and the saddle-node bifurcation to $f_{11} = 140$. Furthermore, the nine-mode approximation predicts a stable single-mode solution when $f_{11} > 366$. Again as in the preceding case, the two-mode approximation fails to predict the correct dynamics.

To check the convergence, we increased the number of modes retained in the approximation to 16. We found out that the additional modes have a negligible effect.
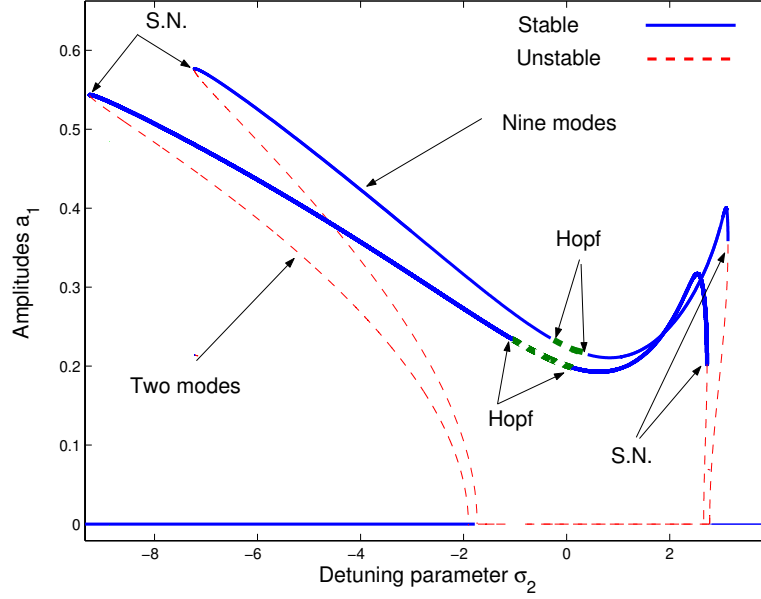
Figure 5.20: Frequency-response curves for a_1 calculated by using two- and nine-mode approximations for the case $\Omega \approx \omega_{13}$.

5.3 Primary Resonance of the Lower-Frequency Mode

We introduce the detuning parameters σ_1 and σ_2 defined by

$$\omega_{13} = 2\omega_{11} + \epsilon\sigma_1 \tag{5.83}$$

$$\Omega = \omega_{11} + \epsilon\sigma_2 \tag{5.84}$$

Substituting Eqs. (5.83) and (5.84) into Eqs. (5.34)-(5.39) and eliminating the terms that produce secular terms, we obtain

$$2i\omega_{11}D_1A_{11} = -(P_{111113} + P_{111311})\bar{A}_{11}A_{13}e^{i\sigma_1\varepsilon t} + \frac{f_{11}}{2}e^{i\sigma_2\varepsilon t} \tag{5.85}$$

$$2i\omega_{13}D_1A_{13} = -P_{131111}A_1^2e^{-i\sigma_1\varepsilon t} \tag{5.86}$$
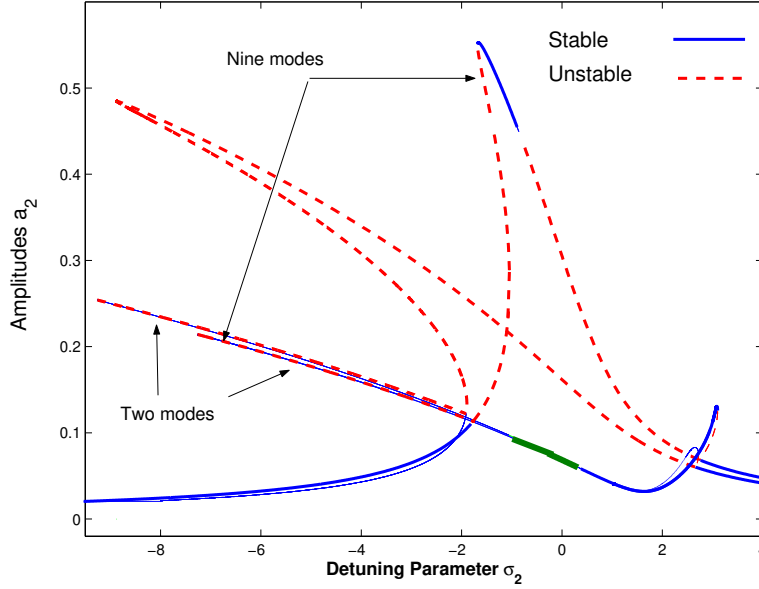
Figure 5.21: Frequency-response curves for a_2 calculated by using two modes and nine modes in the approximation for the case $\Omega \approx \omega_{13}$.

Then, the solution of the second-order equations can be expressed as

$$
\begin{aligned}
W_{11}^{(2)} = \frac{1}{\omega_{11}^2}\Bigg[&- \frac{1}{4}\bar{A}_{13}A_{11}P_{111113}e^{-i(\omega_{13}-\omega_{11})T_0} - \frac{1}{4}\bar{A}_{13}A_{11}P_{111311}e^{-i(\omega_2-\omega_{11})T_0} \\
&+ \frac{1}{8}A_{13}A_{11}P_{111113}e^{i(\omega_{13}+\omega_{11})T_0} + \frac{1}{8}A_{13}A_{11}P_{111311}e^{i(\omega_{13}+\omega_{11})T_0} + \frac{1}{8}f_{13}e^{i\Omega T_0} + \frac{1}{8}f_{13}e^{-i\Omega T_0} \\
&- 2P_{111111}\bar{A}_{11}A_{11} + \frac{1}{3}e^{2i\omega_{11}T_0}P_{111111}A_{11}^2 + \frac{1}{15}e^{-2i\omega_{13}T_0}P_{111313}\bar{A}_{13}^2 + \frac{1}{15}e^{2i\omega_{13}T_0}P_{111313}A_{13}^2 \\
&+ \frac{1}{3}e^{-2i\omega_{11}T_0}P_{111111}\bar{A}_{11}^2 + \frac{1}{8}\bar{A}_{13}\bar{A}_1 P_{111113}e^{-i(\omega_{13}+\omega_{11})T_0} + \frac{1}{8}\bar{A}_{13}\bar{A}_{11}P_{111311}e^{-i(\omega_{13}+\omega_{11})T_0} \\
&- 2P_{111313}\bar{A}_{13}A_{13} - \frac{1}{4}A_{13}\bar{A}_{11}P_{111113}e^{i(\omega_{13}-\omega_{11})T_0} - \frac{1}{4}A_{13}\bar{A}_{11}P_{111311}e^{i(\omega_{13}-\omega_{11})T_0} \Bigg] \quad (5.87)
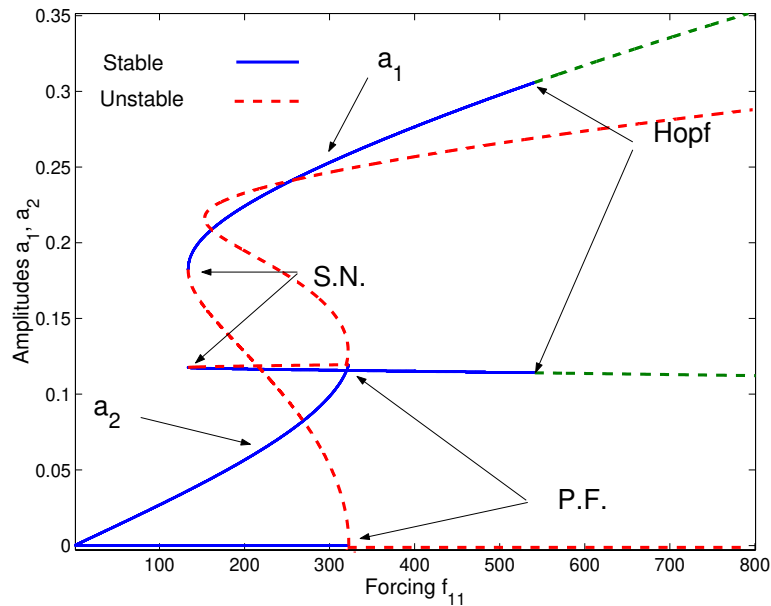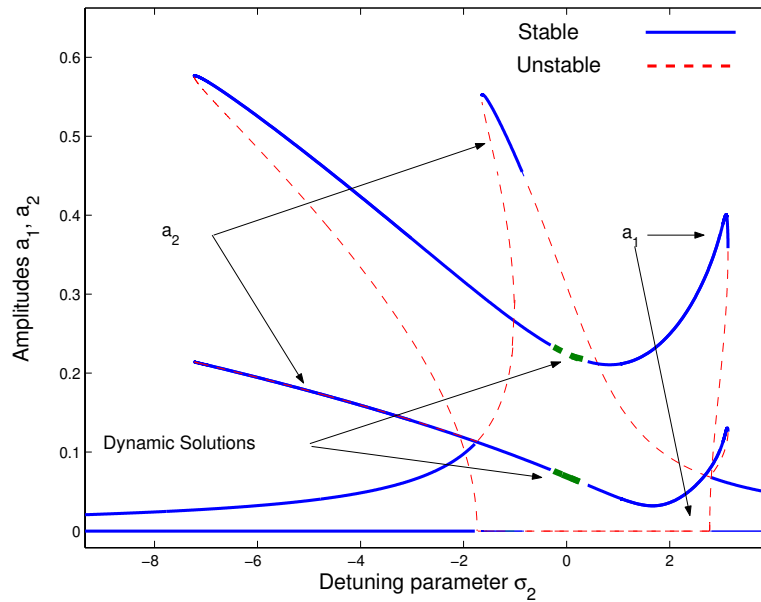\end{aligned}
$$
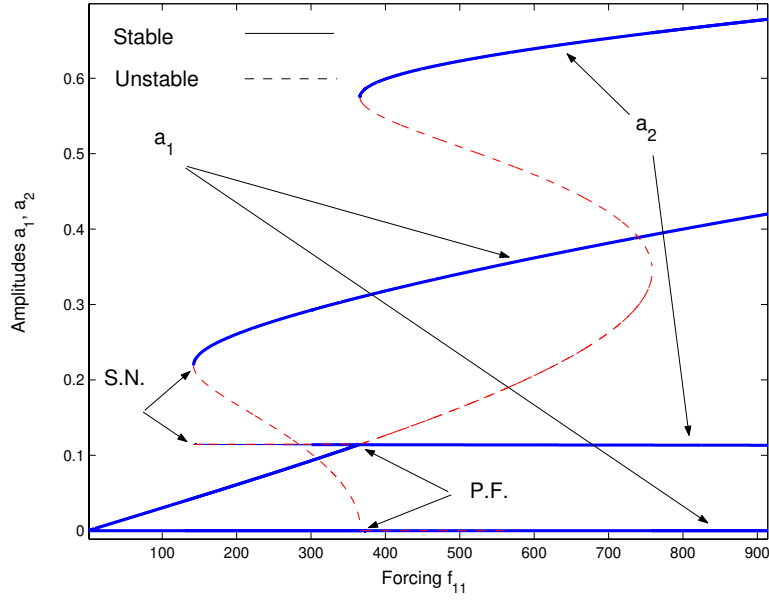
Figure 5.22: Force-response curves for a single-layered shell using a nine-mode approximation when $k_x = 0.33$, $k_y = 0.398$, $\sigma_1 = -1.8$, and $\sigma_2 = -1.8$ for the case $\Omega \approx \omega_{13}$.

$$
\begin{aligned}
v_{11}^{(2)} = \frac{i}{\omega_{11}} \Bigg[&-\frac{2}{3} e^{-2i\omega_{11}T_0} P_{111111} \bar{A}_{11}^2 + \frac{1}{8} f_{13} e^{-i\Omega T_0} + \frac{1}{4} A_{13} \bar{A}_{11} P_{111113} e^{i(\omega_{13}-\omega_{11})T_0} \\
&+ \frac{1}{4} A_{13} \bar{A}_{11} P_{111311} e^{i(\omega_{13}-\omega_{11})T_0} - \frac{1}{8} f_{13} e^{i\Omega T_0} - \frac{4}{15} e^{-2i\omega_{13}T_0} P_{111313} \bar{A}_{13}^2 \\
&- \frac{1}{4} \bar{A}_{13} A_{11} P_{111113} e^{-i(\omega_{13}-\omega_{11})T_0} - \frac{1}{4} \bar{A}_{13} A_{11} P_{111311} e^{-i(\omega_{13}-\omega_{11})T_0} + \frac{4}{15} e^{2i\omega_{13}T_0} P_{111313} A_{13}^2 \\
&+ \frac{3}{8} A_{13} A_{11} P_{111113} e^{i(\omega_{13}+\omega_{11})T_0} + \frac{3}{8} A_{13} A_{11} P_{111311} e^{i(\omega_{13}+\omega_{11})T_0} + \frac{2}{3} e^{2i\omega_{11}T_0} P_{111111} A_{11}^2 \\
&- \frac{3}{8} \bar{A}_{13} \bar{A}_{11} P_{111113} e^{-i(\omega_{13}+\omega_{11})T_0} - \frac{3}{8} \bar{A}_{13} \bar{A}_{11} P_{111311} e^{-i(\omega_{13}+\omega_{11})T_0} \Bigg]
\end{aligned}
\tag{5.88}
$$

$$W_{13}^{(2)} = \frac{1}{\omega_{11}^2}\left[-\frac{1}{16}e^{2i\omega_{11}T_0}P_{131111}A_{11}^2 - \frac{1}{16}e^{-2i\omega_{11}T_0}P_{131111}\bar{A}_{11}^2 + \frac{1}{12}e^{-2i\omega_{13}T_0}P_{131313}\bar{A}_{13}^2 \right.$$

$$+ \frac{1}{12}e^{2i\omega_{13}T_0}P_{131313}A_{13}^2 + \frac{1}{5}A_{13}A_{11}P_{131311}e^{i(\omega_{13}+\omega_{11})T_0} + \frac{1}{5}A_{13}A_{11}P_{131113}e^{i(\omega_{13}+\omega_{11})T_0}$$

$$- \frac{1}{3}A_{13}\bar{A}_{11}P_{131311}e^{i(\omega_{13}-\omega_{11}T_0)} - \frac{1}{3}A_{13}\bar{A}_{11}P_{131113}e^{i(\omega_{13}-\omega_{11})T_0} + \frac{1}{5}\bar{A}_{13}\bar{A}_{11}P_{131311}e^{-i(\omega_{13}+\omega_{11})T_0}$$

$$+ \frac{1}{5}\bar{A}_{13}\bar{A}_{11}P_{131113}e^{-i(\omega_{13}+\omega_{11})T_0} - \frac{1}{2}P_{131111}\bar{A}_{11}A_{11} - \frac{1}{2}P_{131313}\bar{A}_{13}A_{13}$$

$$- \frac{1}{3}\bar{A}_{13}A_{11}P_{131311}e^{-i(\omega_{13}-\omega_{11})T_0} - \frac{1}{3}\bar{A}_{13}A_{11}P_{131113}e^{-i(\omega_{13}-\omega_{11})T_0} + \frac{1}{6}f_{13}e^{i\Omega T_0}$$

$$\left. + \frac{1}{6}f_{13}e^{-i\Omega T_0}\right] \tag{5.89}$$

$$v_{13}^{(2)} = \frac{i}{\omega_{11}}\left[\frac{1}{3}\bar{A}_{13}A_{11}P_{131311}e^{-i(\omega_{13}-\omega_{11})T_0} + \frac{1}{3}\bar{A}_{13}A_{11}P_{131113}e^{-i(\omega_{13}-\omega_{11})T_0} + \frac{1}{3}e^{2i\omega_{13}T_0}P_{131313}A_{13}^2 \right.$$

$$- \frac{1}{3}A_{13}\bar{A}_{11}P_{131113}e^{i(\omega_{13}-\omega_{11})T_0} - \frac{3}{5}\bar{A}_{13}\bar{A}_{11}P_{131311}e^{-i(\omega_{13}+\omega_{11})T_0}$$

$$- \frac{3}{5}\bar{A}_{13}\bar{A}_{11}P_{131113}e^{-i(\omega_{13}+\omega_{11})T_0} - \frac{1}{3}e^{-2i\omega_{13}T_0}P_{131313}\bar{A}_{13}^2 + \frac{3}{5}A_{13}A_{11}P_{131311}e^{i(\omega_{13}+\omega_{11}T_0)}$$

$$+ \frac{3}{5}A_{13}A_{11}P_{131113}e^{i(\omega_{13}+\omega_{11})T_0} - \frac{1}{3}A_{13}\bar{A}_{11}P_{131311}e^{i(\omega_{13}-\omega_{11})T_0} + \frac{1}{6}f_{13}e^{i\Omega T_0} - \frac{1}{6}f_{13}e^{-i\Omega T_0}\right]$$

$$+ \frac{i}{\omega_{11}^2}\left[\frac{1}{16}e^{2i\omega_{11}T_0}\omega_{13}P_{131111}A_{11}{}^2 - \frac{1}{16}e^{-2i\omega_{11}T_0}\omega_{13}P_{131111}\bar{A}_{11}^2\right] \tag{5.90}$$

$$W_{\eta\nu}^{(2)} = -\sum_{n,m=1}^{3}\sum_{l,j=1}^{3}P_{\eta\nu nmlj}\left[\frac{A_{nm}A_{lj}e^{i(\omega_{nm}+\omega_{lj})T_0}}{\omega_{\eta\nu} - (\omega_{nm}+\omega_{lj})^2} + \frac{A_{nm}\bar{A}_{lj}e^{i(\omega_{nm}-\omega_{lj})T_0}}{\omega_{\eta\nu} - (\omega_{nm}-\omega_{lj})^2}\right]$$

$$+ cc \qquad \eta \neq 1, \nu \neq 1, 3 \tag{5.91}$$

Substituting Eqs.(5.30)-(5.33) and (5.87)-(5.91) into Eqs. (5.26)-(5.29), eliminating the terms that lead to secular terms, and using the method of recontitution, we obtain

$$2i\omega_{11}\dot{A}_{11} = \Lambda_1 e^{i\sigma_2\varepsilon t} + i\Xi_1 A_{11} + \Xi_2 A_{11}^2\bar{A}_{11} + \Xi_3 A_{11}A_{13}\bar{A}_{13} + \Xi_5 e^{i\sigma_1\varepsilon t}\bar{A}_{11}A_{13}$$

$$+ \Lambda_2 e^{i\varepsilon t(\sigma_1-\sigma_2)}A_{13} \tag{5.92}$$

$$2i\omega_{13}\dot{A}_{13} = \Lambda_3 e^{-i\varepsilon t(\sigma_1 - \sigma_2)} A_{11} + \xi_5 e^{-i\sigma_1 \varepsilon t} A_{11}^2 + \xi_1 A_{11}\bar{A}_{11}A_{13} + i\xi_2 A_{13} + \xi_3 A_{13}^2 \bar{A}_{13} \quad (5.93)$$

where the Λ_i are defined as

$$\Lambda_1 = \frac{1}{2}\varepsilon f_{11} \quad (5.94)$$

$$\Lambda_2 = -\frac{1}{24\omega_{11}^2}\varepsilon^2 (8P_{111313}f_{13} + 3P_{111311}f_{11} + 3P_{111113}f_{11}) \quad (5.95)$$

$$\Lambda_3 = -\frac{1}{3\omega_{13}^2}\varepsilon^2 (2P_{131113}f_{13} + 3P_{131111}f_{11} + 2P_{131311}f_{13}) \quad (5.96)$$

The Cartesian form of the modulation equations can be obtained by expressing the A_i as

$$A_{11} = \frac{1}{2}(p_1 - iq_1)e^{i\lambda_1(t;\varepsilon)} \quad (5.97)$$

$$A_{13} = \frac{1}{2}(p_2 - iq_2)e^{i\lambda_2(t;\varepsilon)} \quad (5.98)$$

where

$$\lambda_1 = \sigma_2 \varepsilon t - 2n\pi \quad (5.99)$$

$$\lambda_2 = 2\sigma_2 \varepsilon t - \sigma_1 \varepsilon t + 2m\pi - 4n\pi \quad (5.100)$$

Substituting Eqs. (5.97)-(5.100) into Eqs. (5.92) and (5.93), letting $\varepsilon = 1$ and separating real and imaginary parts leads to

$$\dot{p}_1 = -\frac{1}{8\omega_{11}}(8\sigma_2 q_1 \omega_{11} - 4\Xi_2 p_1 + \Xi_3 p_1^2 q_1 + \Xi_3 q_1^3 + \Xi_4 q_1 p_2^2 + \Xi_4 q_1 q_2^2$$
$$+ 2\Xi_5 p_1 q_2 - 2\Xi_5 q_1 p_2 + 4\Xi_6 q_2) \quad (5.101)$$

$$\dot{q}_1 = \frac{1}{8\omega_{11}}(8\sigma_2 p_1 \omega_{11} + 8\Xi_1 + 4\Xi_2 q_1 + \Xi_3 p_1^3 + \Xi_3 p_1 q_1^2 + \Xi_4 p_1 p_2^2 + \Xi_4 p_1 q_2^2$$
$$+ 2\Xi_5 p_1 p_2 + 2\Xi_5 q_1 q_2 + 4\Xi_6 p_2) \quad (5.102)$$

$$\dot{p}_2 = -\frac{1}{8\omega_{13}}(-8q_2\omega_{13}\sigma_1 + 16q_2\omega_{13}\sigma_2 + 4q_1\xi_1 + 4q_1p_1\xi_2$$

$$+ q_2p_1{}^2\xi_3 + q_2q_1{}^2\xi_3 - 4p_2\xi_4 + q_2p_2{}^2\xi_5 + q_2{}^3\xi_5) \tag{5.103}$$

$$\dot{q}_2 = \frac{1}{8\omega_{13}}(16p_2\sigma_2\omega_{13} - 8p_2\sigma_1\omega_{13} + 4\xi_1p_1 + 2\xi_2p_1^2 - 2\xi_2q_1^2$$

$$+ \xi_3p_1{}^2p_2 + \xi_3q_1{}^2p_2 + 4\xi_4q_2 + \xi_5p_2{}^3 + \xi_5p_2q_2{}^2) \tag{5.104}$$

To express the modulation equation in polar form, we let

$$A_{11} = \frac{1}{2}a_1e^{i\beta_1} \tag{5.105}$$

$$A_{13} = \frac{1}{2}a_2e^{i\beta_2} \tag{5.106}$$

Substituting Eqs. (5.105) and (5.106) into Eqs. (5.92) and (5.93) and separating real and imaginary parts, we obtain

$$\dot{a}_1 = \frac{1}{4\omega_{11}}\left[a_2\Xi_5\sin(\gamma_1 + \gamma_2)a_1 + 2a_2\Xi_6\sin(\gamma_1) + 2\Xi_2a_1 + 4\Xi_1\sin(\gamma_2)\right] \tag{5.107}$$

$$\dot{a}_2 = \frac{1}{4\omega_{13}}[2\xi_4a_2 - \xi_2\sin(\gamma_1 + \gamma_2)a_1^2 - 2\xi_1\sin(\gamma_1)a_1] \tag{5.108}$$

$$a_1\dot{\gamma}_1 = \frac{1}{8\omega_{11}\omega_{13}a_2}[a_2{}^3\omega_{13}\Xi_4a_1 - \xi_5a_2{}^3a_1\omega_{11} + 2a_2{}^2\omega_{13}\Xi_5\cos(\gamma_1 + \gamma_2)a_1$$

$$+ 4a_2{}^2\omega_{13}\Xi_6\cos(\gamma_1) + a_2\omega_{13}\Xi_3a_1{}^3 - \xi_3a_1{}^3a_2\omega_{11} + 8a_2\sigma_1\omega_{13}a_1\omega_1$$

$$- 8a_2\sigma_2\omega_2a_1\omega_{11} + 8a_2\omega_{13}\Xi_1\cos(\gamma_2) - 2a_1{}^3\omega_{11}\xi_2\cos(\gamma_1 + \gamma_2)$$

$$- 4\xi_1a_1{}^2\cos(\gamma_1)\omega_{11}] \tag{5.109}$$

$$a_2\dot{\gamma}_2 = \frac{1}{8\omega_{11}a_1}[a_2{}^3\Xi_4a_1 + 2a_2{}^2\Xi_5\cos(\gamma_1 + \gamma_2)a_1 + 4a_2{}^2\Xi_6\cos(\gamma_1) + a_2\Xi_3a_1{}^3$$

$$+ 8a_2a_1\sigma_2\omega_{11} + 8a_2\Xi_1\cos(\gamma_2)] \tag{5.110}$$

where

$$\gamma_1 = -\beta_1 + \sigma_1 \varepsilon t - \sigma_2 \varepsilon t + \beta_2 \tag{5.111}$$

$$\gamma_2 = -\beta_1 + \sigma_2 \varepsilon t \tag{5.112}$$

5.3.1   Numerical Results

We consider the shell parameters defined in (5.81). In Fig. 5.23, we show typical frequency-response curves for a single-layered shell with $k_x = 0.33$ and $k_y = 0.398$ obtained by using a nine-mode approximation. Starting with $\sigma_2 = 3$ and decreasing its value, we find that the amplitudes a_1 and a_2 increase until a_1 reaches a maximum at $\sigma_2 = 2.1$ where this solution loses stability through a Hopf bifurcation. Decreasing σ_2 further results in a decrease in a_1 and an increase in a_2 until $\sigma_2 = -0.4$, an enlarged picture for these bifurcations are shown in Fig. 5.24,. The system gains stability through another Hopf bifurcation at $\sigma_2 = -1.17$. This stable solution continues as we decrease σ_2 until it loses stability through a saddle-node bifurcation, causing a jump to the lower branch of stable solutions. Starting on the lower branch and increasing σ_2 increases the values of a_1 and a_2. This solution loses stability at $\sigma_2 = -3.79$ through a saddle-node bifurcation, causing a jump to the upper branch.

In Fig. 5.25, we plot the force-response curves for the shell parameters defined in (5.81) by using only the two interacting modes. We can see that, as we increase the forcing from zero, both a_1 and a_2 increase. At $f_{11} = 48$ the system loses stability through a saddle-node bifurcation. Tracking this unstable solution as the forcing is decreased both a_1 and a_2 increase. The system gains stability through another saddle-node bifurcation at $f_{11} = 41$. Increasing f_{11} to 91, the system loses stability through a Hopf bifurcation generating a dynamic solution. At $f_2 = 560$ the system gains stability through a Hopf bifurcation. We can see that the value of a_2 is larger that a_1 when the value of f_2 is larger than 430.

To see the effect of multi-mode analysis on the force-response curves, we plot in Fig. 5.26 the force-response curves obtained by using nine modes in the approximation. We can
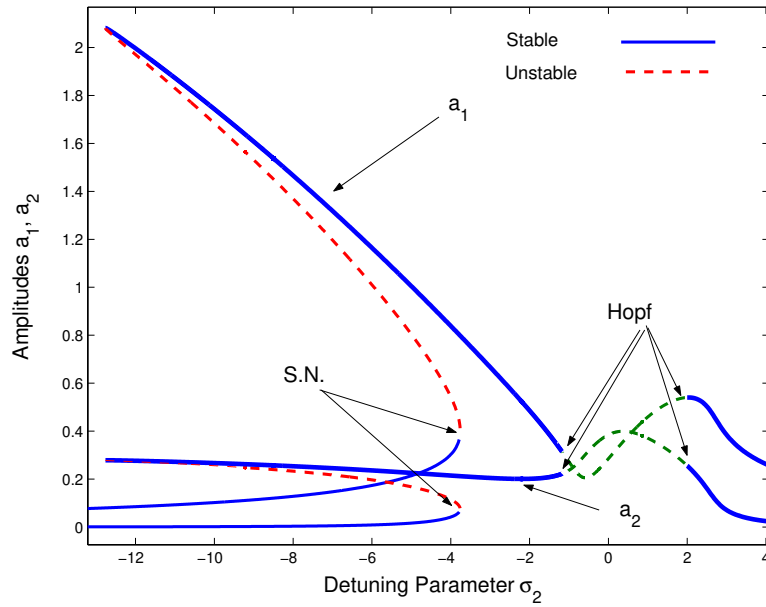
Figure 5.23: Frequency-response curves for a single-layered shell when $k_x = 0.33$, $k_y = 0.398$, $\sigma_1 = -1.8$, and $f_{11} = 350$ for the case $\Omega \approx \omega_{11}$.
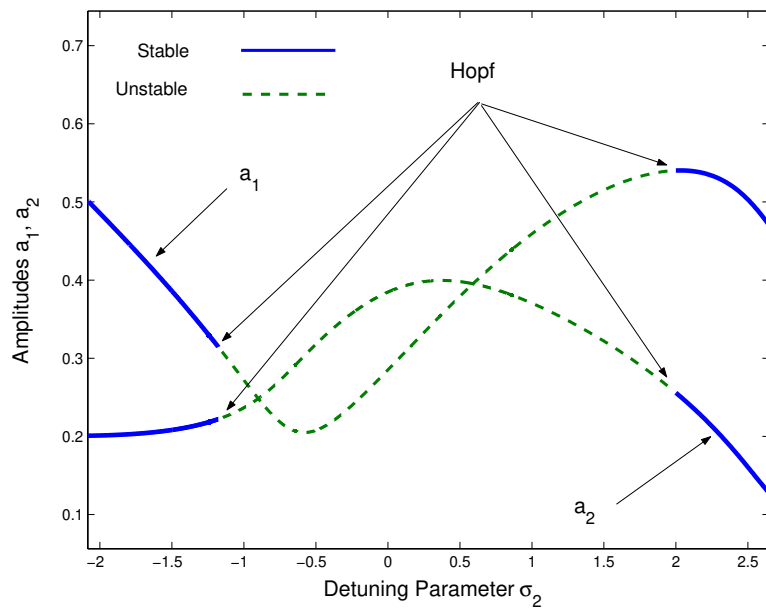
Figure 5.24: An enlagment of the frequency-response curves in Fig. 5.23 near the Hopf bifurcations.
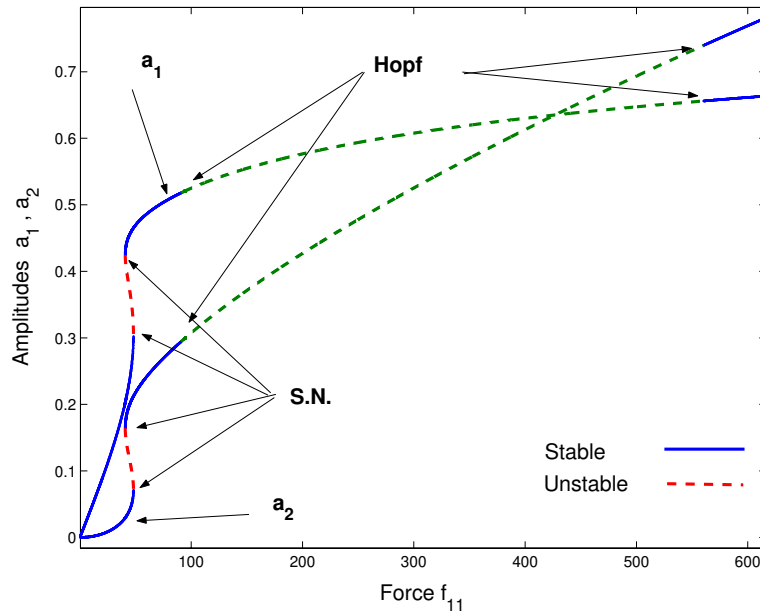
Figure 5.25: Force-response curves for a single-layered shell using a two-mode approximation when $k_x = 0.33$, $k_y = 0.398$, $\sigma_1 = -1.8$, and $\sigma_2 = -1.8$ for the case $\Omega \approx \omega_{11}$.
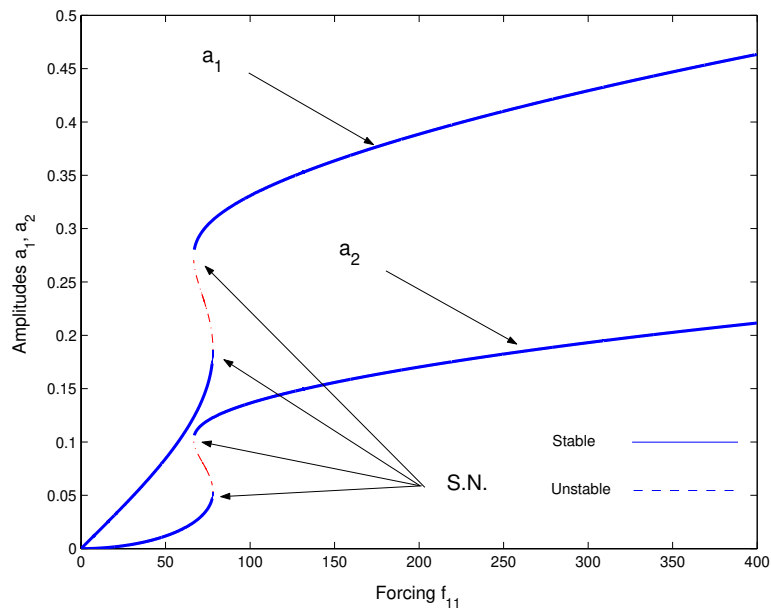
Figure 5.26: Force-response curves for a single-layered shell using a nine-mode approximation when $k_x = 0.33$, $k_y = 0.398$, $\sigma_1 = -1.8$, and $\sigma_2 = -1.8$ for the case $\Omega \approx \omega_{11}$.

see that, as we increase the forcing from zero, both a_1 and a_2 increase. At $f_{11} = 78$, the system loses stability through a saddle-node bifurcation. Tracking this unstable solution as the forcing is decreased, we find that both a_1 and a_2 increase. The system gains stability through another saddle-node bifurcation at $f_{11} = 67$. Increasing f_{11} further increases a_1 and a_2. From Figs 5.25 and 5.26, we can see that using only the two interacting modes shifts the bifurcation points, underestimates or overestimates the amplitudes, and predicts erroneous behaviors.

In this analysis, both the frequency- and force-response curves have only two-mode solutions, while in the case of primary resonance of the higher-frequency mode both single- and two-modes solutions can be activated. To study the effect of changing σ_1 on the shell dynamics, we plot in Fig. 5.27 the force-response curves when $\sigma_2 = 0$. Starting from zero, we see that a_1 and a_2 increase with increasing f_{11}. At $f_{11} = 123$, the system suffers a Hopf bifurcation, which generates dynamic solutions. At $f_{11} = 200.3$, the amplitude of the second mode becomes larger than that of the first mode.
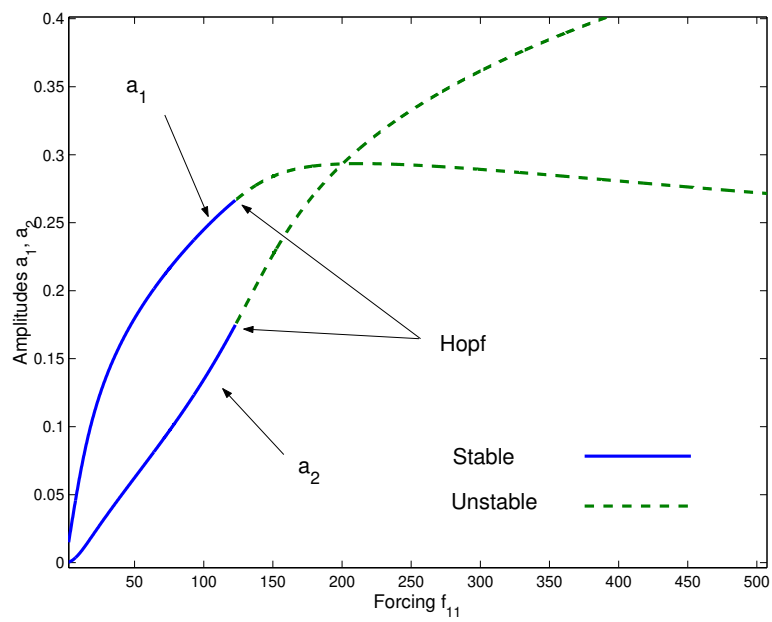
Figure 5.27: Force-response curves for a single-layered shell when $k_x = 0.33, k_y = 0.398$, $\sigma_1 = -1.8$, and $\sigma_2 = 0$ for the case $\Omega \approx \omega_{11}$.

Chapter 6

Conclusions

6.1 Summary

We analyzed the nonlinear vibrations of a doubly curved cross-ply shallow shell in the cases of primary resonance, subharmonic resonance of order one-half, and two-to-one internal resonance. We used the Galerkin procedure to reduce the governing nonlinear partial-differential equations of motion and associated boundary conditions to an infinite system of nonlinearly coupled second-order ordinary-differential equations. We used the method of multiple scales to determine a second-order approximate solution of the discretized equations. We derived a system of first-order nonlinear equations governing the modulation of the amplitudes and phases and obtained expression for the effective nonlinearity. The modulation equations were then used to generate frequency-response curves for a varying number of modes retained in the approximation. Also, the effect of the number of layers on the predicted responses was investigated.

6.1.1 Response of a Shallow Shell to a Primary Resonance Excitation

We analyzed the nonlinear vibrations of a doubly curved cross-ply shell in the case of a primary resonance excitation of its fundamental mode of vibration. We found that even modes do not effect the response of the fundamental mode to a primary-resonance excitation. Furthermore, we found that a single-mode approximation, and even a two-mode approximation, fails to predict the dynamics of the shell. In fact, we found that, for some parameters, the single-mode and two-mode approximations lead not only to quantitatively but also to qualitatively erroneous frequency-response curves. The number of modes that needed to be retained for convergence depends on the shell parameters; a twelve-mode approximation is sufficient for most cases. The second-order approximate solution predicts, for some shell parameters, that the fundamental mode of vibration is involved in a two-to-one internal resonance with another mode. The two-to-one internal resonance manifests itself in a singular value for the effective nonlinearity.

We analyzed the effect of the number of layers on the predicted response. It was shown that increasing the number of layers from 1 to 3 has a great effect on the shell characteristics. This large effect is due to the large change in the stiffness in one direction. It was also shown that, as the number of layers increases, the change in the shell characteristics decreases. Due to the change in shell parameters, such as the natural frequencies, the two-to-one internal resonance is shifted in the k_x and k_y plane.

6.1.2 Global Dynamics

We investigated the vibrations and stability of doubly curved cross-ply laminated shallow shells in the case of primary resonance. We used the reduced-order model to investigate numerically the effect of the number of modes on the predicted responses. We used a combination of a shooting technique and Floquet theory to calculate limit cycles and their

stability. We showed that a single-mode approximation may miss important dynamical responses, underestimate the location of bifurcations, and provide an inaccurate solution for the vibration amplitude. On the other hand, using a multi-mode approximation, we found period-doubling bifurcations, chaos, saddle-node bifurcations and a two-to-one internal resonance. Increasing the number of modes retained over four, in this case, did not affect either the qualitative or the quantitative dynamic behavior of the shell. We used six modes and nine modes in checking for convergence.

6.1.3 Direct Approach

We applied the method of multiple scales directly to the governing partial-differential equations of motion and associated boundary conditions to obtain a second-order uniform approximate solution. We used a Fourier series expansion to satisfy the boundary conditions at second order. The obtained modulation equations were derived and compared with those obtained by using a multi-mode Galerkin approximation. We found that both methods give the same results if the number of terms used in the approximation is large enough. Results were obtained by using 32 terms in the Fourier series expansion.

6.1.4 Responses of a Shallow Shell to a Subharmonic Excitation

We considered the nonlinear forced vibrations of a doubly curved cross-ply laminated shallow shell with simply supported boundary conditions. We investigated its response to a subharmonic resonance of the form $\Omega \approx 2\omega_{11}$. An approximate solution of the reduced-order equations was obtained. These equations were solved by using the method of multiple scales. Numerical results for isotropic, single-layered, and multi-layered shells were obtained. The influence of the number of modes retained in the discretization and the number of layers was investigated. We foundout that a single-mode approximation may underestimate or overestimate the effective forcing. For a single-layered shell, we foundout a large change in

the behavior of the shell as the number of modes is increased from 2 to 3. We foundout that increasing the number of modes beyond 4 has a negligible effect. We also studied the influence of the number layers on the response. We found that changing the number of layers from 1 to 3 produces a large change in the effective forcing.

6.1.5   Two-to-One Internal Resonance

We investigated modal interactions between the first and second modes in the case of the two-to-one internal resonance $\omega_{13} = 2\omega_{11}$. We investigated the shell responses and stability for two cases of primary resonance: $\Omega \approx \omega_{13}$ and $\Omega \approx \omega_{11}$. We used the method of multiple scales to determine the modulation equations that govern the slow dynamics of the response. A pseudo-arclength scheme was then used to determine the fixed points and the stability of these points was investigated. We studied the effect of changing the driving frequency and the forcing amplitude on the predicted response. In some cases, we found that the fixed points may undergo Hopf bifurcations, which result in dynamic responses. A combination of a long-time integration and Floquet theory was used to determine detailed branches of limit cycles and chaotic solutions and their stability. We found that the limit cycles may undergo symmetry-breaking, saddle node, and period-doubling bifurcations. Furthermore, we found that neglecting the effect of the modes not involved in the internal resonance may produce erroneous dynamic responses.

6.2   Recommendations for Future Work

The work presented in this work can be expanded and enhanced by undertaking the following tasks:

1. During our study, we considered simply supported boundary conditions. Other boundary conditions are also important to be considered.

2. When the excitation is direct, combination resonances may occur. These types of resonances should be investigated.

3. The effect of heat on the nonlinear vibrations of shells is of great practical importance and should be studied.

4. Throughout our analysis, we only considered cross-ply shallow shells. This work should be expanded to include angle-ply composite shells.

5. Experimental work needs to be conducted to validate our results.

Bibliography

[1] Abe, A., Kobayashi, Y. and Yamada, G. (1998a). Analysis of Subharmonic Resonance of Moderately Thick Antisymmetric Angle-Ply Laminated Plates by Using Method of Multiple Scales. *Journal of Sound and Vibration*, 217(3):467–484.

[2] Abe, A., Kobayashi, Y. and Yamada, G. (1998b). Three-Mode Response of Simply Supported Rectangular Laminated Plates. *JSME International Journal*, 41(1):51–59.

[3] Abe, A., Kobayashi, Y. and Yamada, G. (1998c). Two-Mode Response of Simply Supported Rectangular Laminated Plates. *International Journal of Non-Linear Mechanics*, 33(4):675–690.

[4] Abe, A., Kobayashi, Y. and Yamada, G. (2000). Non-linear Vibration Characteristics of Clamped Laminated Shallow Shells. *Journal of Sound and Vibration*, 3(234):405–426.

[5] Ahmed, J. and Lee, H. C. (1975). Nonlinear Acoustic Response of a Cylindrical Shell. *Journal of the Franklin Institute*, 299(3):171–189.

[6] Alfonso, S. and Hinton, E. (1995). Free Vibration Analysis and Shape Optimization of Variable Thickness Plates and Shells: 1- Finite Element Studies. *Computing Systems in Engineering*, 6(1):27–46.

[7] Alwar, R. S. and Narasimhan, M. C. (1991). Analysis of Laminated Orthotropic Spherical Shells Subjected to Asymmetric Loads. *Computers & Structures*, 41(4):611–620.

[8] Amabili, M., Pellicano, F. and Paidoussis, M. P. (1998). Nonlinear Vibrations of Simply Supported Circular Cylindrical Shells Coupled to Quiescent Fluid. *Journal of Fluid and Structures*, 12:883–918.

[9] Amabili, M., Pellicano, F. and Paidoussis, M. P. (1999). Non-Linear Dynamics and Stability of Circular Cylindrical Shells Containing Flowing Fluid. Part I: Stability. *Journal of Sound and Vibration*, 225(4):655–699.

[10] Ambartsumian, S. A. (1974). *A General Theory of Anisotropic Shells*. Nauka Publ. Moscow.

[11] Anderson, T. J. and Nayfeh, A. H. (1996). Natural Frequencies and Mode Shapes of Laminated Composite Plates: Experiments and Finite Element Analysis. *Journal of Vibration and Control*, 2(4):381–414.

[12] Andrianov, I. V. and Kholod, E. G. (1993). Non-linear Free Vibration of Shallow Cylindrical Shell By Bolotin's Asymptotic Method. *Journal of Sound and Vibration*, 165(1):9–17.

[13] Andrianov, I. V. and Kholod, E. G. (1996). Approximate Non-Linear Boundary Value Problems for Reinforced Shell Dynamics. *Journal of Sound and Vibration*, 194(3):369–387.

[14] Aron, H. (1874). Das Gleichgewicht und die Bewegung einer Unendlich Dunnen. *Beliebig Gekrummten Elastischen Schale, Journal of Math (Crelle)*, 78.

[15] Atluri, S. (1972). A Perturbation Analysis of Non-Linear Free Flexural Vibration of a Circular Cylindrical Shell. *International Journal of Solids and Structures*, 8:549–569.

[16] Barik, M. and Mukhopadhyay, M. (1998). Finite Element Free Flexural Vibration Analysis of Arbitrary Plates. *Finite Elements in Analysis and Design*, 29(2):137–151.

[17] Berger, H. M. (1955). A New Approach to the Analysis of Large Deflections of Plates. *Journal of Applied Mechanics*, 22:465–472.

[18] Bert, C. W. (1969). Dynamics of Composite, Sandwich and Stiffened Shell-Type Structures. *Spacecraft Rockets*, 6(12):1345–1361.

[19] Bieniek, M. P., Fan, T. C. and Lackman, L. M. (1966). Dynamic Stability of Cylindrical Shells. *AIAA Journal*, 4(3):495–500.

[20] Bogdanovich, A. (1991). *Non-Linear Dynamic Problems for Composite Cylindrical Shells*. Elsevier Applied Science. London.

[21] Chai, G. (1996). Free Vibration of Laminated Composite Plates with a Central Circular Hole. *Composite Structures*, 35(4):357–368.

[22] Chandrashekhara, K. and Karekar, M. S. (1992). Bending Analysis of a Truncated Conical Shells Subjected to Asymmetric Load. *Journal of Thin-Walled Structures*, 13:299–318.

[23] Chen, J. C. and Babcock, C. D. (1975). Nonlinear Vibration of Cylindrical Shells. *AIAA Journal*, 13(7):868–876.

[24] Cheung, Y. K. and Fu, Y. M. (1995). Nonlinear Static and Dynamic Analysis for Laminated, Annular, and Spherical Caps of Moderate Thickness. *Nonlinear Dynamics*, 8:251–268.

[25] Cheung, Y. K. and Zhou, D. (1999). The Free Vibrations of Tapered Rectangular Plates Using a New Set of Beam Functions with the Rayleigh-Ritz Method. *Journal of Sound and Vibration*, 223(5):703–722.

[26] Chia, C. Y. (1980). *Nonlinear Analysis of Plates*. McGraw Hill. New York.

[27] Chia, C. Y. (1988). Nonlinear Analysis of Doubly Curved Symmetrically Laminated Shallow Shells with Rectangular Planform. *Ingenieur-Archiv*, 58:252–264.

[28] Chien, W. Z. (1943). The Intrinsic Theory of Thin shells and Plates 1. General Theory. *Quarterly Journal of Applied Mathematics*, 1(4):297–327.

[29] Chien, W. Z. (1944a). The Intrinsic Theory of Thin Shells and Plates 2. Application to Thin Plates. *Quarterly Journal of Applied Mathematics*, 2(1):43–59.

[30] Chien, W. Z. (1944b). The Intrinsic Theory of Thin Shells and Plates 3. Application to Thin Shells. *Quarterly Journal of Applied Mathematics*, 2(2):120–135.

[31] Chin, C-M and Nayfeh, A. H. (1996). Bifurcation and Chaos in Externally Excited Circular Cylindrical Shells. *Journal of Applied Mechanics*, 63(3):163–173.

[32] Connor, J. Jr. (1962). Nonlinear Transverse Axisymmetric Vibrations of Shallow Spherical Shells. *NASA TN-D1510*, 623–642.

[33] Cummings, B. E. (1964). Large-Amplitude Vibration and Response of Curved Panels. *AIAA Journal*, 2(4):709–716.

[34] Cunha, J. (1997). Free Vibration of Composite Laminated Plates by Using Finite Element Technique with a Higher-Order Theory. *Science and Engineering Journal*, 6(2):73–81.

[35] De Almeida, S. F. and Hansen, J. S. (1997). Free Vibration Analysis of Composite Plates with Tailored Thermal Residual Stresses. *ASME International Mechanical Engineering Congress and Exposition*, AD 55 ASME:183–190.

[36] Delpak, R., Peshkam, V. and Azizian, Z. G. (1986). A Theoretical Energy Approach in Predicting the Elastic Nonlinear Behavior of Thin Rotational Shells and Other Continua. *Computers & Structures*, 22(5):867–876.

[37] Ding, Z. (1996). Natural Frequency of Rectangular Plates Using a Set of Static Beam Functions in Rayleigh-Ritz Method. *Journal of Sound and Vibration*, 189(1):81–87.

[38] Donnell, L. H. (1933). *Stability of Thin Walled Tubes Under Torsion*. NACA Report. 479.

[39] Donnell, L. H. (1934). A New Theory for the Buckling of Thin Cylinders Under Axial Compression and Bending. *ASME*, 56:795–806.

[40] Efstathiades, G. J. (1971). A New Approach to the Large-Deflection Vibrations of Imperfect Circular Disks Using Galerkin's Procedure. *Journal of Sound and Vibration*, 16:231–253.

[41] El-Zaouk, B. R. and Dym, C. L. (1973). Non-Linear Vibrations of orthotropic Doubly-Curved Shallow Shells. *Journal of Sound and Vibration*, 31(1):89–103.

[42] Evensen, D. A. and Fulton, R. E. (1965). *Some Studies on the Nonlinear Dynamics Response of Shell-Type Structures*. NASA TMX-56843.

[43] Fan, J. and Ye, J. (1990). An Exact Solution for the Statics and Dynamics of Laminated Thick Plates with Orthotropic Layers. *International Journal of Solids and Structures*, 26(5/6):655–662.

[44] Fan, J. and Zhang, J. (1992). Analytical Solutions for Thick, Doubly Curved, Laminated Shells. *Journal of Engineering Mechanics*, 118(7):1338–1356.

[45] Fan, S. C. and Luah, M. H. (1995). Free Vibration Analysis of Arbitrary Thin Shell Structures by Using Spline Finite Element. *Journal of Sound and Vibration*, 179(5):763–776.

[46] Farag, N. H. and Pan, J. (1998). Free and Forced In-Plane Vibration of Rectangular Plates. *Journal of the Acoustical Society of America*, 103(1):408–413.

[47] Flügge, W. (1934). *Statik and Dynamik der Schalen*. Springer-Verlag. New York.

[48] Flügge, W. (1962). *Stresses in Shells.* Springer-Verlag. New York.

[49] Foale, S., Thompson, M. T. and McRobie, F. A. (1998). Numerical Dimension-Reduction Methods for Non-Linear Shell Vibration. *Journal of Sound and Vibration,* 215(3):527–545.

[50] Fu, Y. M. and Chia, C. Y. (1993). Non-Linear Vibration and Post buckling of Generally Laminated Circular Cylindrical Thick Shells with Non-Uniform Boundary Conditions. *Nonlinear Dynamics,* 28(3):313–327.

[51] Galerkin, B. G. (1934). On the Theory of Elastic Cylindrical Shells. *D.A.N,* 4(5-6).

[52] Galerkin, B.G. (1942). Equilibrium of an Elastic Spherical Shells. *Prikl. Math. Mekh, U.S.S.R.,* 6(6).

[53] Galimov, A. K. (1977). *Theory of Shells with Allowance for Transverse Shear.* Gostekhizdat Publ. Moscow.

[54] Germaine, S. (1821). *Recherches sur la Theorie des Surfaces Elastiques.* Paris.

[55] Gershtein, M. S. (1976). On One Variant of the Non-Linear Dynamic Theory for Thin Multilayer Shells. *Applied Mathematics and Mechanics,* 40(1):180–185.

[56] Ghazi, S. (1998). Determination of Natural Frequencies of Regular Polygonal Plates of Nonuniform Thickness. *Alexandria Engineering Journal,* 37(1):7–18.

[57] Gol'denveiser, A. L. (1961). *Theory of Thin Shells.* Pergamon Press. New York.

[58] Gol'denveiser, A. L. (1979). *A Theory of Elastic Thin-Wall Shells.* Gostekhizdat Publ. Moscow.

[59] Gol'denveiser, A. L., Kaplunov, J. D. and Nolde, E. V. (1993). On Timoshenko-Reissner Type Theories of Plates and Shells. *International Journal of Solids and Structures,* 30(5):675–694.

[60] Gould, P. L. (1998). *Analysis of Plates and Shells.* Prentice-Hall. New York.

[61] Grigolyuk, E. I. (1953). On the Strength and Stability of Cylindrical Bimetallic Shells. *Engineering Collect*, 116:119–148.

[62] Grigolyuk, E. I. and Chulkov, P. P. (1964). A Theory of Visco-Elastic Multilayer Shells Containing a Solid Core at Finite Deflection. *Appl. Mech. Tech. Phys*, 150(5):1012–1015.

[63] Grigolyuk, E. I. and Kabanov, V. V. (1967). *Stability of Circular Cylindrical Shells.* Scientific Totals. Moscow.

[64] Grigolyuk, E. I. and Kabanov, V. V. (1978). *Stability of Shells.* Nauka Publ. Moscow.

[65] Grigolyuk, E. I. and Mamai, V. I. (1974). About One Variant of Equations in a Theory of Finite Displacements of Shallow Shells. *Journal of Applied Mechanics*, 10(2):3–13.

[66] Grossman, P. L., Koplik, B. and Yu, Y. Y. (1969). Nonlinear Vibrations of Shallow Spherical Shells. *Journal of Applied Mechanics*, 36:451–458.

[67] Hadian, J. and Nayfeh, A. H. (1990). Modal Interaction in Circular Plates. *Journal of Sound and Vibration*, 142(2):279–292.

[68] Harichandran, R. S. and Naja, M. K. (1997). Random Vibration of Laminated Composite Plates with Material Nonlinearity. *International Journal of Non-Linear Mechanics*, 32(4):707–720.

[69] Hui, D. (1983). Large-Amplitude Axisymmetric Vibrations of Geometrically Imperfect Circular Plates. *Journal of Sound and Vibration*, 91(2):239–246.

[70] Hui, D. (1983). Large-Amplitude Vibrations of Geometrically Imperfect Shallow Spherical Shells with Structural Damping. *AIAA Journal*, 21(12):1736–1741.

[71] Hui, D. (1984). Influence of Geometric Imperfections and In-Plane Constraints on the Nonlinear Vibrations of Simply Supported Cylindrical Panels. *Journal of Applied Mechanics*, 51:383–389.

[72] Hui, D. (1985). Soft-Spring Nonlinear Vibrations of Anti Symmetrically Laminated Rectangular Plates. *International Journal of Mechanical Science*, 27(6):397–408.

[73] Hui, D. and Leissa, A. W. (1983). Effects of Uni-Directional Geometric Imperfections on Vibrations of Pressurized Shallow Spherical Shells. *International Journal of Non-Linear Mechanics*, 18(4):279–285.

[74] Ip, K. H., Chan, W. K., Tse, P. C. and Lai, T. C. (1996). Vibration Analysis of Orthotropic Thin Cylindrical Shells with Free Ends by the Rayleigh-Ritz Method. *Journal of Sound and Vibration*, 195(1):117–135.

[75] Jiashen, F. and Lei, F. (1991). Closed Form Solution for Nonlinear Dynamic Response in Shallow Shells. *Applied Mathematics Modeling*, 15:416–424.

[76] Khdeir, A. A. (1993). Dynamic Response of Cross-Ply Laminated Circular Cylindrical Shells with Various Boundary Conditions. *Acta Mechanica*, 112:117–134.

[77] Killian, D. E., Kamat, M. P. and Nayfeh, A. H. (1983). Numerical Perturbation Solution for the Vibration of Prestressed, Clamped Cylindrical Shells. *Journal of Sound and Vibration*, 86(1):9–22.

[78] Kobayashi, Y. and Leissa, A. W. (1995). Large Amplitude Free Vibration of Thick Shallow Shells Supported by Shear Diaphragms. *International Journal of Non-Linear Mechanics*, 30(1):57–66.

[79] Koiter, W. T. (1966). On the Non-Linear Theory of Thin Elastic Shells 1,2,3. *Proc. K. Nederl. Acad. Wet.*, B69(1):1–54.

[80] Kulikov, G. M. (1979). On the Theory of Multilayer Shallow Shells at Finite Deflection. *Trans. USSR Acad. Sci. Mech. Solids.*, 3:188–192.

[81] Lacarbonara, W. (1999). Direct Treatment and Discretization of Non-Linear Spatially Continuous System. *Journal of Sound and Vibration*, 221(5):849–866.

[82] Lacarbonara, W., Nayfeh, A. H. and Kreider, W. (1998). Experimental Validation of Reduction Methods for Nonlinear Vibrations of Distributed-Parameter Systems: Analysis of a Buckled Beam. *Nonlinear Dynamics*, 17:95–117.

[83] Lee, J. M., Chung, J. H. and Chung, T. Y. (1997). Free Vibration Analysis of Symmetrically Laminated Composite Rectangular Plates. *Journal of Sound and Vibration*, 199(1):71–85.

[84] Leissa, A. W. (1993). *Vibration of Shells*. Acoustical Society of America. Sewickly, PA.

[85] Leissa, A. W. and Kadi, A. S. (1971). Curvature Effects of Shallow Shell Vibration. *Journal of Sound and Vibration*, 16(2):173–187.

[86] Leissa, A. W., Lee, J. K. and Wang, A. J. (1983). Vibration of Cantilevered Doubly-Curved Shallow Shells. *International Journal of Solids and Structures*, 19(5):411–424.

[87] Leissa, A. W. and Narita, Y. (1984). Vibration of Completely Free Shallow Shells of Rectangular Planform. *Journal of Sound and Vibration*, 96(2):207–218.

[88] Leissa, A. W. and Qatu, M. S. (1991). Equations of Elastic Deformation of Laminated Composite Shallow Shells. *Journal of Applied Mechanics*, 58(1):181–188.

[89] Leung, A. Y. T. and Mao, S. G. (1995). A Simplistic Galerkin Method for Non-Linear Vibration of Beams and Plates. *Journal of Sound and Vibration*, 183(3):475–491.

[90] Li, W. Y., Tham, L. G., Cheung, Y. K. and Fan, S. C. (1990). Free Vibration Analysis of Doubly Curved Shells by Spline Finite Strip Method. *Journal of Sound and Vibration*, 140(1):39–53.

[91] Libai, A. and Simmond, J. G. (1988). *The Nonlinear Theory of Elastic Shells: One Spatial Dimension*. Academic Press. New York.

[92] Librescu, L. (1987). Refined Geometrically Nonlinear Theories of Anisotropic Laminated Shells. *Quarterly of Applied Mathematics*, 45(1):1–22.

[93] Liew, K. M. and Lim, C. W. (1996). A Higher-Order Theory for Vibration of Doubly Curved Shallow Shells. *Journal of Applied Mechanics*, 63:587–592.

[94] Liew, K. M. (1997). Vibration of Shallow Shells: A Review with Bibliography. *Applied Mechanics Reviews*, 50(8):431–444.

[95] Love, A. E. H. (1944). *A Treatise on the Mathematical Theory of Elasticity*. Dover. New York.

[96] Lur'ye, A. I. (1937). A Study in the Theory of Thin Shells. *Trudy L.P.I U.S.S.R.*, 6.

[97] Maewal, A. (1978). Nonlinear Flexural Vibrations of an Elastic Ring. *Journal of Applied Mechanics*, 45:428–429.

[98] Maganty, S. P. and Bickford, W. B. (1987). Large Amplitude Oscillation of Thin Circular Rings. *Journal of Applied Mechanics*, 54:315–322.

[99] Masunaga, H. (1999). Vibration and Stability of Thick Simply Supported Shallow Shells Subjected to In-Plane Stress. *Journal of Sound and Vibration*, 225(1):41–60.

[100] McIvor, I. K. (1966). The Elastic Cylindrical Shell under Radial Impulse. *Journal of Applied Mechanics*, 33(4):831–837.

[101] McIvor, I. K. and Lovell, E. G. (1968). Dynamic Response of Finite-Length Cylindrical Shells to Nearly Uniform Radical Impulse. *AIAA Journal*, 6(12):2346–2351.

[102] Meirovitch, L. (1997). *Principles and Techniques of Vibration*. Printice-Hall International. New York.

[103] Mente, L. J. (1973). Dynamic Nonlinear Response of Cylindrical Shells to Asymmetric Pressure Loading. *AIAA Journal*, 11(6):793–800.

[104] Mirza, S. (1991). Recent Research in Vibration of Layered Shells. *Journal of Pressure Vessel Technology*, 113:321–325.

[105] Moussaoui, F., Benamar, R. and White, R. G. (2000). The Effects of Large Vibration Amplitudes on the Mode Shapes and Natural Frequencies of Thin Elastic Shells, Part I: Coupled Transverse-Circumferential Mode Shapes of Isotropic Circular Cylindrical Shells of Infinite Length. *Journal of Sound and Vibration*, 232(5):917–943.

[106] Mukherjee, K. and Chakraborty, S. K. (1985). Exact Solution for Large Amplitude Free and Forced Oscillation of a Thin spherical Shell. *Journal of Sound and Vibration*, 100(3):339–342.

[107] Mushtari, H. M. and Galimov, K. Z. (1957). *A Non-Linear Theory of Elastic Shells*. Tatknigoizdat Publ. Moscow.

[108] Mushtari, H. M. and Teregulov, I. G. A Theory of Shallow Orthotropic Shells of Medium Thickness. *Trans. USSR Acad Sci.*, 6:60–67, 1959.

[109] Naghdi, P. M. and Berry, J. G. (1964). On the Equations of Motion of Cylindrical Shells. *Journal of Applied Mechanics*, 21(2):160–166.

[110] Nash, W. A. and Modeer, J. R. (1959). Certain Approximation Analysis of the Nonlinear Behavior of Plates and Shallow Shells. *Proceedings of the Symposium on the Theory of thin Elastic Shells, New York*, pp. 331–353.

[111] Nayfeh, A. H. (1973). *Perturbation Methods*. Wiley. New York.

[112] Nayfeh, A. H. (1981). *Introduction to Perturbation Techniques*. Wiley. New York.

[113] Nayfeh, A. H. (1987). Nonlinear Forced Response of Infinitely Long Circular Cylindrical Shells. *Journal of Applied Mechanics*, 54:571–577.

[114] Nayfeh, A. H. (1993). *Method of Normal Forms*. Wiley. New York.

[115] Nayfeh, A. H. (1998). Reduced-Order Models of Weakly Nonlinear Spatially Continuous Systems. *Nonlinear Dynamics*, 16:105–125.

[116] Nayfeh, A. H. and Lacarbonara, W. (1988). On the Discretization of Spatially Continuous Systems with Quadratic and Cubic Nonlinearities. *JSME International Journal*, 4(3):2–23.

[117] Nayfeh, A. H. and Lacarbonara, W. (1997). On the Discretization of Distributed-Parameter System with Quadratic and Cubic Nonlinearities. *Nonlinear Dynamics*, 13:203–220.

[118] Nayfeh, A. H. and Mook, D. T. (1979). *Nonlinear Oscillations*. Wiley. New York.

[119] Nayfeh, A. H., Nayfeh, J. F. and Mook, D. T. (1992). On Methods for Continuous Systems with Quadratic and Cubic Nonlinearities. *Nonlinear Dynamics*, 3:145–162.

[120] Nayfeh, A. H. and Balachandran, B. (1995). *Applied Nonlinear Dynamics*. Wiley. New York.

[121] Novozhilov, V. V. (1953). *Foundations of the Nonlinear Theory of Elasticity*. Dover. New York.

[122] Novozhilov, V. V. (1964). *The Theory of Thin Elastic Shells*. Norodhoff. Moscow.

[123] Nowacki, W. (1963). *Dynamics of Elastic Systems (Trans. from Polish)*. Chapman and Hall. New York.

[124] Nowinski, J. (1958a). Note on an Analysis of Large Deflections of Rectangular Plates. *MRC Technical Summary Report No.34 Mathematics Research Center US Army*, The University of Wisconsin.

[125] Nowinski, J. (1958b). Some Mixed Boundary-Value Problems for Plates with Large Deflection. *MRC Technical Summary Report No.42 Mathematics Research Center US Army*, The University of Wisconsin.

[126] Nowinski, J. (1959). Large Deflections of Circular Plates Supported Along their Boundary and Along Concentric Circumferences. *MRC Technical Summary Report No.67 Mathematics Research Center US Army*, The University of Wisconsin.

[127] Nowinski, J. L. (1963). Nonlinear Transverse Vibration of Orthotropic Cylindrical Shells. *AIAA Journal*, 1(3):617–620.

[128] Oh, K. and Nayfeh, A. H. (1998). High- to Low-Frequency Modal interactions in a Cantilever Composite Plate. *Journal of Vibration and Acoustics*, 120(2):579–587.

[129] Pai, P. and Nayfeh, A. H. (1992). A Nonlinear Composite Shell Theory. *Nonlinear Dynamics*, 3:431–463.

[130] Pakdemirli, M., Nayfeh, S. A. and Nayfeh, A. H. (1995). Analysis of One-to-One Autoparametric Resonances in Cable- Discretization vs. Direct Treatment. *Nonlinear Dynamics*, 8:65–83.

[131] Popov, A. A., Thompson, J. M. and McRobie, F. A. (1998). Low Dimensional Models of Shell Vibrations, Parametrically Excited Vibrations of Cylindrical Shells. *Journal of Sound and Vibration*, 209(1):163–186.

[132] Prathap, G. and Varadan, T. K. (1977). On the Nonlinear Vibrations of Rectangular Plates. *Journal of Sound and Vibration*, 56(4):521–530.

[133] Prusakov, A. P. (1971). Finite Deflection in Multilayer Shallow Shells. *Trans. USSR Acad. Sci. Mech. Solids*, 3:119–125.

[134] Pshenichnov, G. I. (1993). *A Theory of Latticed Plates and Shells*. World Scientific. London.

[135] Qatu, M. S. (1992). Review of Shallow Shells Vibration Research. *Shock and Vibration Digest*, 24(9):3–15.

[136] Qatu, M. S. and Leissa, A. W. (1991a). Free Vibrations of Completely Free Doubly-Curved Laminated Composite Shallow Shells. *Journal of Sound and Vibration*, 151(1):9–29.

[137] Qatu, M. S. and Leissa, A. W. (1991b). Natural Frequency for Cantilevered Doubly-Curved Laminated Composite Shallow Shells. *Composite Structures*, 17:227–255.

[138] Qatu, M. S. and Leissa, A. W. (1993). Vibration of Shallow Shells with Two Adjacent Edges Clamped and the Others Free. *Mech. Struct. & Mach.*, 21(3):285–301.

[139] Rajalingham, C., Bhat, R. B. and Xistris, G. D. (1996). Vibration of Rectangular Plates Using Plate Characteristic Functions as Shape Functions in the Rsyleigh-Ritz Method. *Journal of Sound and Vibration*, 193(2):497–509.

[140] Ramesh, G. and Krishnamoorthy, C. S. (1995). Geometrically Non-Linear Analysis of Plates and Shallow Shells by Dynamic Relaxation. *Computer Methods and Applied Mechanics Engineering*, 123:15–32.

[141] Raouf, R. A. (1989). *Modal Interaction in Shell Dynamics*. Doctoral Thesis. Virginia Tech, Blacksburg, VA.

[142] Raouf, R. A. and Nayfeh, A. H. (1990). One-to-One Autoparametric Resonance in Infinitely Long Cylindrical Shells. *Computers & Structures*, 35(2):163–173.

[143] Raouf, R. A. and Palazotto, A. N. (1994). On the Non-Linear Free Vibrations of Curved Orthotropic Panels. *International Journal of Non-Linear Mechanics*, 29(4):507–514.

[144] Reddy, J. N. (1997). *Mechanics of Laminated Composite Plates*. CRC Press. New York.

[145] Reddy, J. N. and Liu, C. F. (1985). A Higher-Order Shear Deformation Theory of Laminated Elastic Shells. *International Journal of Engineering Science*, 23(3):319–330.

[146] Rega, G., Lacarbonara, W., Nayfeh, A. H. and Chin, C. M. (1999). Multiple Resonances in Suspended Cables: Direct Versus Reduced-Order Models. *International Journal of Non-Linear Mechanics*, 34:901–924.

[147] Reissner, E. (1941). A New Derivation of the Equations of the Deformation of Elastic Shells. *American Journal of Mathematics*, 63(1):177–184.

[148] Sanders, J. L. (1959). *An Improved First Approximation Theory for Thin Shells.* NASA TR-R24.

[149] Sanders, J. L. (1963). Non-Linear Theories for Thin Shells. *Quarterly Journal of Applied Mathematics*, 21(1):21–36.

[150] Sathyamoorthy, M. (1994). Vibration of Moderately Thick Shallow Spherical Shells at Large Amplitudes. *Journal of Sound and Vibration*, 172(1):63–70.

[151] Shtaerman, I. (1924) On the Theory of Symmetric Deformations of Anisotropic Elastic Shells. *Trans. Kiev Polytech. Agric. Inst.*, 1(1):54–72.

[152] Simmonds, J. G. (1979). Accurate Nonlinear Equations and Perturbation Solution for the Free Vibrations of a Circular Elastic Ring. *Journal of Applied Mechanics*, 46:156–160.

[153] Simmonds, J. G. (1985). A New Displacement Form for the Nonlinear Equations of Motion of Shells of Revolution. *Journal of Applied Mechanics*, 52:507–509.

[154] Singh, A. V. and Kumar, V. (1996). Vibration of Laminated Shallow Shells on Quadrangular Boundary. *Journal of Aerospace Engineering*, 9(2):52–57.

[155] Sinharay, G. C. and Banerjee, B. (1985). A New Approach to Deflection Analysis of Spherical and Cylindrical Shells. *Journal of Applied Mechanics*, 52:872–876.

[156] Soedel, W. (1993). *Vibrations of Shells and Plates.* Marcel Dekker. New York.

[157] Sokolnikoff, I. S. (1956). *Mathematical Theory of Elasticity.* McGraw-Hill. New York.

[158] Sridhar, S., Mook, D. T. and Nayfeh, A. H. (1975). Nonlinear Resonances in the Forced Responses of Plates, Part I: Symmetric Responses of Circular Plates. *Journal of Sound and Vibration*, 41:359–373.

[159] Sridhar, S., Mook, D. T. and Nayfeh, A. H. (1978). Nonlinear Resonances in the Forced Responses of Plates, Part II: Asymmetric Responses of Circular Plates. *Journal of Sound and Vibration*, 59:159–170.

[160] Stavridis, L. T. (1998). Dynamic Analysis of Shallow Shells of Rectangular Base. *Journal of Sound and Vibration*, 218(5):861–882.

[161] Stricklin, J. A., Martinez, J. E., Tillerson, J. R., Hong, J. H. and Haisler, W. E. (1971). Nonlinear Dynamic Analysis of Shells of Revolution by Matrix Displacement Method. *AIAA Journal*, 9(4):629–636.

[162] Suzuki, K., Shikanai, G. and Leissa, A. W. (1994). Free Vibrations of Laminated Composite Noncircular Thin Cylindrical Shells. *Journal of Applied Mechanics*, 61:861–870.

[163] Tenneti, R. and Chandrashekhara, K. (1994). Nonlinear Vibration of Laminated Plates Using a Refined Shear Flexible Element. *Advanced Composite Materials*, 4(2):145–160.

[164] Timarci, T. and Soldatos, K. P. (1995). Comparative Dynamic Studies for Symmetric Cross-Ply Circular Cylindrical Shells on the Basis of a Unified Shear Deformation Shell Theory. *Journal of Sound and Vibration*, 187(4):609–624.

[165] Timoshenko, S. P. and Woinowsky-Krieger, S. (1959). *Theory of Plates and Shells.* McGraw-Hill. New York.

[166] Troger, H. and Steindl, A. (1991). *Non-linear Stability and Bifurcation Theory.* Springer-Verlag, New York.

[167] Vlasov, V. Z. (1949). *General Theory for Shells and its Application in Engineering.* Gostekhizdat Publ. Moscow.

[168] Vorovich, I. I. (1956). About Bubnov-Galerkin's Method in the Non-Linear Theory of Vibrations of Shallow Shells. *Rep. USSR Acad. Sci.*, 110(5):723–726.

[169] Vorovich, I. I. (1990). *Nonlinear Theory of Shallow Shells.* Springer-Verlag. New York.

[170] Watawala, L. and Nash, W. A. (1983). Influence of Initial Geometric Imperfections on Vibrations of Thin Cylindrical Shells. *Computers & Structures*, 16:125–130.

[171] Wu, C.-P. and Chi, Y.-W. (1999). Asymptotic Solutions of Laminated Composite Shallow Shells with Various Boundary Conditions. *Acta Mechanica*, 132:1–18.

[172] Wu, C. and Liu, C. (1994). Stress and Displacement of Thick Doubly Curved Laminated Shells. *Journal of Engineering Mechanics*, 120(7):1403–1429.

[173] Yasuda, K. and Kushida, G. (1984). Nonlinear Forced Oscillations of a Shallow Spherical Shell. *Bulletin of the JSME*, 27(232):2233–2240.

[174] Ye, Z. M. (1997). The Nonlinear Vibration and Dynamic Instability of Thin Shallow Shells. *Journal of Sound and Vibration*, 202(3):303–311.

[175] Young, T. H. and Chen, F. Y. (1995). Non-linear Vibration of Cantilever Skew Plates Subjected to Aerodynamic and In-Plane Exciting Forces. *Journal of Sound and Vibration*, 182(3):427–440.

[176] Zenkour, A. M. (1998). Vibration of Axisymmetric Shear Reformable Cross-Ply Laminated Cylindrical Shells - A Variational Approach. *International Journal of Engineering Science*, 36(3):219–231.

[177] Zerna, W. (1960). *Theory of Thin Elastic Shells.* IUTAM Symp, Moscow.

[178] Zhang, J., Van Campen, D. H., Zhang, G . Q., Bouwman, V. and TerWeeme, J. W. (2001). Dynamic Stability of Doubly Curved Orthotropic Shallow Shells under Impact. *AIAA Journal*, 39(5):956–961.

[179] Zhu, J., Datta, S. K. and Shah, A. H. (1995). Modal Representation of Transient Dynamics of Laminated Plates. *Composite Engineering*, 5(12):949–963.

<u>Appendix A</u>

Definition of the Coefficients

$$A1_{nm} = \frac{D^*\pi^4}{4l_x^4 l_y^4} \left[K_{11} n^4 l_y^4 + n^2 m^2 l_x^2 l_y^2 (2K_{12} + K_{66}) + K_{22} m^4 l_x^4 \right] \tag{6.1}$$

$$A2_{nm} = -\frac{h\pi^2 \left(k_x m^2 l_x^2 + k_y n^2 l_y^2\right)}{4l_x^2 l_y^2} \tag{6.2}$$

$$A3 = \frac{h^2 \pi^4}{l_x^2 l_y^2} \tag{6.3}$$

$$C1_{nm} = \frac{h\pi^4}{4l_x^4 l_y^4} \left[D_{11} n^4 l_y^4 + 2n^2 m^2 l_x^2 l_y^2 (D_{12} + 2D_{66}) + D_{22} m^4 l_x^4 \right] \tag{6.4}$$

$$C2_{nm} = \left(-\frac{k_x D^* m^2 \pi^2}{4l_y^2} - \frac{k_y D^* n^2 \pi^2}{4l_x^2} \right) \tag{6.5}$$

$$C3_{nm} = \frac{h\sqrt{\frac{D^*}{\rho h}}}{l_x^2} \int_0^1 \int_0^1 C \sin^2(n\pi x) \sin^2(m\pi y) dx dy \tag{6.6}$$

$$C4 = \frac{D^* h}{4l_x^4} \tag{6.7}$$

$$C5 = -\frac{D^* h \pi^4}{l_x^2 l_y^2} \tag{6.8}$$

$$f_{nm} = \frac{-l_x^3}{D^* h} \int_0^1 \int_0^1 F_{nm} \sin(n\pi x) \sin(m\pi y) dx dy \tag{6.9}$$

$$G_{\eta\nu nmlj} = \int_0^1 \int_0^1 \left[\sin(\pi\eta x) \sin(\pi\nu y) \sin(\pi n x) \right.$$
$$\left. \sin(\pi m y) \sin(\pi l x) \sin(\pi j y) \right] dx dy \tag{6.10}$$

$$\bar{G}_{\eta\nu nmlj} = \int_0^1 \int_0^1 \left[\sin(\pi\eta x) \sin(\pi\nu y) \cos(\pi nx) \right.$$

$$\left. \cos(\pi my) \cos(\pi lx) \cos(\pi jy) \right] dx dy \tag{6.11}$$

$$2\mu_{nm} = \frac{C3_{nm}}{C4} \tag{6.12}$$

$$\omega_{nm}^2 = \frac{A_{1nm} C1_{nm} + C2_{nm} A2_{nm}}{C4 A_{1nm}} \tag{6.13}$$

$$P_{\eta\nu nmlj} = \frac{C2_{\eta\nu} A3(mnlj \bar{G}_{\eta\nu nmlj} - n^2 j^2 G_{\eta\nu nmlj})}{A1_{\eta\nu} C4}$$

$$+ \frac{A2_{lj} C5[(n^2 j^2 + m^2 l^2) G_{\eta\nu nmlj} - 2nmlj \bar{G}_{\eta\nu nmlj}]}{A1_{lj} C4} \tag{6.14}$$

$$S_{\eta\nu nmljpqrs} = \frac{A3 C5 \left(pqrs \bar{G}_{ljpqrs} - p^2 s^2 G_{ljpqrs} \right)}{A1_{lj} C4}$$

$$.[(n^2 j^2 + m^2 l^2) G_{\eta\nu nmlj} - 2nmlj \bar{G}_{\eta\nu nmlj}] \tag{6.15}$$

Vita

Khaled A. Alhazza was born on June 15, 1972 in the city of Kuwait. He graduated from Al-bra' Ibn Malk high school in June 1990. He then attended the College of Engineering at Kuwait University where he obtained his Bachelor of Science degree in Mechanical Engineering in January 1996. Then in March 1996, he was employed by the Kuwait Institute of Scientific Research (KISR). In August 1996, he Joined the Mechanical Engineering department at Rensselaer Polytechnic Institute (RPI), in Troy, New York, where he obtained his Master of Science in Mechanical Engineering, May 1998. Finally, he joined the Mechanical Engineering department at Virginia Polytechnic Institute and State University (Virginia Tech), in Blacksburg, Virginia in August 1998. In December 2002, he successfully defended his dissertation to receive a Doctor of Philosophy degree in Mechanical Engineering.